Whole-Core Magnetic Susceptibility Measurements During the VNTR01 Expedition, 1989: Dating Quaternary Sediments Using Climate-Susceptibility Correlations

by

Pórdur Arason

Geophysics
College of Oceanography
Oregon State University
Corvallis, Oregon 97331

March 1990

Report OSU-CO-90-1-149

Data report no. 149, per publisher.

Table of Contents

List of Figures

List of Tables

Abstract

Whole-core magnetic susceptibilities were measured on unopened sections of sediment cores collected from the eastern equatorial Pacific during the Venture expedition Leg 1 on the R/V Thomas Washington. The measurements were finished within hours of retrieving the cores on deck and were processed, plotted and stratigraphic correlations between cores were made during the cruise. Furthermore, by correlating down-core variations in the magnetic susceptibility to known Pleistocene global climatic fluctuations (glacial-interglacial), estimates of the absolute chronology and sedimentation rates were made. This report is a compilation of the measurements and stratigraphic correlations made during the cruise, supported by shorebased finetuning of the chronology of the cores. The reliability of the susceptibility-chronostratigraphy is unknown, since obtaining an absolute chronology using only correlations between the cheap and fast magnetic susceptibilities and climatic timescales during a coring cruise have very little or no precedence. Therefore, further traditional chronostratigraphy (magnetostratigraphy, biostratigraphy, oxygen isotope stratigraphy, etc.) of discrete samples are warranted to verify the results. At publication time of this report (March 1990), the cores have not been opened; splitting and sampling of the cores is scheduled for May 1990.

Abstract in Icelandic - Ágrip

Segulviðtak var mælt á heilum óopnuðum úthafssetkjörnum, sem teknir voru í borleiðangri um austurhluta Kyrrahafsins á bandaríska hafrannsóknarskipinu Thomas Washington. Mælingum var lokið innan fárra klukkustunda frá því borkjarnarnir komu á þilfar, úrvinnsla, teiknun línurita og tengingar milli kjarna voru gerðar í leiðangrinum. Með því að tengja sveiflur í segulviðtaki setsins við þekktar langtímaveðurfarsbreytingar (ísaldir og hlýskeið) var unnt að aldursákvarða setkjarnana og áætla sethraða. Skýrsla þessi lýsir mælingum, tengingum og aldursákvörðunum á setkjörnunum í leiðangrinum sem og nánari útfærslum í landi. Áreiðanleiki aldursákvörðunar með þessum hraðvirku og ódýru segulviðtaksmælingum er óviss, þar sem lítil sem engin reynsla er af aðferðinni. Því er nauðsynlegt að taka niðurstöðunum með ákveðinni varúð þar til niðurstöður fást úr frekari aldursákvörðunum á einstökum sýnum úr kjörnunum með hefðbundnum aðferðum (fornsegulfræði, steingerfingafræði, mælingum á súrefnissamsætum, o.s.frv.). Á útgáfudegi þessarar skýrslu í mars 1990 er ekki enn búið að opna setkjarnana, en áformað er að kljúfa þá og hefja sýnatöku í maí 1990.

Acknowledgments

I would like to thank my major advisor Shaul Levi for continued support throughout this work, also Carl Kocher teacher who requested a student project in Fall term 1987, Dennis Schultz for lab assistance and for his idea to interface the susceptibility meter with the Macintosh. Bob Karlin made good suggestions during trials of the Core-Scanner system at the OSU corelab, and discussions with John Nábelek and Gary Egbert on deconvolution are appreciated.

Special thanks go to Nick Pisias chief scientist of the Venture cruise who also helped me with the inverse correlations. I would also like to thank the scientists on board: Steve Clemens, Steve Hovan (I hope my photographic expertise was appreciated), Pete Kalk, Mitch Lyle, Larry Mayer, Alan Mix, Stacey Moore, Dave Mosher, Dave Murray, Carolyn Peterson, Dave Rea, Bill Rugh, the crew and Tom Desjardins Master of the R/V Thomas Washington.

Introduction

All materials have a certain magnetic susceptibility, although most natural substances have relatively low susceptibilities. Obviously, downcore variations in magnetic susceptibility reflect some compositional changes. However, many unrelated factors can cause such changes in the susceptibility. Increased water content and carbonate content will decrease the susceptibility since water and carbonate have very low susceptibilities (actually slightly negative). On the other hand the major contributors to the susceptibility are clays, volcanogenic material and in particular remanence domain wall movements of magnetic material such as magnetite.

Background

In the early 1970's paleomagnetic and paleoclimatic studies of deep-sea sediment cores showed a striking correlation between the intensity of remanent magnetization and paleoclimatic indices [e.g., *Wollin et al.*, 1971]. Since the intensity of remanence is proportional to the ancient magnetic field strength (keeping other factors constant) it was suggested that there might be a link between the strength of the geomagnetic field and climate. *Amerigian* [1974] pointed out that climate would affect the sediment composition and that the variation in the intensity of remanence could be explained by climatic control over the concentration of magnetic grains in the sediment. In a very good article, *Kent* [1982] showed examples of deep-sea sediment cores where the climate affects the calcium carbonate content which dilutes the amount of magnetic material as indicated by the sediments magnetic susceptibility (correlation coefficient between susceptibility and carbonate content was $r = -0.93$), and the concentration of magnetic material in turn controls the intensity of remanent magnetization. Recently some workers have correlated glacial- interglacial fluctuations to concentration dependent magnetic properties (including susceptibility) in cores from the central Atlantic Ocean [*Robinson*, 1986], eastern equatorial Atlantic Ocean [*Bloemendal et al.*, 1988], and Gulf of Mexico [*King*, 1986]. *Robinson* [1986] points out the possibility to use whole-core measurements of magnetic susceptibility on board ship during a coring cruise to reveal the paleoclimatic record and therefore dating the sediment in a fast manner. This report represents such an attempt to reveal a paleoclimatic signal through whole-core measurements of magnetic susceptibility during a coring cruise.

Systems for measuring whole-core susceptibilities have been available for some time, for instance *Radhakrishnamurty et al.* [1968] designed such a system and it was used to measure many Pacific Ocean sediment cores [*Somayajulu et al.*, 1975]. Another similar system was designed by *Molyneux and Thompson* [1973]. However, the usefulness of the susceptibility measurements was not at all obvious from these studies. In the 1980's convenient portable

magnetic susceptibility meters became available for a relatively low price.

Units and Magnitudes

Unfortunately, there has not been harmony among magnetists when it comes to unit systems. Units for magnetic susceptibility are a good example of this, for magnetic susceptibilities have been published in the following units: unitless SI, unitless cgs (due to inconsistencies in rationalization between definitions in SI units and the cgs system the "unitless" quantity depends on unit system: SI values are higher by a factor of 4π than cgs), other units: $m^3\ kg^{-1}$, $H\ m^{-1}$, $H\ m^2\ kg^{-1}$, $G\ Oe^{-1}$, $G\ Oe^{-1}\ cm^3\ g^{-1}$, $cm^3\ g^{-1}$, emu, emu g^{-1}, emu cm^{-3}, emu $Oe^{-1}\ g^{-1}$, to name a few (H=henry, G=gauss, Oe=Oersted). The saying "the nice thing about standards is that there are so many of them to choose from" fits this field very well.

Currently two types of susceptibilities are generally accepted in the SI system: mass susceptibility χ ($m^3\ kg^{-1}$) and volume susceptibility κ (unitless SI). The volume and mass susceptibilities are related through the density ρ ($kg\ m^{-3}$) by

$$\chi = \kappa / \rho$$

Volume susceptibility is used for whole-core measurements, and generally when the measured sample has poorly defined boundaries. Mass susceptibility is preferred for discrete dry samples when one wants to account for different compactness between samples.

Magnetic volume susceptibility κ is defined by

$$\kappa = M / H$$

where M is the induced magnetization per unit volume and H is the inducing magnetic field strength. Both M and H have units of $A\ m^{-1}$; hence volume susceptibility is unitless.

The whole-core volume susceptibilities of this study range between -4×10^{-6} (unitless SI) and 867×10^{-6} (unitless SI). Table 1 shows a collection of volume susceptibilities of various materials [from: *Collinson*, 1983; *Chikazumi*, 1964; *Dankers*, 1978; *Thompson and Oldfield*, 1986] (units have been transformed). Some of the numbers are only rough estimates, for instance igneous rocks are plus or minus an order of magnitude, and the magnetite number is an extrapolation of the susceptibility of dispersed non-interacting grains and is also grain size dependent. Note that water and calcium carbonate have very low susceptibilities and that the clay content of a sediment can contribute slightly to its susceptibility. However, it is thought that magnetite contributes a major part of the observed susceptibility of marine sediments.

TABLE 1. Volume susceptibilities of selected materials

Material	Volume Susceptibility (10^{-6} unitless SI)
Air	0·4
Water	–9
Plastic	–5
Calcium carbonate	–10
Quartz	–16
Smectite	350
Illite	400
Igneous rocks	10,000
Magnetite (5 μm)	2,000,000
Supermalloy	100,000,000,000
Ideal wet sediment (80% porosity)	
100% $CaCO_3$	–9
90% $CaCO_3$ + 10% clay	0
100% clay	75
99% $CaCO_3$ + 1% Magnetite	2000
Marine sediments	1–1000

Some numbers are rough estimates (see text).

This Report

This report shows results of whole-core susceptibility measurements during a coring cruise of the R/V Thomas Washington on the eastern equatorial Pacific Ocean. The cruise was named "Venture Expedition, Leg 1", or "VNTR01". The ship left San Diego, California on August 28, 1989 and returned to Manzanillo, Mexico on October 2, 1989. Figures 1 and 2 are location maps. Eighteen piston cores (7.42–14.33 m long) and 16 gravity cores (0.40–2.96 m long) were taken from the area between 5°S–14°N and 89°W–111°W. The sub-bottom depths to the top of individual sections is shown in Table 2, and the section boundaries and the core lengths are summarized in Figure 3.

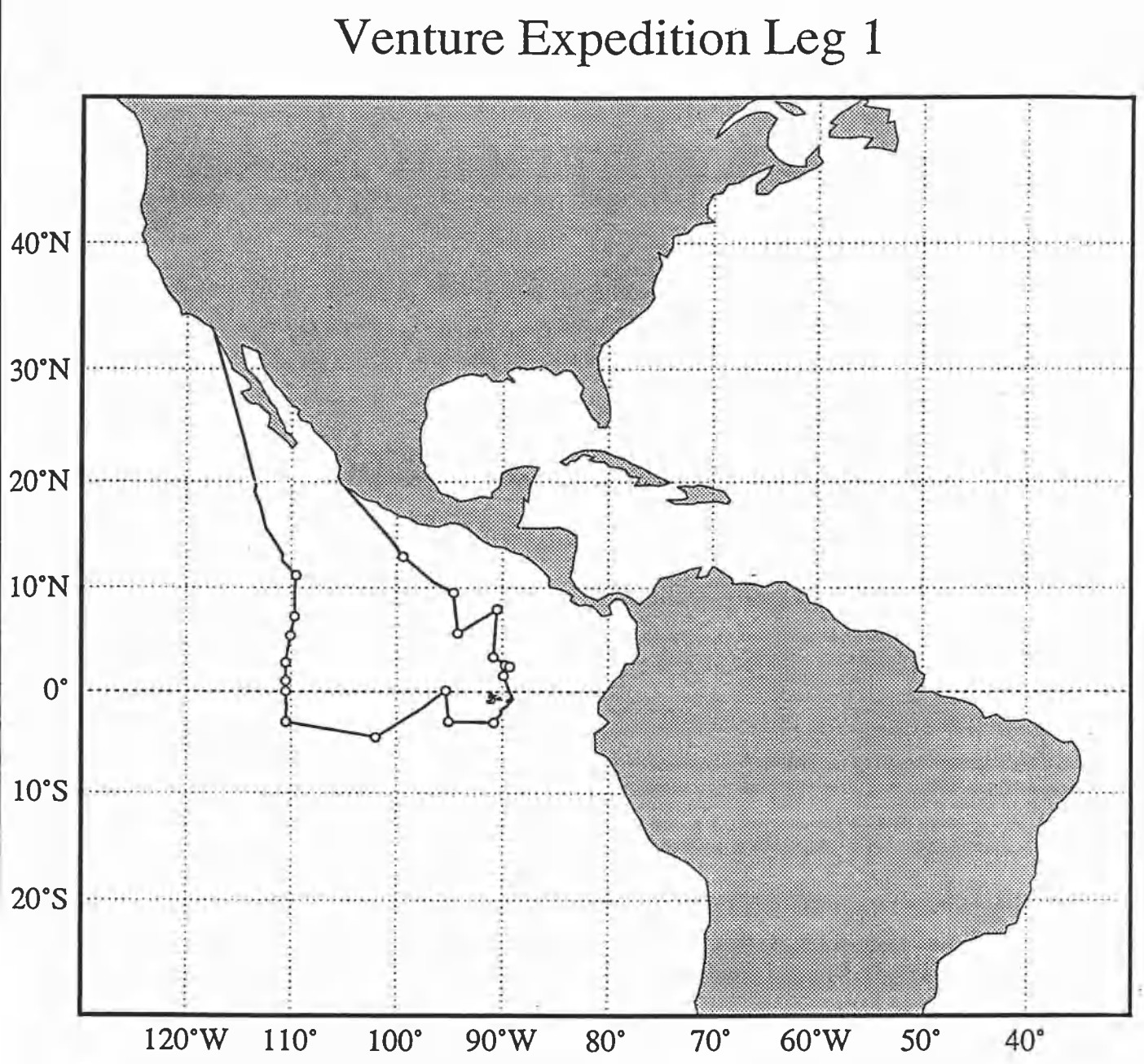

Figure 1. Location map.

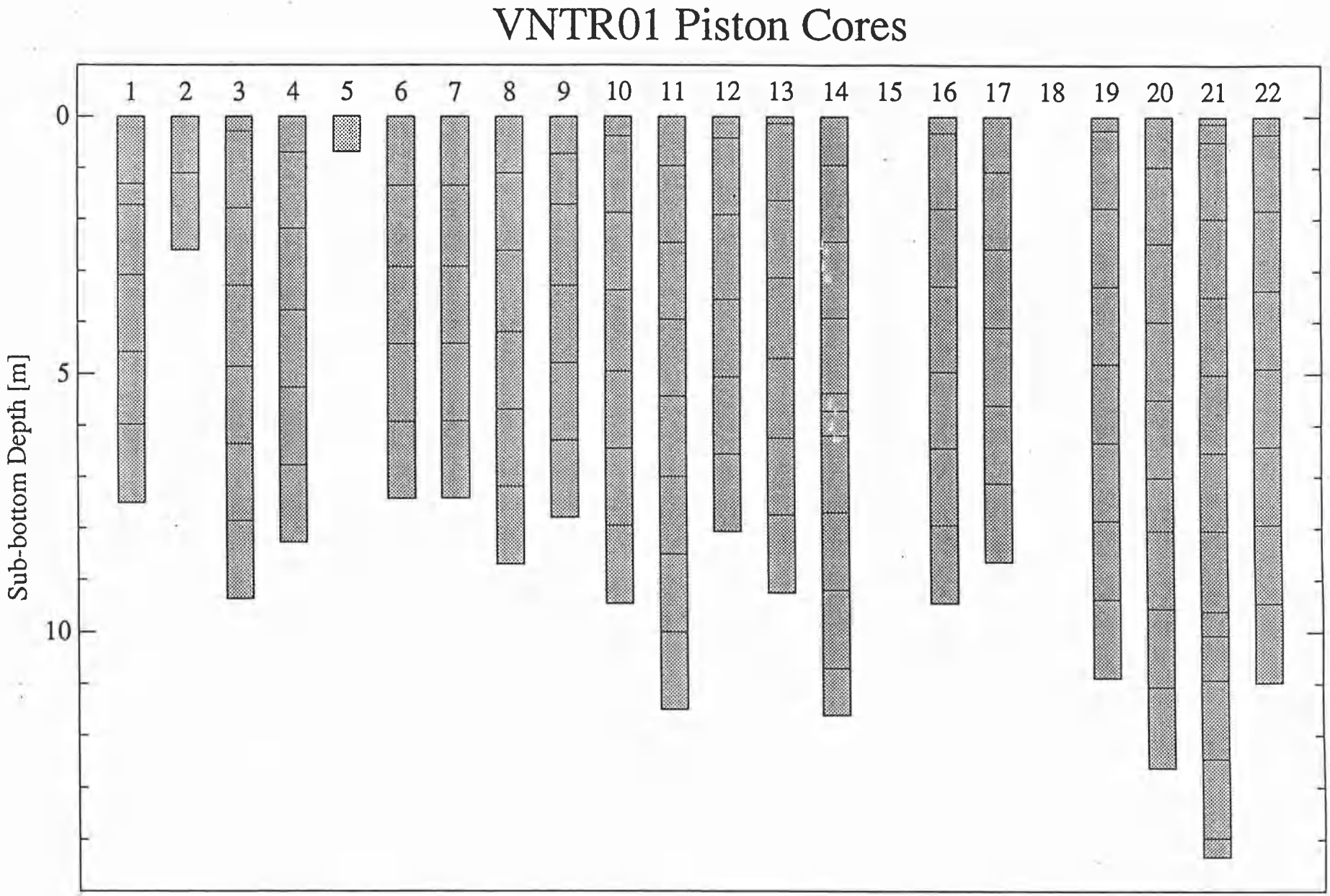

Figure 3. Summary of core lengths and section boundaries (see also Table 2).

TABLE 3. Coring and measurement times (GMT)

	Coring Times				Susceptibility Measurements		
Core	Launch Date	Corer Launch	On Bottom	Core On Deck	Begin	End	Figure Ready
01PC	3-Sep-1989	10:07	11:52	13:10	13:50	14:41	
03PC	5-Sep-1989	07:35	09:21	11:04	11:30	13:04	
04PC	6-Sep-1989	13:47	16:42	18:50	19:25	20:14	21:30
06PC	8-Sep-1989	01:40	03:21	05:13	05:55	07:58	
07PC	8-Sep-1989	21:24	23:14	00:50	02:00	03:16	05:36
08PC	9-Sep-1989	14:00	15:39	17:32	18:00	19:47	20:47
09PC	10-Sep-1989	18:54	20:49	22:30	23:04	02:06	05:07
10PC	13-Sep-1989	13:03	14:40	16:30	16:50	19:23	
11PC	16-Sep-1989	23:06	00:33	02:47	03:19	06:25	
12PC	18-Sep-1989	10:51	12:53	14:57	16:20	19:41	
13PC	20-Sep-1989	04:05	06:02	08:22	08:53	11:26	
14PC	22-Sep-1989	00:23	01:29	02:42	03:21	07:21	
16PC	22-Sep-1989	16:16	17:08	18:22	19:00	21:47	
17PC	23-Sep-1989	04:11	05:12	06:27	06:57	09:18	
19PC	25-Sep-1989	11:45	13:36	15:35	15:58	17:07	19:13
20PC	27-Sep-1989	09:11	11:05	13:04	13:58	15:30	
21PC	29-Sep-1989	01:23	03:21	05:09	05:43	10:24	
22PC	30-Sep-1989				19:06	22:59	

Blanks in the table represents times not recorded.

The susceptibility of the gravity cores (102 mm inner diameter and 114 mm outer diameter of liner) was not measured since our sensor loop had only 100 mm inner diameter. On the other hand the susceptibility of the piston cores (81 mm inner diameter and 86 mm outer diameter of liner) was measured within hours of retrieving them on deck. Individual unopened sections (usually about 150 cm long) were put through the sensor loop and the magnetic susceptibility measured every 2 cm. A total of 8063 susceptibility determinations of the piston cores are in this report.

One of the major advantage of the susceptibility measurements is how fast they are. Table 3 and Figure 4 compare the coring times and susceptibility measurement times. The time from launching corer into water, taking core on bottom, and retrieving the core on deck was on average 3 hours and 29 minutes (ranging from 2:06 to 5:03). The susceptibility measurements were started on average 39 minutes after the core was on deck (ranging from 0:20 to 1:23), and

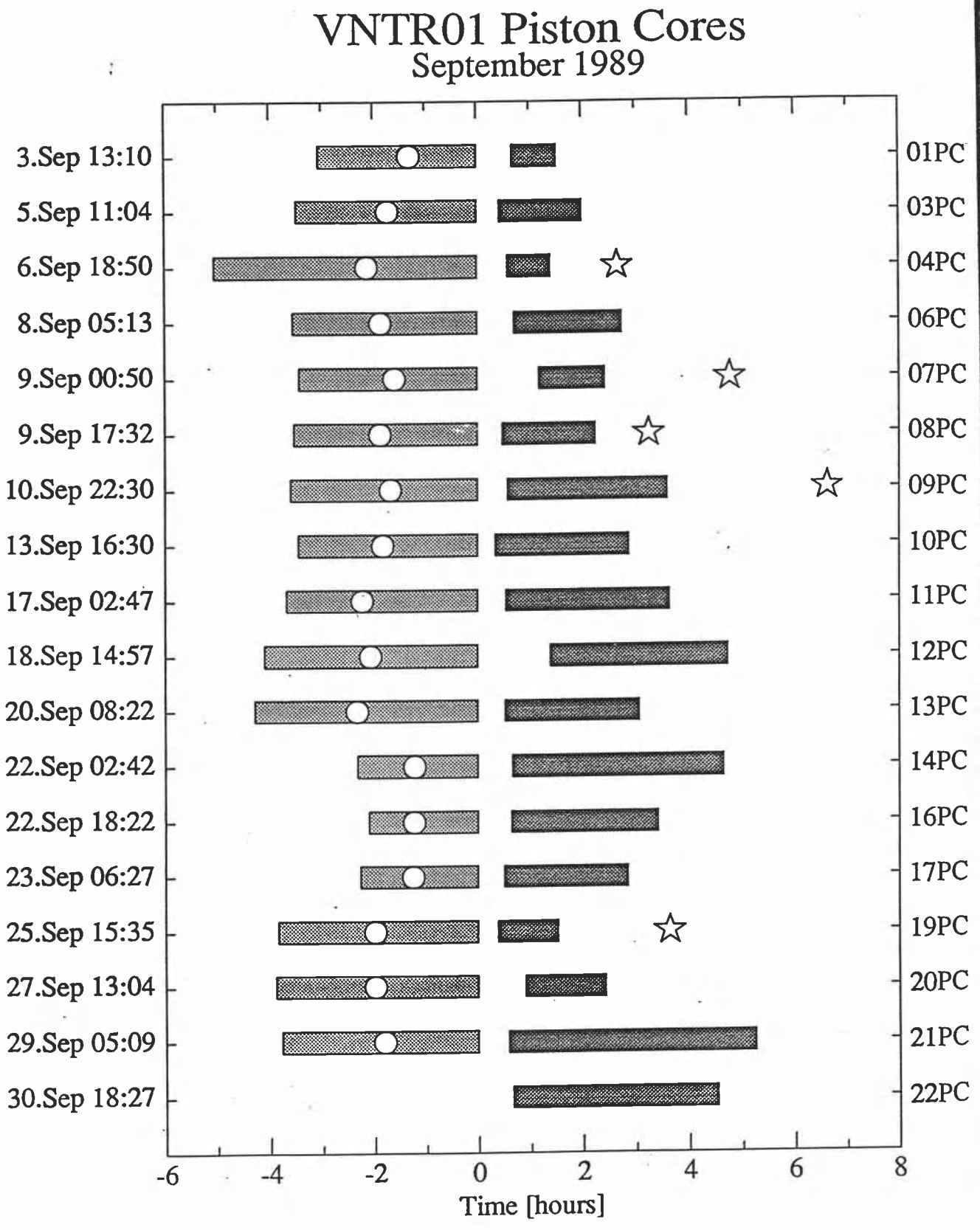

Figure 4. Coring and measurement times (see also Table 3).

were finished on average in 2 hours and 24 minutes (ranging from 0:49 to 4:41). The data were then processed and plotted on a dot matrix printer. This way we usually had graphs of the downcore variation of the susceptibility a few hours after the coring.

Figure 5 shows a good example of a correlation between the measured susceptibility in piston core 06PC (Figure 5a) and the oxygen isotope timescale of *Imbrie et al.* [1984] (Figure 5c), representing global climate. The inverse correlation method of *Martinson et al.* [1982] was used to define a smooth mapping function between the depths in 06PC and time, resulting in the age scale for 06PC shown in Figure 5b. The smooth depth-time mapping function (degree N=10) shown in Figure 6 results in a correlation of r = –0.84 between the susceptibility signal in Figure 5b and the oxygen isotope timescale in Figure 5c.

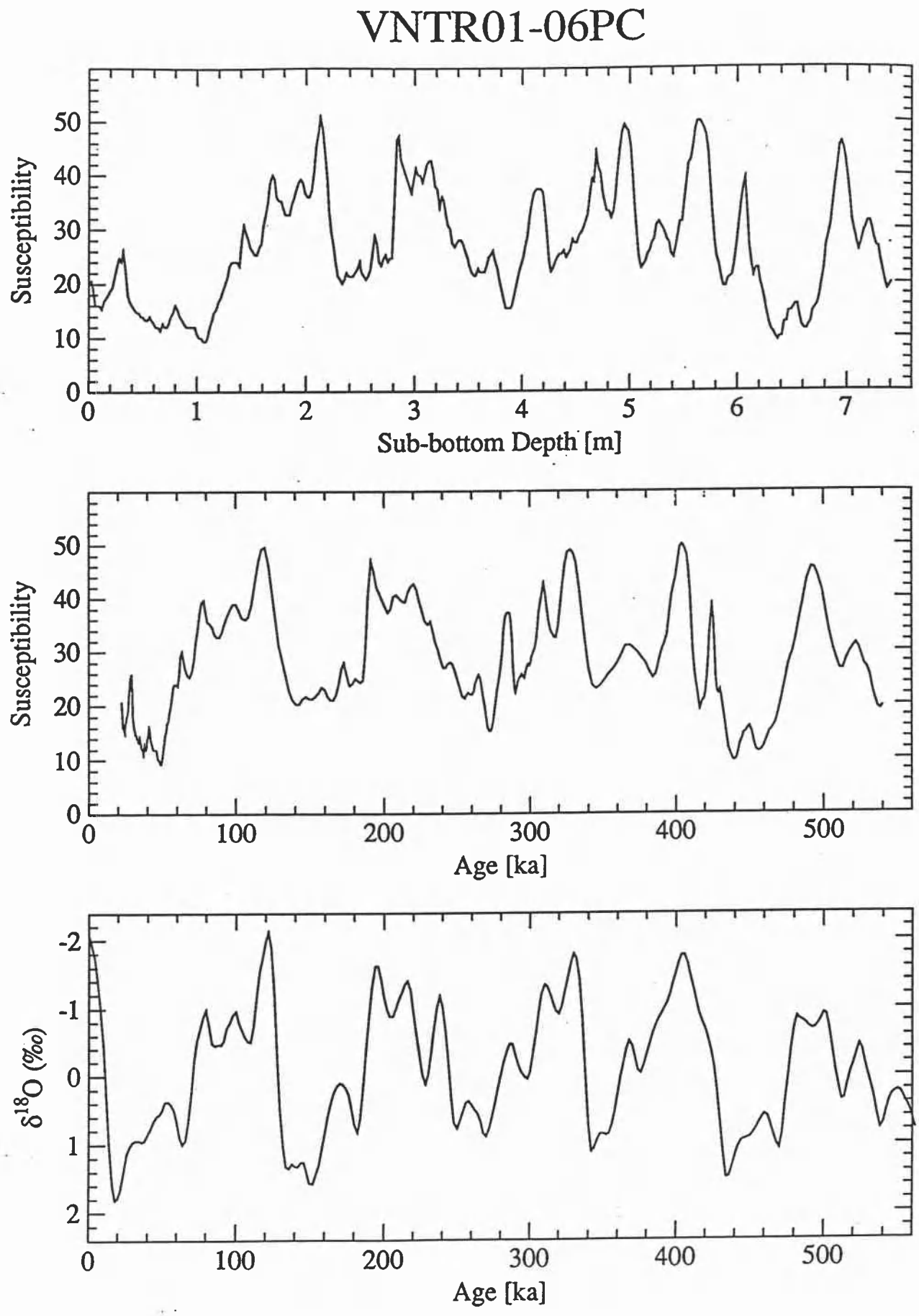

Figure 5. Correlation of the susceptibility in core 06PC to the oxygen isotope timescale.

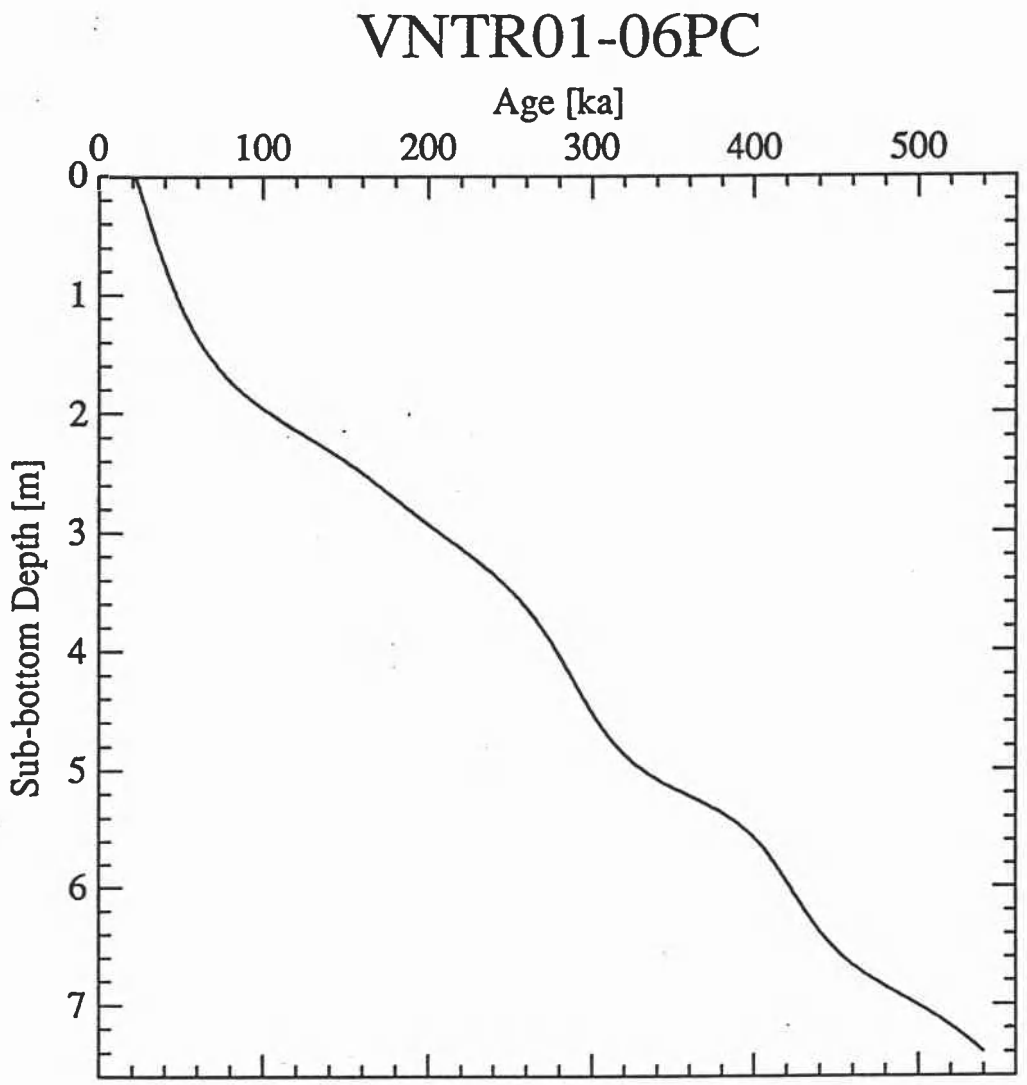

Figure 6. Depth-age mapping function for the correlation in Figure 5. The mapping function was obtained by maximizing the correlation between the susceptibility and the oxygen isotope timescale (see Figure 5c) by the method of *Martinson et al.* [1982] using degree N=10. This mapping function transforms the depth scale to age (i.e. Figure 5a to 5b) resulting in correlation of r = 0.84 between the signals in Figure 5b and 5c.

The Core-Scanner System

As a student project in the course *PH 461 - Computer Interfacing and Instrumentation* in Fall term 1987 I interfaced a Bartington magnetic susceptibility meter with a Macintosh computer, and wrote the program Core-Scanner to control measurements, recording and primary analysis of the data [*Arason*, 1987]. The system was tested in the Oregon State University corelab in 1988 resulting in slight modifications [*Arason*, 1988].

The Bartington Magnetic Susceptibility Meter

In 1987 the paleomagnetics laboratory in the College of Oceanography at Oregon State University acquired a portable digital magnetic susceptibility meter, model M.S.2. (dimensions: $23.5 \times 22 \times 7$ cm), produced by Bartington Instruments Ltd., Oxford, England. The meter comes with a digital display and a RS-232 serial output interface. The user chooses between two sensitivity scales on the meter (coarse and fast vs. sensitive and slow). On the coarse scale (1.0) a measurement takes about 1 s and 10 s on the more sensitive scale (0.1). For the particular combination of sensor and cores of this study, the meter can measure volume magnetic susceptibilities in the range 10^{-6} to 10^{-1} (unitless SI). Core scanning sensors are available for the meter, model M.S.2.C. A borecore is put through the sensor-loop and the susceptibility at a given depth horizon measured. The sensor operates on a 565 Hz, 0.1 mT (r.m.s.) alternating field. The low alternating field should not affect the magnetic remanence of the sediment (typically 10–50 mT alternating field is used for remanence demagnetization).

Connections between Meter and Computer

The serial port on the meter has three active plugs, marked A, B, and C. The manual with the meter shows that A is ground, B is transmission line, and C is receive line [*Bartington Instruments*, 1987]. The meter comes with a cable, that can be connected to the serial port socket, and a 25 pin D type connector on the other end.

There are two serial ports on the Macintosh, one called printer port and the other modem port. I chose to use the modem port. The socket is circular with a metal shield (the ground). I identified a data transmission line as the rightmost (on the port) in middle row, and a receiver line as the leftmost in middle row (see Figure 7).

I made an adaptor cable from the computer serial port to a 25 pin D type connector, where I connected the grounds of the meter and computer, and transmission line of the computer goes to receive line on the meter, and the receive line of the computer to the transmission line of the

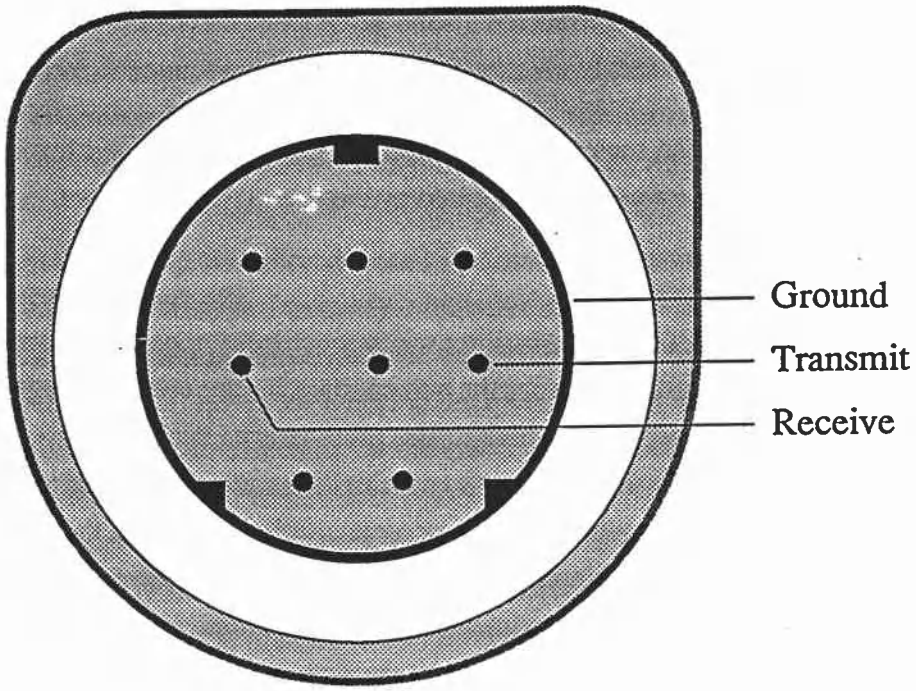

Figure 7. Configuration on the modem port of the computer. The figure shows the position of the ground, transmit and receive conductors.

meter.

From the susceptibility meter manual, I learned that it required 1200 baud, no parity check, 7 bit word length, 2 stop bits, and no handshaking. The meter will take a measurement when receiving an ASCII "M", and zero adjust it self when receiving a "Z". It will repeat the last command until it receives some character other than "M" or "Z". Then it will send the measurement in the order:

1: sign
2: most significant digit
3: second most significant digit
4: second least significant digit
5: least significant digit
6: carriage return

all on an ASCII form. The meter does not send the decimal point and information about the sensitivity scale of the meter has to be supplied by the user to the computer.

The Program Core-Scanner

The program Core-Scanner, controlling the susceptibility measurements, splits the screen into four areas: a graph output area on the screen, data listing area, highlighted measurement area, and a central command menu, which the program returns back to after each operation. The user can view specific sections of the data graphically on the graph area of the screen, he can also view it numerically as a table in the listing area. While measuring, the present measurement is highlighted, so the user can view it from some distance. On the command menu there are eleven operations for the user to choose from: Measure core, View core, Zero meter, Adjust parameters, Display data, Enter comment, reWrite screen, Clear buffers, Read data, Save data, and Quit. Operations are launched by typing the first letter in the command (except reWrite screen "w") : (m, v, z, a, d, e, w, c, r, s, q). A brief description of each operation is appropriate:

Measure core. This operation is used to measure and record a given depth interval of the core in fixed increments. The user is asked to give the depth that he is going to start measuring at, the depth he wants to end measuring at, and the depth increments. Default values are shown, with each question, and will be used if the user presses [*return*] button. The user should be ready with the core at the starting depth, when he answers the three questions, since there is very short waiting time. The computer gives the user sound signals as to when to move the core (one beep). The computer shows "Measuring at xxx cm" (where xxx is the current depth level) highlighted while the meter is taking a reading, which takes 1 or 10 seconds depending on meter sensitivity setting. Meanwhile the user should keep the core still at the right depth level. When

the meter reports the measurement reading to the computer, the computer gives a beep, indicating the user to move to next depth level, reports the new value on the screen, and waits for a while (see *pause* in "Adjust parameters") for the next reading. The data are listed continuously on the screen, in a table and graph. The user can at any time stop the measurements by pressing "i" (interrupt) on the computer keyboard.

View core. This is similar to measuring core, but no special depths are assigned to each reading, and even though the data is shown on the screen, it is not recorded in memory. This operation is mainly for viewing the core, get a feeling for ranges and special features; finding highs and lows. To return to central command menu press "i" (interrupt).

Zero meter. The meter can drift a little bit during measurements, so regularly one wants to zero the drift. The core should be taken at least 10 cm away from the loop while zeroing is conducted. Zeroing is done in two parts; a reading of air susceptibility is taken and recorded, followed by zeroing the meter. At very low susceptibilities one may need to apply a linear drift correction to the data.

Adjust parameters. Nine parameters, used by the program, can be adjusted by this command. Default values are assigned to every parameter, and are shown on the screen with each question. By setting a value, the user defines the default value for the next time he uses "Adjust parameters". Default is chosen by ignoring the question and answering by the [*return*] button. First the user can set the plotting axes on the graph, by defining the starting value on the x-axis, length of the x-axis (in depth units), starting value on the y-axis, and the length of the y-axis (in susceptibility meter units). For "View core", the user defines the time duration of one sweep on the graph. One can also adjust the time pause between individual measurements in "Measure core". The settings of the meter and sensor are recorded with the data into the data file, and the user has to supply information on those settings. The user can change the selected parameters at any time.

Display data. Used to look at data, already measured, in a specific depth range, both graphically and numerically. The user gives starting and ending depth, unless using default values.

Enter comment. The user can record notes, or sediment descriptions, with the measured data. The user gives depth of a feature, and describes it in words. These comments will be saved with the susceptibility data. No defaults are assigned.

Rewrite screen. Used to rewrite screen if wanted, that is replot graph and list recorded measurement values. For instance, after "View core", or "Display data" one might want to replot the recorded values and continue from there on.

Clear buffers. Used to erase data from memory, to get ready for the next core. Note that if this is done by mistake, then the data is not retrievable, therefore the user has to reconfirm

command.

Read data. One can read in old data that has previously been saved. This way one can later use the plotting ability of the program for further analysis, or one can continue measuring the same core.

Save data. Used to save the current data from memory to a disk file. The user will be asked to give a file name. The user can identify the data by writing a data file header and subheading (two lines).

Quit. Closes all open files, and quits running the program Core-Scanner. Returns the user to the desktop. If any data is not yet saved the user has to reconfirm the quit command.

The program Core-Scanner does not give the option of printing data tables or graphs, but the saved data files can be printed with an editor program and plotted by several graph programs.

Data Processing

After measurements and recording by the Core-Scanner system the data were processed in four steps; 1) correction for a linear meter drift over a section, 2) section end corrections, 3) combining all sections in a core and converting section depths to sub-bottom depths, and 4) scaling meter values to volume susceptibilities (unitless SI).

Meter Drifts

The measured susceptibility values drift slowly, and the meter needs to be zeroed after a certain measurement time. The zeroing is done by measuring and recording an air susceptibility and then set that level to a zero. Piston cores 01PC, 03PC, 04PC, 19PC, and 20PC were measured on the less sensitive meter scale (1.0), the drift turned out to be insignificant (partly due to high susceptibilities of these cores) and no correction was applied to the data. In these cores (39 sections including cores 2 and 5) the drift was always in the range –1 to +1 (meter units), see Table 4 and Figure 8a. On the other hand piston cores 06PC, 07PC, 08PC, 09PC, 10PC, 11PC, 12PC, 13PC, 14PC, 16PC, 17PC, 21PC, and 22PC were all measured on the more sensitive meter scale (0.1). For these thirteen cores (94 sections) drifts ranged from –1.9 to 0.9, (see Table 5 and Figure 8b) and drift corrections were nessecary (especially for the low susceptibility cores).

TABLE 4. Meter drifts after measuring sections on 1.0 scale

Drift in meter units	Frequency
–1.	17
0.	19
1.	3
	total 39 sections

TABLE 5. Meter drifts after measuring sections on 0.1 scale

Drift in meter units	Frequency
–1.9	1
–1.8	0
–1.7	1
–1.6	2
–1.5	0
–1.4	1
–1.3	0
–1.2	0
–1.1	0
–1.0	0
–0.9	2
–0.8	2
–0.7	5
–0.6	1
–0.5	4
–0.4	3
–0.3	5
–0.2	7
–0.1	6
0.0	10
0.1	11
0.2	10
0.3	13
0.4	3
0.5	1
0.6	1
0.7	1
0.8	1
0.9	3
	total 94 sections

When the meter was turned on (on the more sensitive scale 0.1) there was an initial period of about 15 minutes of strong drift that decayed exponentially to a much lower and nearly constant drift. An example of this initial drift is shown in Figure 9 (from 30 September 1989, before 22PC). Part of the strong initial drift was probably due to temperature changes inside the meter and/or sensor. Old rechargeable batteries may also have affected the initial drift. Before measuring a core the Core-Scanner system was set up and kept busy for 30 to 60 minutes by

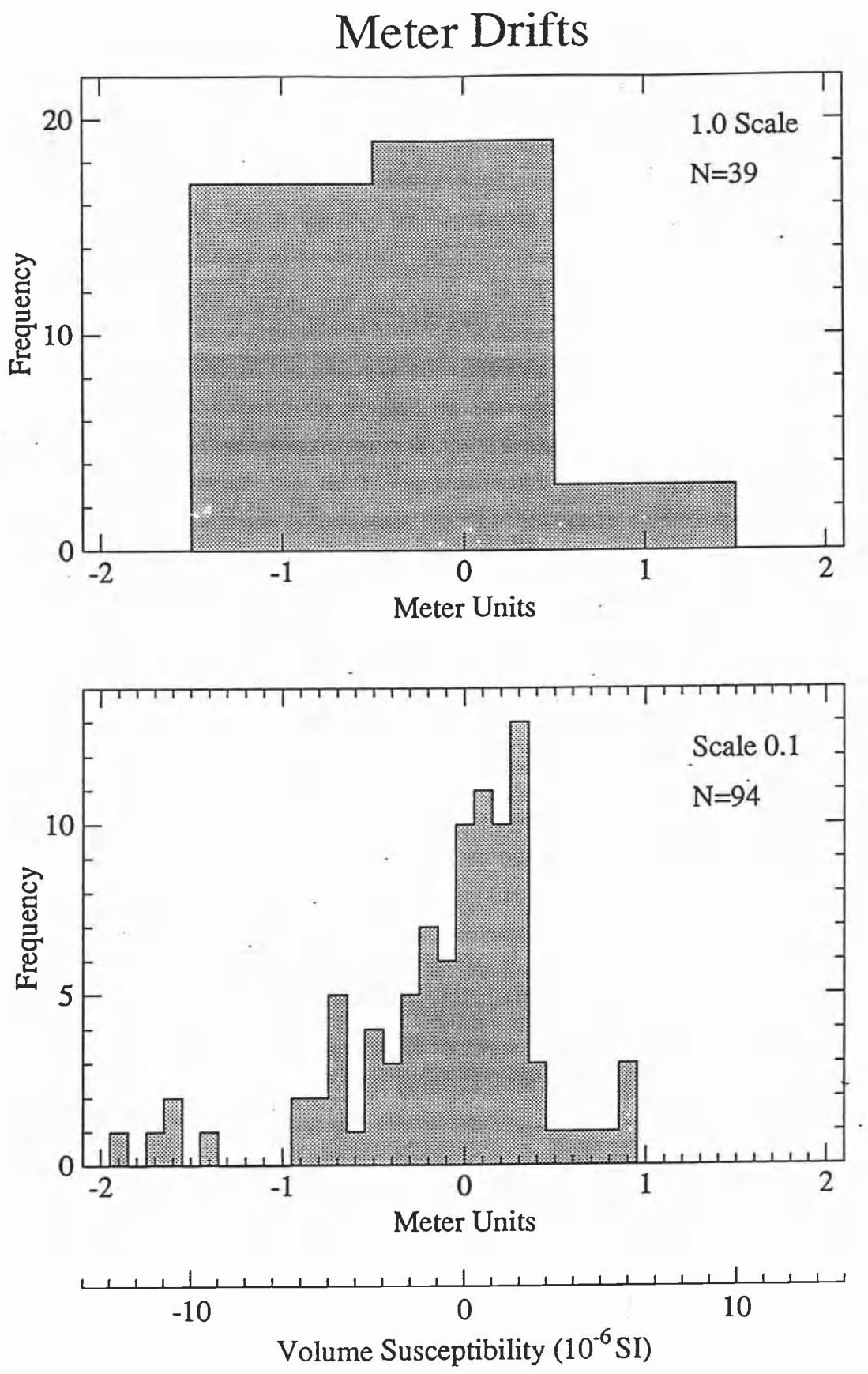

Figure 8. Distribution of observed meter drifts over individual sections.

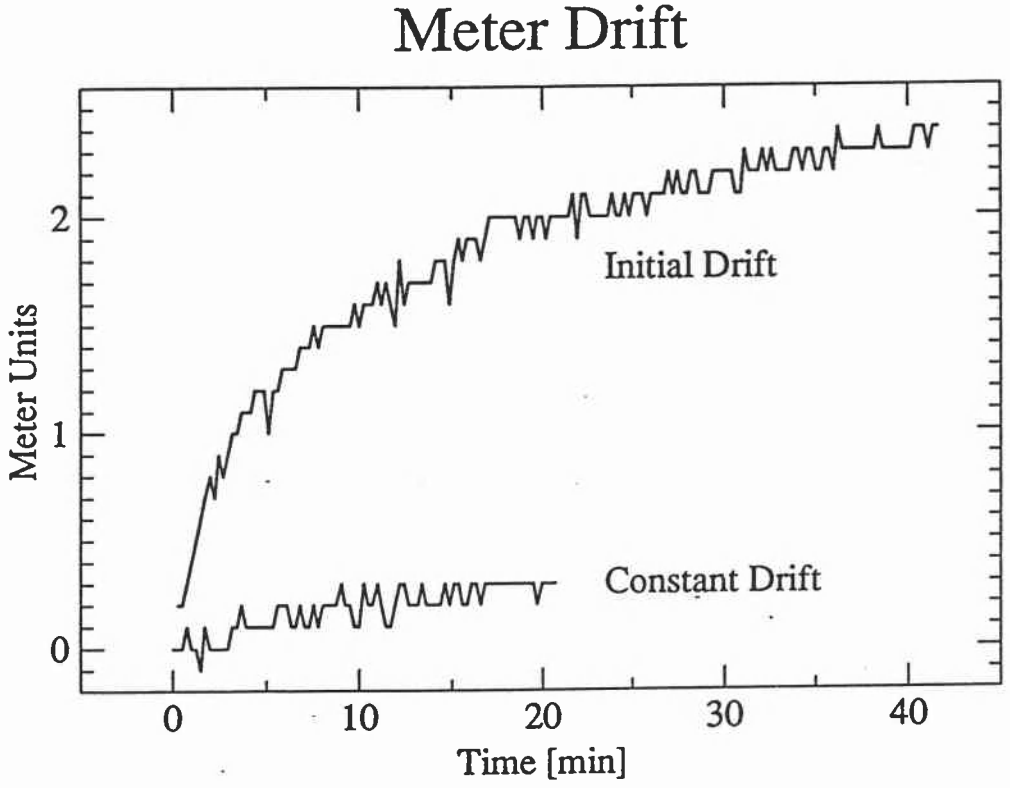

Figure 9. Characteristics of meter drifts. When the meter was turned on it showed significant initial drift. After about 15 minutes the drift became nearly constant allowing for linear drift corrections over sections. The cores were never measured during the initial drift phase.

measuring air susceptibility at the same rate as measurements were planned with the same pause (5 seconds) between measurements. Pause between measuring sections also affected the drift, and that time was either kept at a minimum or by continuous air measurements.

After the initial drift phase, the drift appeared to be close to a constant (see Figure 9). The meter was zeroed before measuring each section (which took about 20 minutes) and an air reading taken after measuring the section. The air reading was used to apply a linear drift correction to the measurements.

Section End Corrections

When measuring section ends, the sensor will see sediment on one side and nothing on the other side, resulting in a fraction of the true value. It is possible to correct these lower values close to the ends by knowing the impulse response of the sensor. The impulse response of the susceptibility sensor (100 mm inner diameter) was measured by a very thin disk (< 1 mm), 81 mm diameter (same as the diameter of the piston cores). By integrating the impulse response function it is possible to estimate the step response of the sensor. The impulse and the step responses are shown in Figure 10 and Table 6. The inverse of the step response is used as an estimate of end correction factors in Table 7. These end corrections are usually reasonable (smooth continuations between sections) but in some instances they produce spikes at the very end. For this reason the end measurements were deleted (at 0 cm and 150 cm).

Scaling Meter Units to Volume Susceptibility

The susceptibility meter does not take into account the sensor diameter or the diameter of the cores. Wider core of the same material gives higher meter values. Furthermore, the same core would give weaker signal if we used a sensor with larger diameter. Therefore, the meter values have to be scaled in order to obtain other than relative values. The meter manual [*Bartington Instruments*, 1987] shows that the meter units (on the SI meter setting) have to be multiplied by 10^{-5} for a certain core/coil diameter ratio to result in SI volume susceptibility. To correct for other core/coil ratios the manual gives a graph [*Bartington Instruments*, 1987, graph 1]. The effective coil diameter of the 100 mm sensor is given in the manual to be 108 mm, and for the ratio (81 mm / 108 mm) = 0.753 the graph shows that the meter gives 1.50 times too high value. Therefore, in order to obtain volume susceptibilities in the SI unit system, the meter units have to be multiplied by $(10^{-5} / 1.50) = 6.667 \times 10^{-6}$.

All the susceptibility measurements of the VNTR01 piston cores have been converted to units of 10^{-6} (unitless SI), by multiplying the meter values by 6.667.

TABLE 6. Impulse and step response of the susceptibility sensor

Distance from sensor (cm)	Measured impulse response	Normalized impulse response	Normalized step response
–16	0	0.0000	0.0000
–15	1	0.0002	0.0001
–14	2	0.0004	0.0004
–13	3	0.0006	0.0009
–12	4	0.0008	0.0016
–11	5	0.0010	0.0026
–10	8	0.0016	0.0039
–9	13	0.0027	0.0061
–8	20	0.0041	0.0095
–7	34	0.0070	0.0150
–6	56	0.0115	0.0243
–5	95	0.0196	0.0399
–4	166	0.0342	0.0668
–3	292	0.0602	0.1140
–2	503	0.1037	0.1959
–1	766	0.1579	0.3267
0	915	0.1886	0.5000
1	766	0.1579	0.6733
2	503	0.1037	0.8041
3	292	0.0602	0.8860
4	166	0.0342	0.9332
5	95	0.0196	0.9601
6	56	0.0115	0.9757
7	34	0.0070	0.9850
8	20	0.0041	0.9905
9	13	0.0027	0.9939
10	8	0.0016	0.9961
11	5	0.0010	0.9974
12	4	0.0008	0.9984
13	3	0.0006	0.9991
14	2	0.0004	0.9996
15	1	0.0002	0.9999
16	0	0.0000.	1.0000

The response curves are only valid for the particular combination of a 100 mm inner diameter sensor and a 81 mm diameter core. The measured impulse response was measured several times and symmetrically averaged. The normalized impulse and step responses are calculated from the measured impulse response.

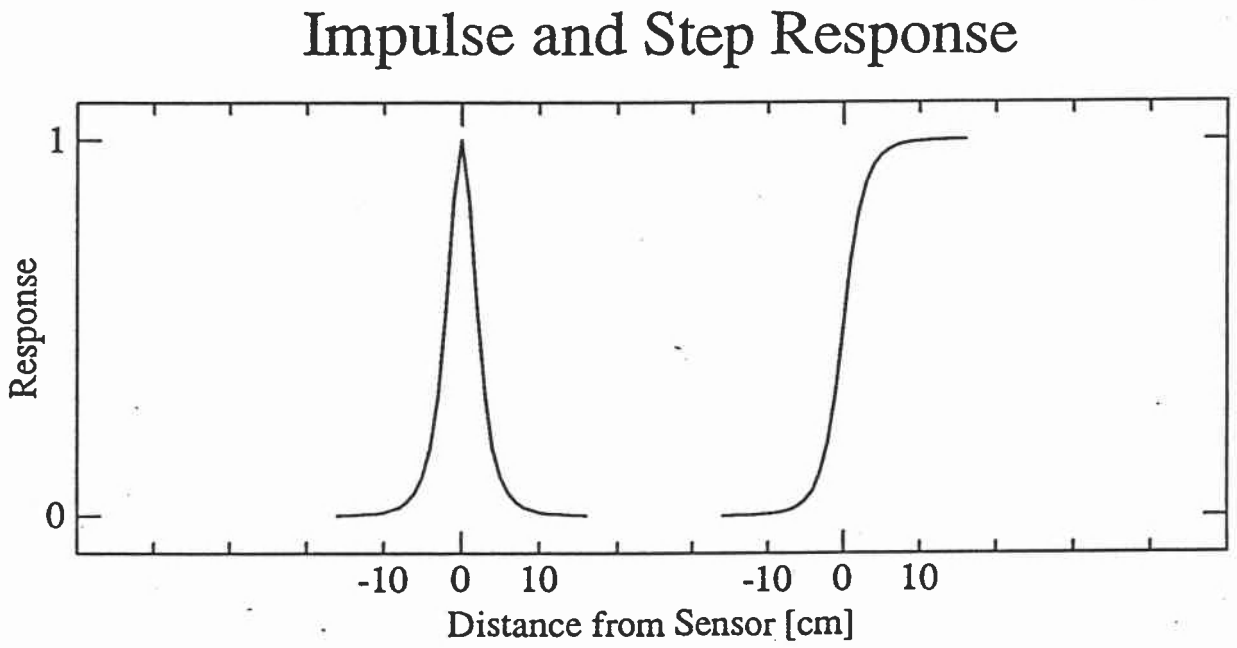

Figure 10. Impulse and step response of the susceptibility sensor. The impulse response was measured for a very thin (< 1 mm) disk with the same diameter as the piston cores (81 mm). The step response was then calculated by convolution of the impulse response with a step function. The impulse and step response are used to make section end corrections and synthetic calculations.

TABLE 7. Section end correction factors

Distance from end (cm)	Correction factor
0	2.000
1	1.485
2	1.244
3	1.129
4	1.072
5	1.042

Accuracy

On the less sensitive meter scale (1.0) the accuracy in each measurement is mainly defined by the steps in meter units ±1, and the error due to drift is comparable in magnitude. The errors in the measurements (both relative and absolute) are therefore close to $\pm 10 \times 10^{-6}$ SI.

The errors on the more sensitive meter scale (0.1) are mainly due to inadequate correction of the slow drift. Table 8 and Figure 11 show results of an experiment in determining typical errors in the linear drift correction. Air was measured for as long as a typical section, then the linear drift correction was applied to the three measurement sequences (each with 86 data points). The residual represents an error in the linear drift assumption. The errors in the absolute values are estimated to be ±2 to 3×10^{-6} SI. However, the shape of individual short features in the cores are probably accurate in a relative sense to about $\pm 1 \times 10^{-6}$ SI.

TABLE 8. Estimates of errors after linear drift corrections

Error in meter units	Susceptibility 10^{-6} SI	Frequency
–0.2	–1.3	6
–0.1	–0.7	38
0.0	0.0	96
0.1	0.7	69
0.2	1.3	37
0.3	2.0	12
	total	3×86

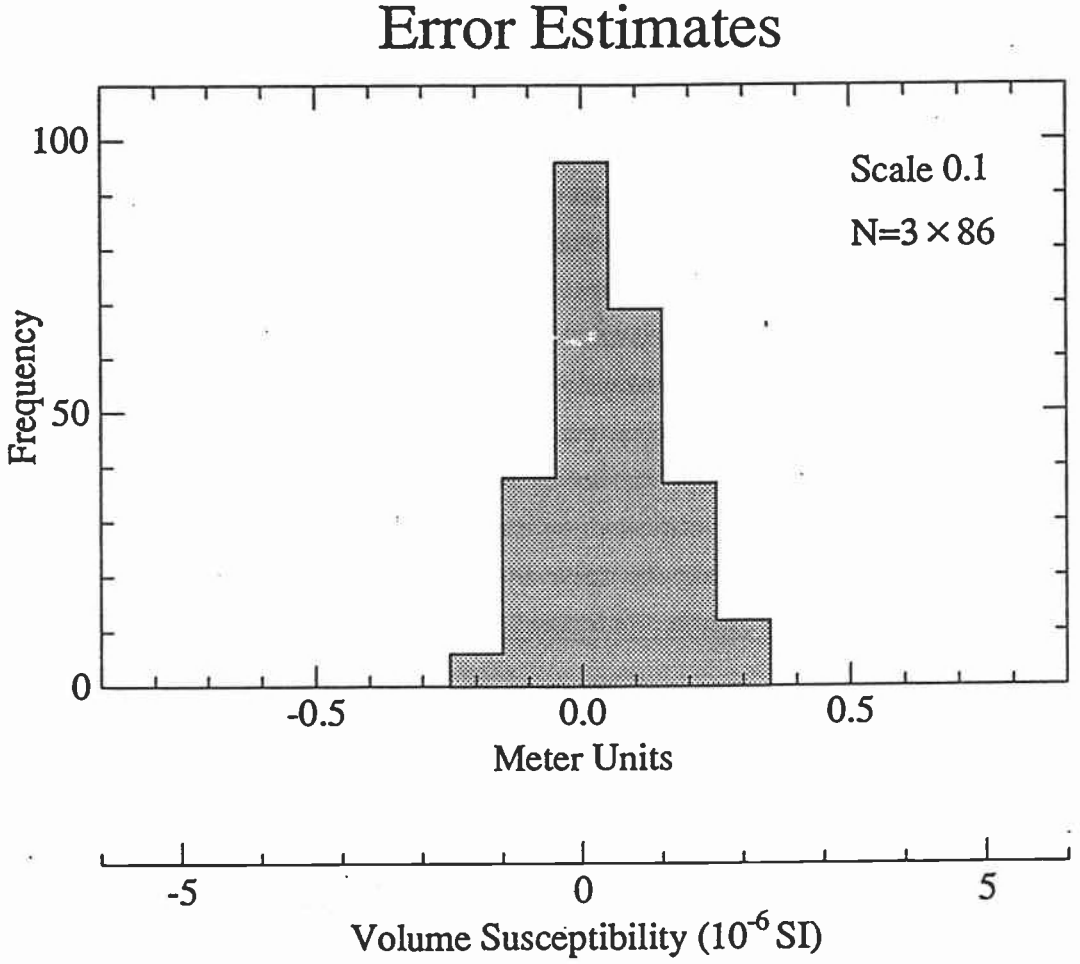

Figure 11. Error estimates of the linear drift corrections. Three empty sections were measured and corrected for linear drift. The errors in the susceptibility are estimated to be about $\pm 2 \times 10^{-6}$ (unitless SI).

Pulse Smoothing

Since the impulse response of the sensor is a bell shaped curve (see Figure 10), sharp individual features will be slightly smoothed. Figures 12 and 13 show the calculated response for sharp thin layers. First, as the layer gets thinner the height of the observed pulse decreases relative to the true value (see Figure 12). Second, the thickness of the observed pulse, as measured by the thickness at half the maximum height, overestimates the true layer thickness, especially when the layer is less than 5 cm thick (see Figure 13). Figure 13 also shows that a very thin layer (< 1 mm) would appear to be about 4 cm thick. Since the measurements were taken at 2 cm intervals a spike defined by one point (thickness 2 cm) is noise, defined by 2 points (thickness 4 cm) might be a very thin and strong layer or a metallic contamination such as rust flakes [e.g., *Sager*, 1986]. Figure 13 also suggests that we can not get much more information by measuring the cores every 1 cm.

It is possible to decrease the smoothing by deconvolving the impulse response with the measurements. Deconvolution was tried on the signals during the cruise but did not result in more pleasing curves. The reason seems to be twofold: First, there are very few sharp boundaries in the cores so deconvolution does not change the appearance of the signals. Second, the deconvolution does magnify noise in the measurements. Deconvolution was therefore terminated and is not shown in this report.

Synthetic Pulse Smoothing

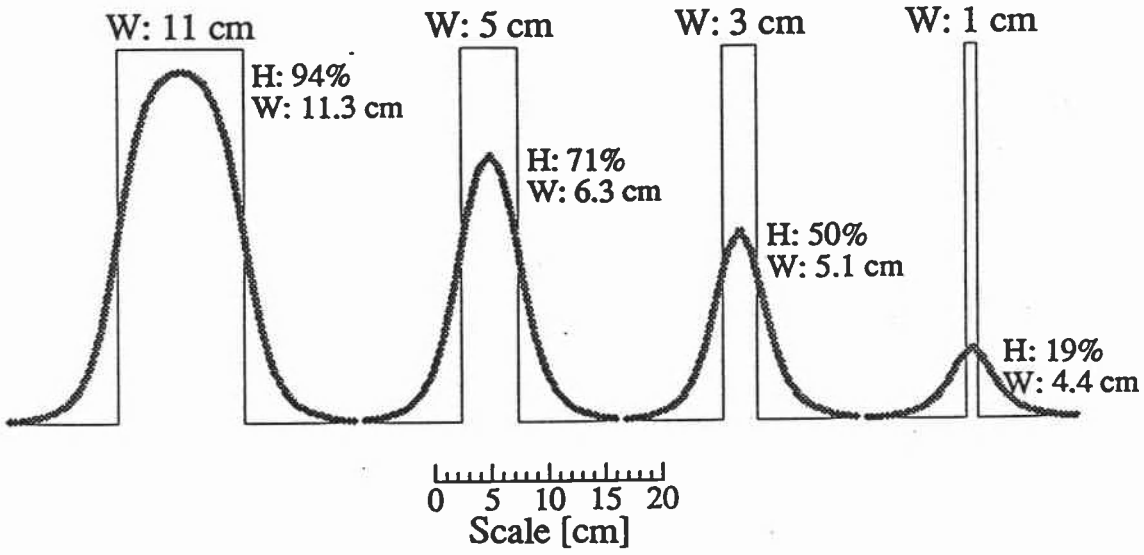

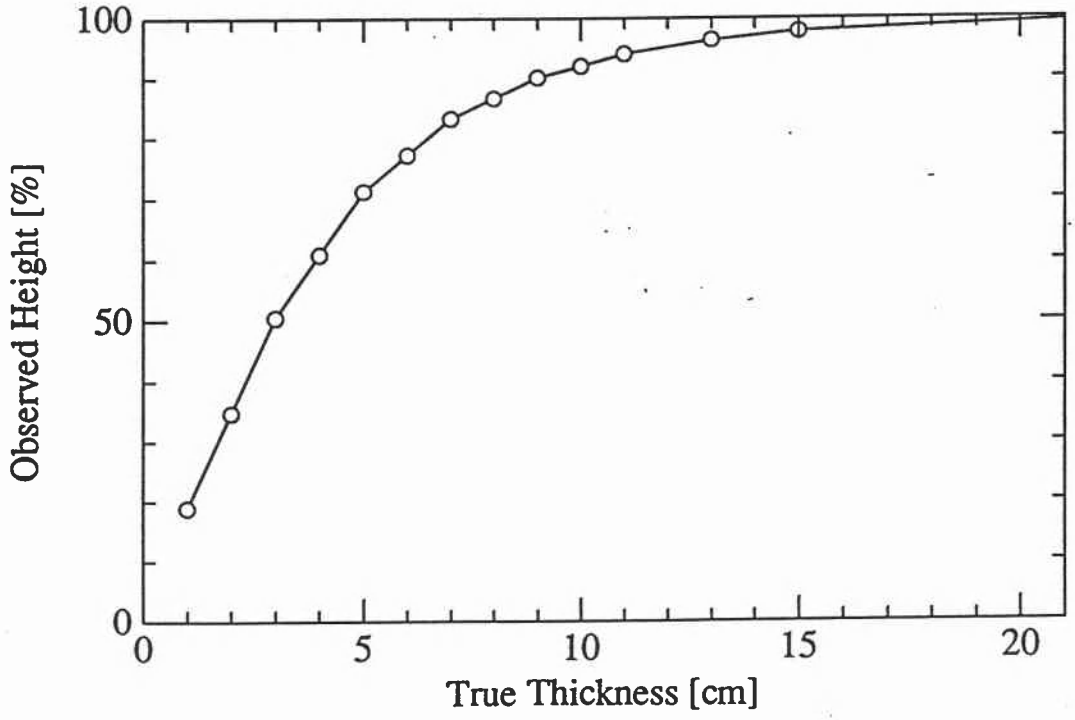

Figure 12. Effects of sensor smoothing on pulse height.

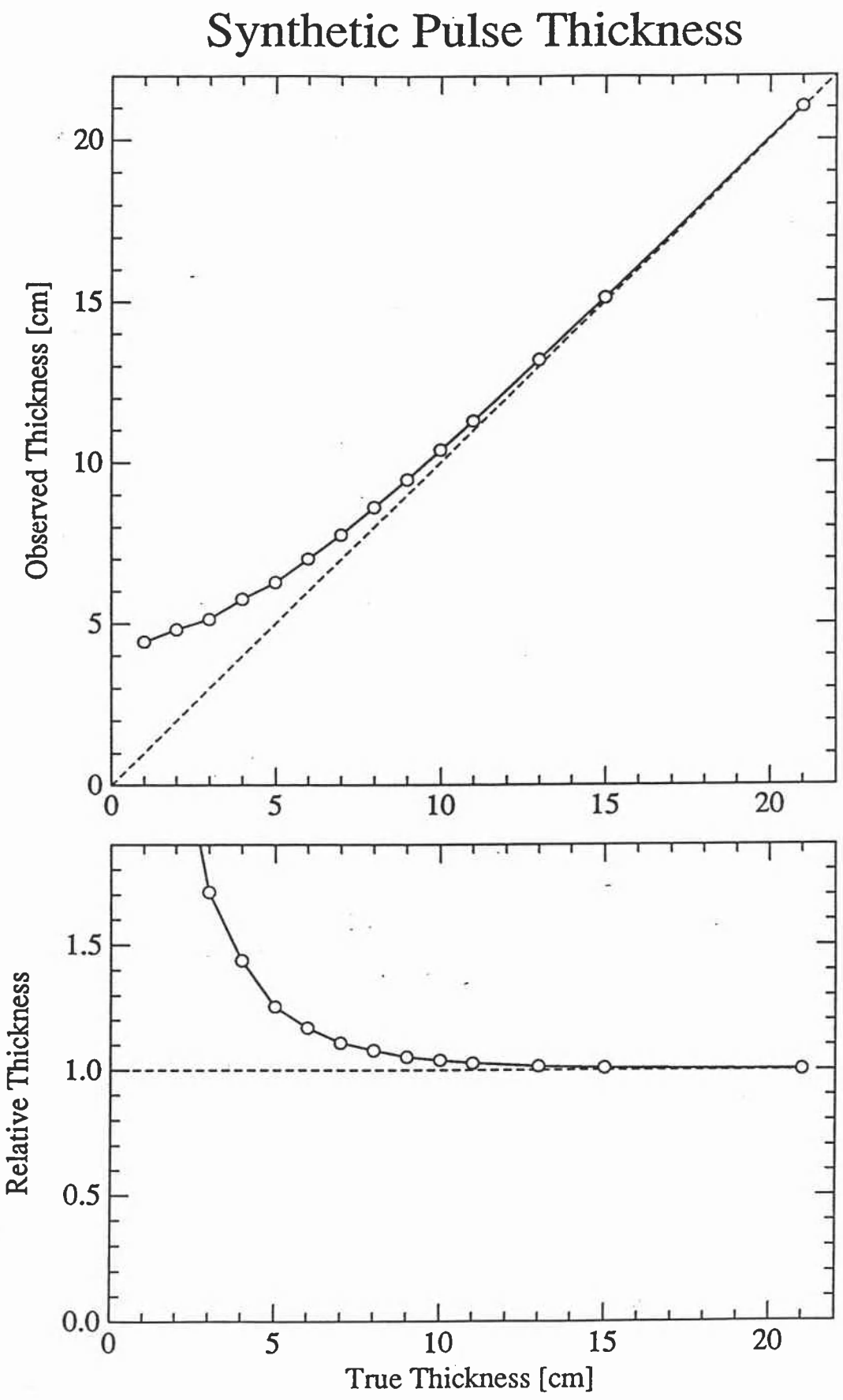

Figure 13. Effects of sensor smoothing on pulse thickness.

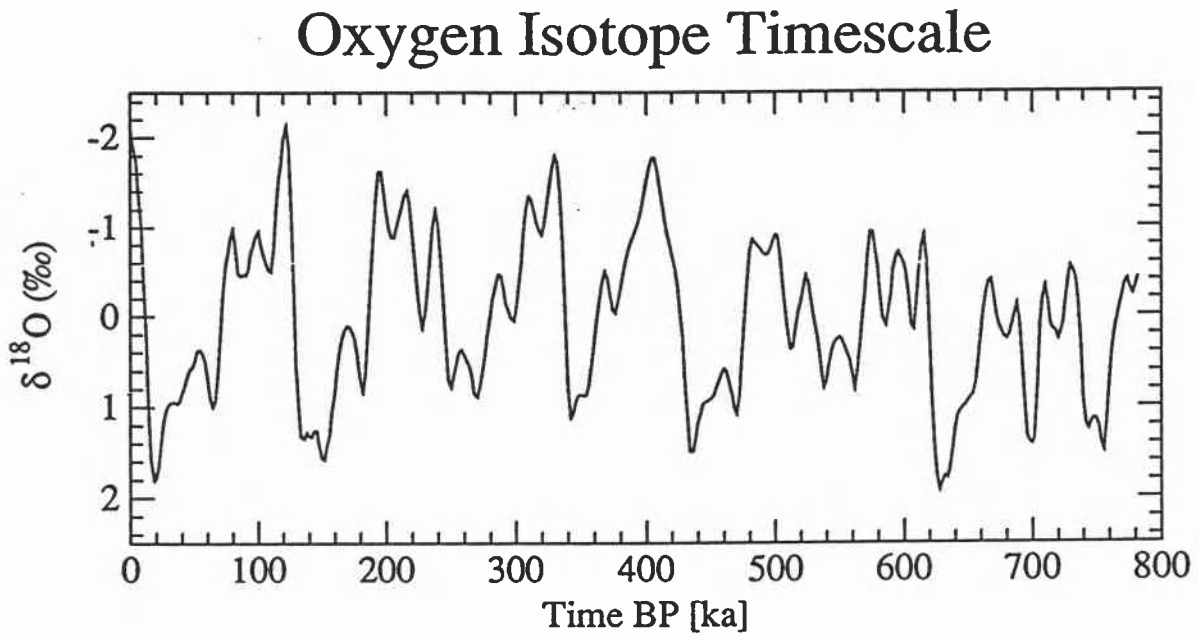

Figure 14. The oxygen isotope timescale of *Imbrie et al.* [1984]. The oxygen isotope composition is related to global ice volume. Lows on the graph (positive $\delta^{18}O$ values) reflect glacial times and highs (negative $\delta^{18}O$ values) are interglacial periods.

Susceptibilities of the VNTR01 Piston Cores

Following are chapters for all the piston cores. Each chapter has a description of the core and the susceptibility data. The downcore variation in the susceptibility signal is shown on a graph where section boundaries are shown as dotted lines (liner joints are shown as heavy dotted lines). Detailed graphs show the data points by sections. Chronological correlations are summarized in tables. The ages and event names of the oxygen isotope timescale are adopted from *Martinson et al.* [1987] for 0 to 300 ka, and from *Imbrie et al.* [1984] for 300 ka to 800 ka. The oxygen isotope timescale of *Imbrie et al.* [1984] is shown in Figure 14. Slightly different (but not significantly) age estimates were used during the cruise (shown in the tables).

VNTR01-01PC

Piston core 01 was taken on 3-Sep-1989 (11.254°N, 109.614°W, 3536 m water depth). The core is 7.51 m long, consisting of calcareous pelagic ooze. After the data selection we use 371 susceptibility determinations (range: 120.0 to 866.7, arithmetic mean: 212.8 (all 10^{-6} unitless SI)). The downcore susceptibility is shown in Figures 15 and 16, and Figure 17 shows details of individual measurements by sections.

Data selection. The measurements seem to be smooth across all the section boundaries and no data were deleted.

Chronology. Table 9 shows age-depth correlations, and the sedimentation rate is estimated to be about 1.3 cm/ky. There is a consistent sedimentation rate by correlating a major spike in the susceptibility to ash layer "K".

TABLE 9. Age-depth estimates from susceptibility correlations of 01PC

Piston Core	Event Name	Event Age (ka)	Position of Event Section (S-cm)	Position of Event Depth (m)	Sedimentation Rate (from top) (cm/ky)	Core Length (m)	Bottom Age (ka)
			Estimates Made During the Cruise:				
01	6.0	128		1.69	1.3		
			Estimates of this Report:				
01	6.0	130	5-38	1.69	1.30		
01	Ash K	330	3-112	4.20	1.27	7.51	550–650

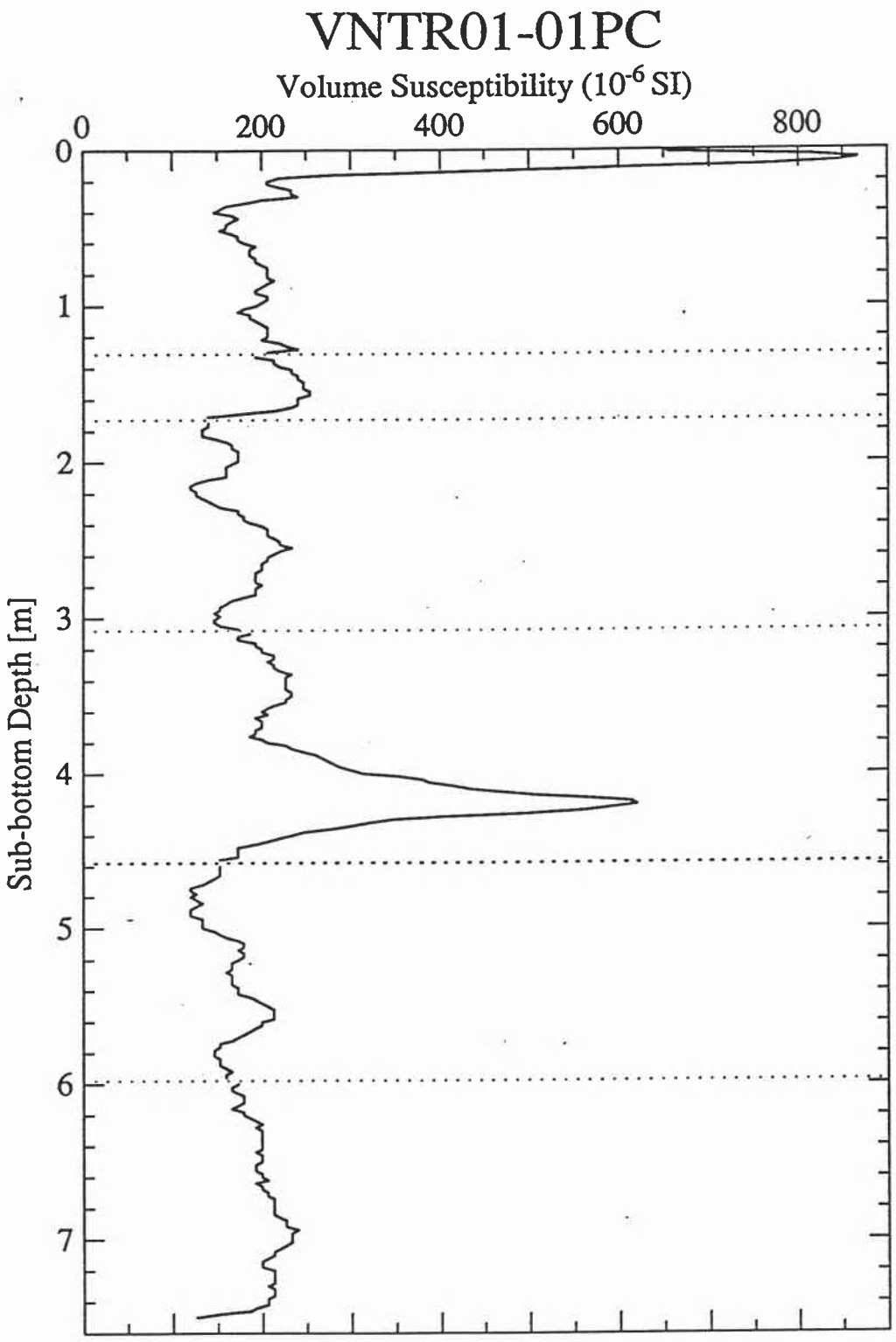

Figure 15. The downhole susceptibility in core VNTR01-01PC (11°N, 110°W). Section boundaries are shown by dotted lines.

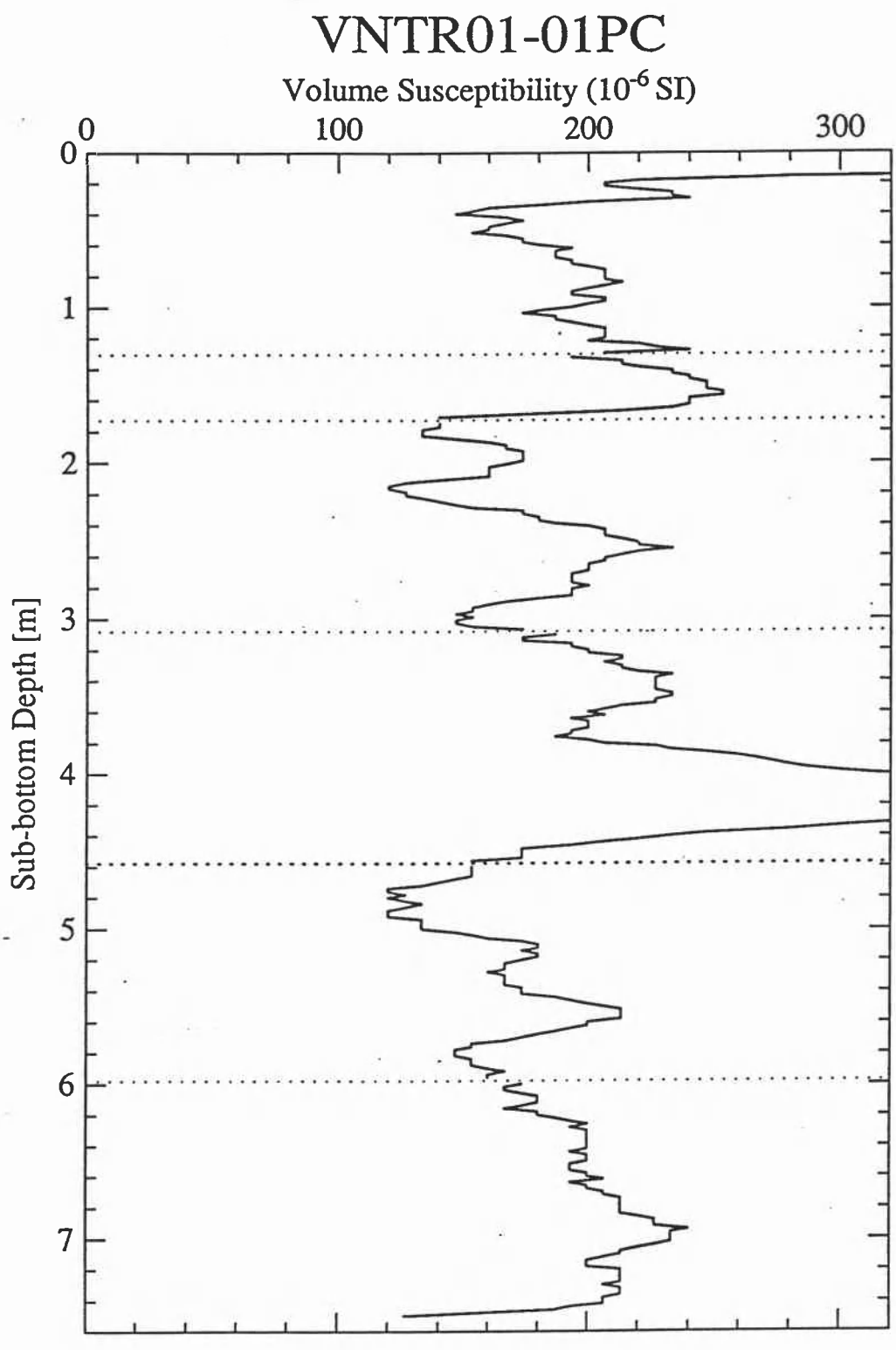

Figure 16. Blown up version of the downhole susceptibility in core VNTR01-01PC. Section boundaries are shown by dotted lines.

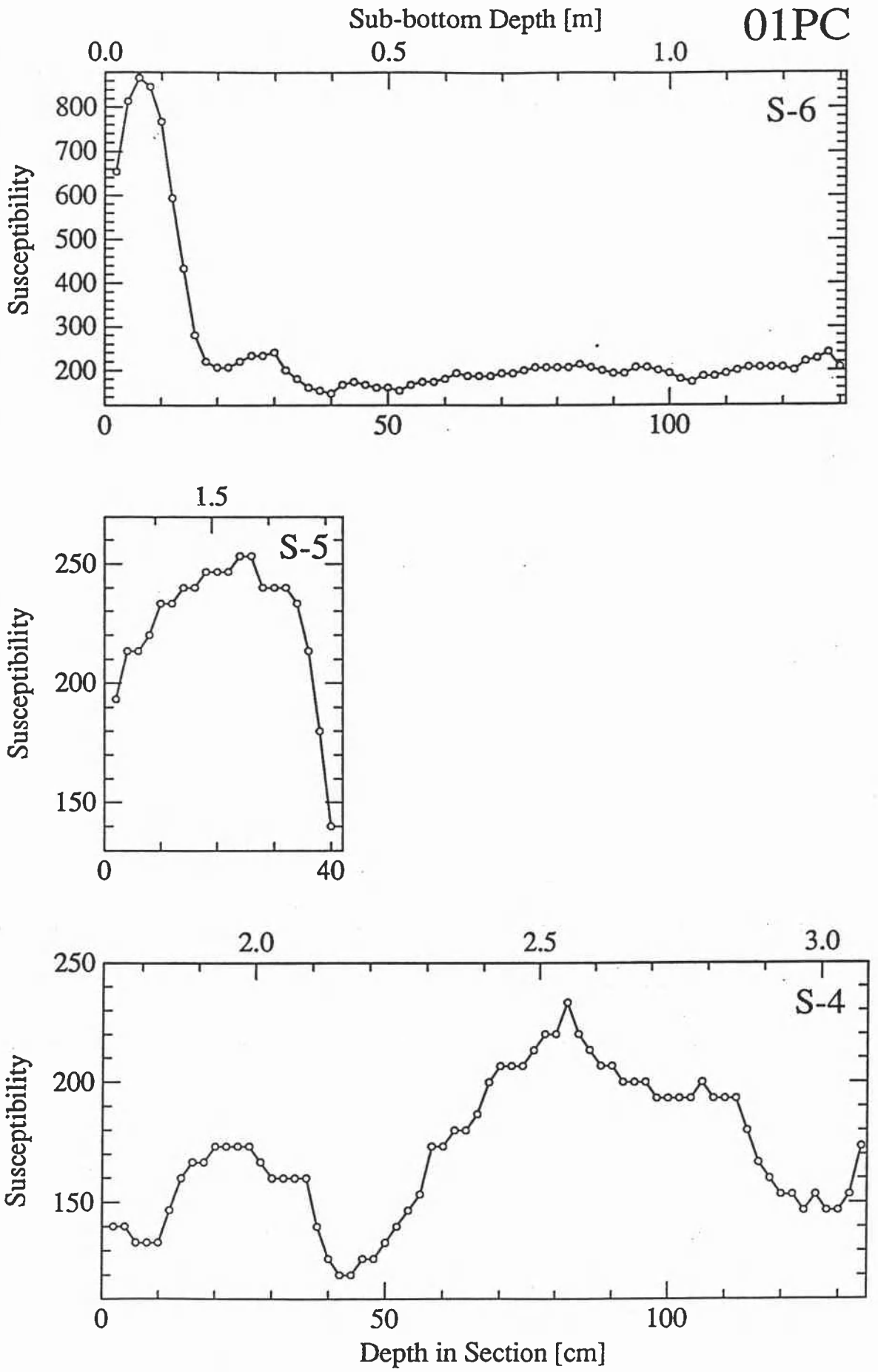

Figure 17. Details of the susceptibility data in core VNTR01-01PC by sections.

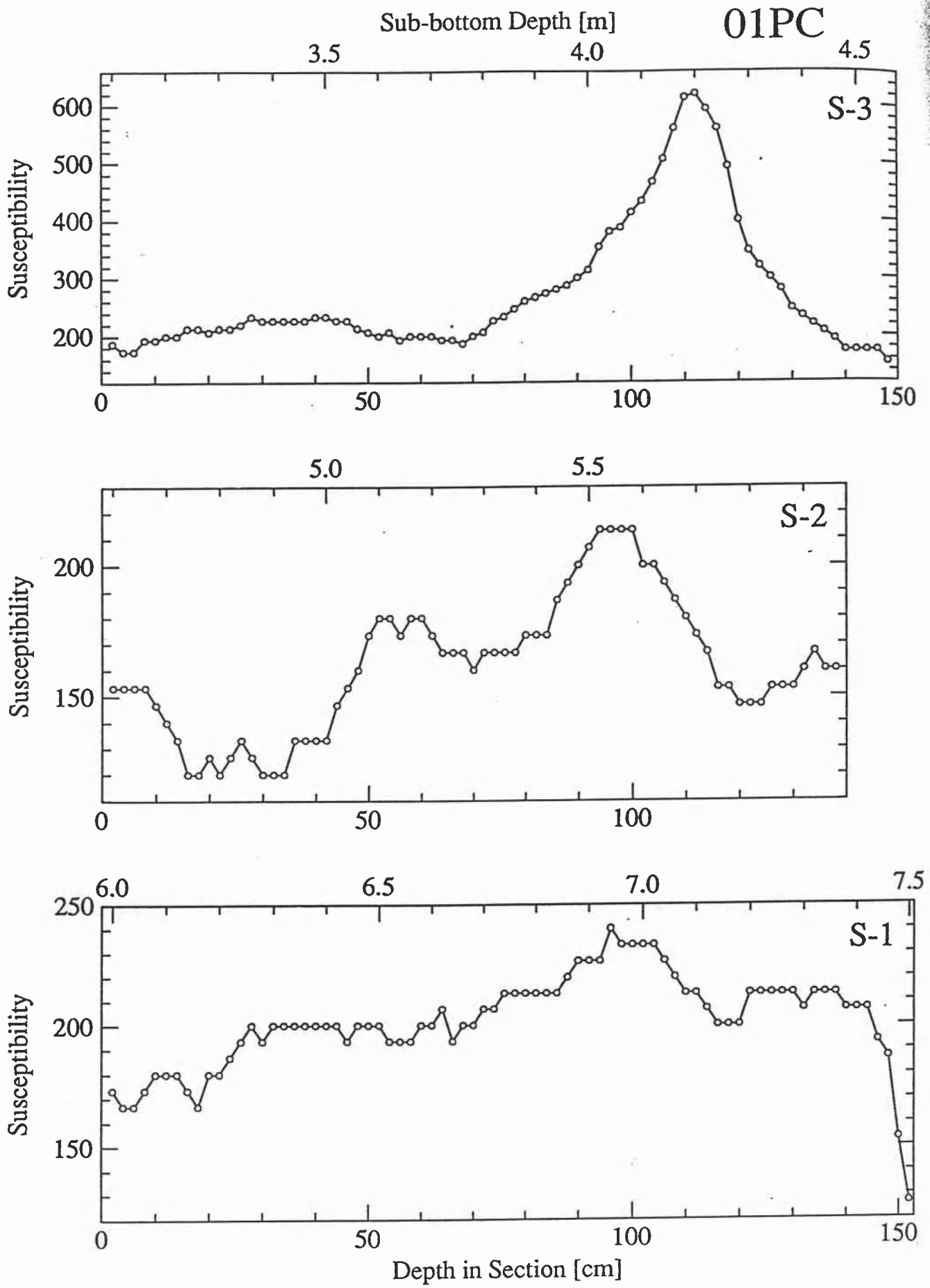
Sub-bottom Depth [m]
01PC
3.5
4.0
4.5
600
500
400
300
200
Susceptibility
S-3
0
50
100
150
5.0
5.5
S-2
200
150
Susceptibility
0
50
100
6.0
6.5
7.0
7.5
250
S-1
200
150
Susceptibility
0
50
100
150
Depth in Section [cm]

VNTR01-02PC

Coring for piston core 02 was attempted on 5-Sep-1989 (7.190°N, 109.783°W, 3731 m water depth), but the piston corer pretripped and although 2.60 m of sediment were recovered, this core is not considered in this report. Piston core 03 was subsequently taken from the same site.

VNTR01-03PC

Piston core 03 was taken on 5-Sep-1989 (7.167°N, 109.740°W, 3725 m water depth). The core is 9.36 m long, consisting of calcareous pelagic ooze. After the data selection we use 458 susceptibility determinations (range: 33.3 to 166.7, arithmetic mean: 104.5 (all 10^{-6} unitless SI)). The downcore susceptibility is shown in Figure 18 and Figure 19 shows details of individual measurements by sections.

Data selection. Sharp spikes at top of S-5 and bottom of S-4 were deleted. Four values were deleted (S-5: 2 cm and 4 cm, S-4: 154 cm and 156 cm)

Chronology. Table 10 shows age-depth correlations, and the sedimentation rate is estimated to be about 0.9 cm/ky. This core penetrates probably well into the Matuyama Chron (possibly through Jaramillo).

TABLE 10. Age-depth estimates from susceptibility correlations of 03PC

Piston Core	Event Name	Event Age (ka)	Position of Event Section (S-cm)	Position of Event Depth (m)	Sedimentation Rate (from top) (cm/ky)	Core Length (m)	Bottom Age (ka)
			Estimates Made During the Cruise:				
03	6.0	128		1.16	0.9		
			Estimates of this Report:				
03	5.0	74	6-45	0.92	1.24		
03	6.0	130	6-87	1.16	0.89	9.36	900–1200

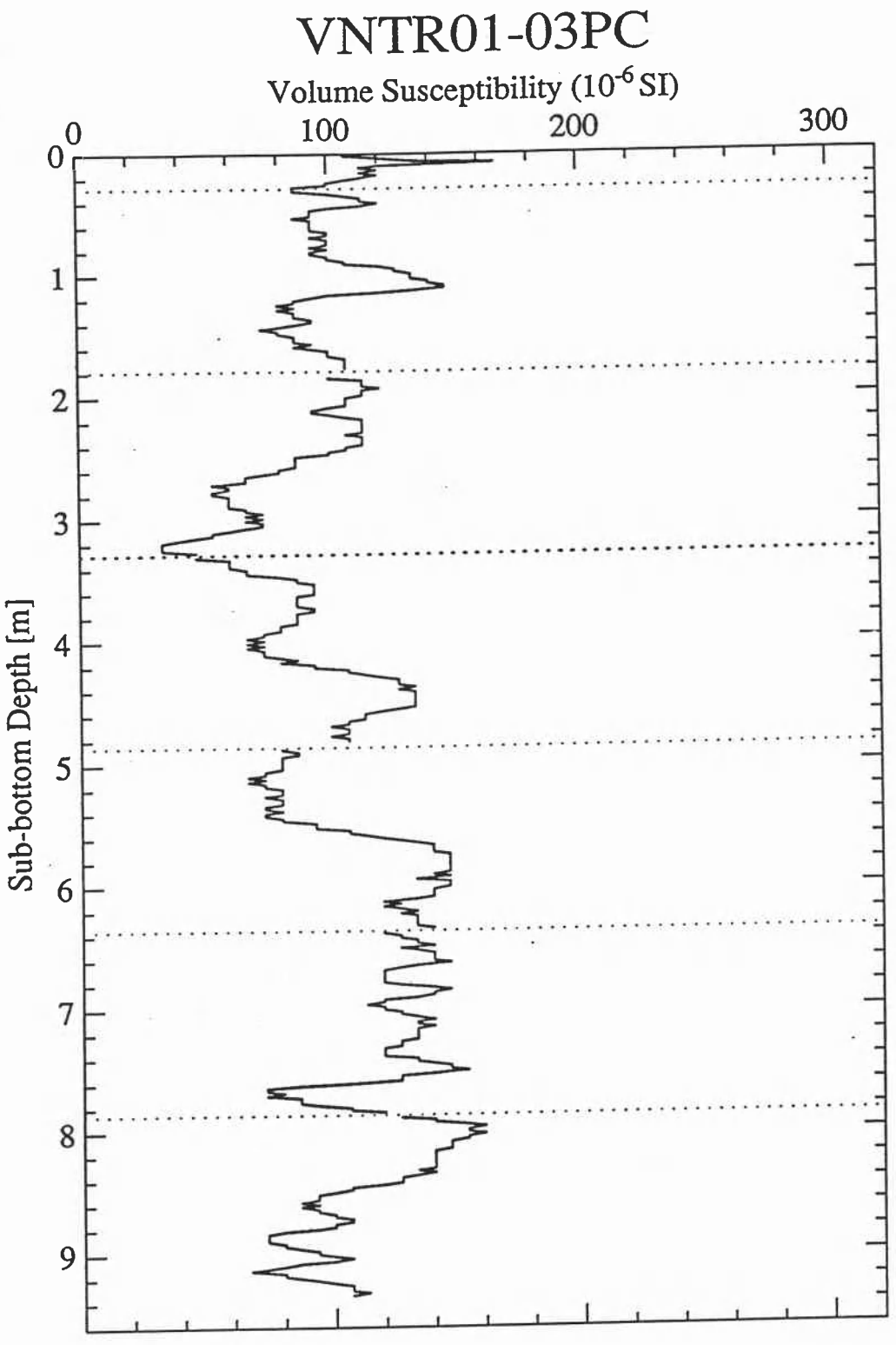

Figure 18. The downhole susceptibility in core VNTR01-03PC (7°N, 110°W). Section boundaries are shown by dotted lines.

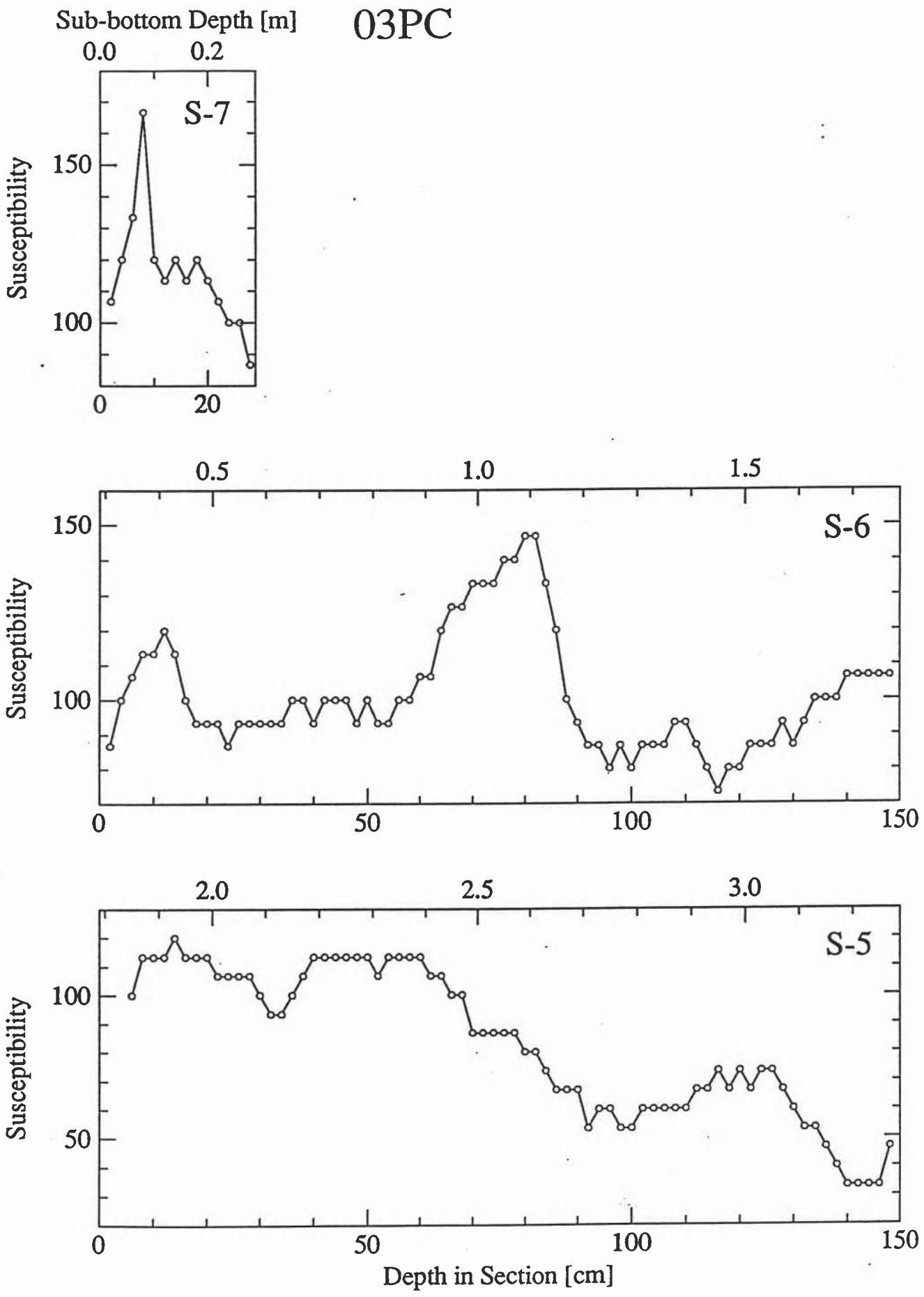

Figure 19. Details of the susceptibility data in core VNTR01-03PC by sections.

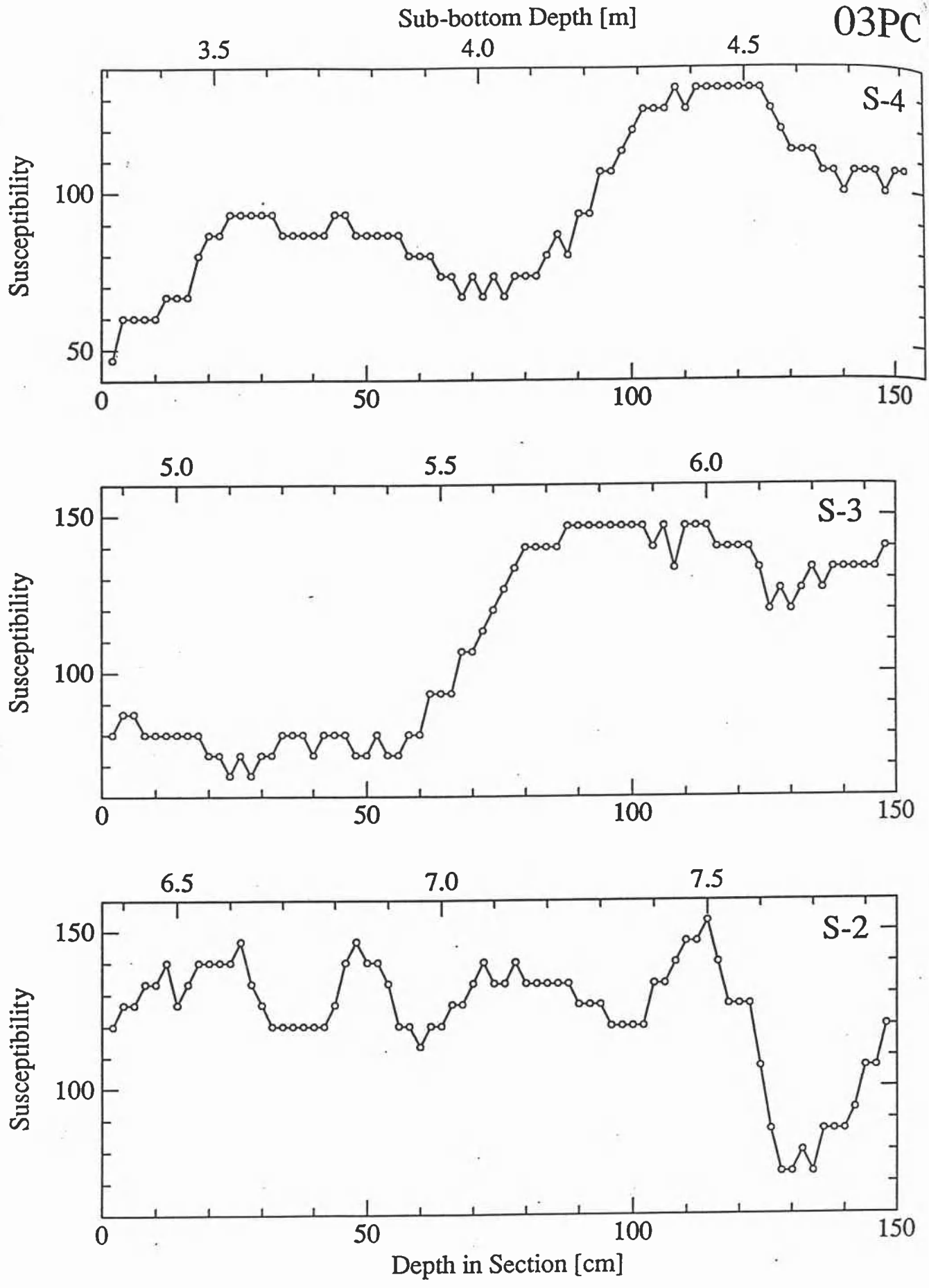
03PC
Sub-bottom Depth [m]
3.5
4.0
4.5
S-4
Susceptibility
100
50
0
50
100
150
5.0
5.5
6.0
S-3
Susceptibility
150
100
0
50
100
150
6.5
7.0
7.5
S-2
Susceptibility
150
100
0
50
100
150
Depth in Section [cm]

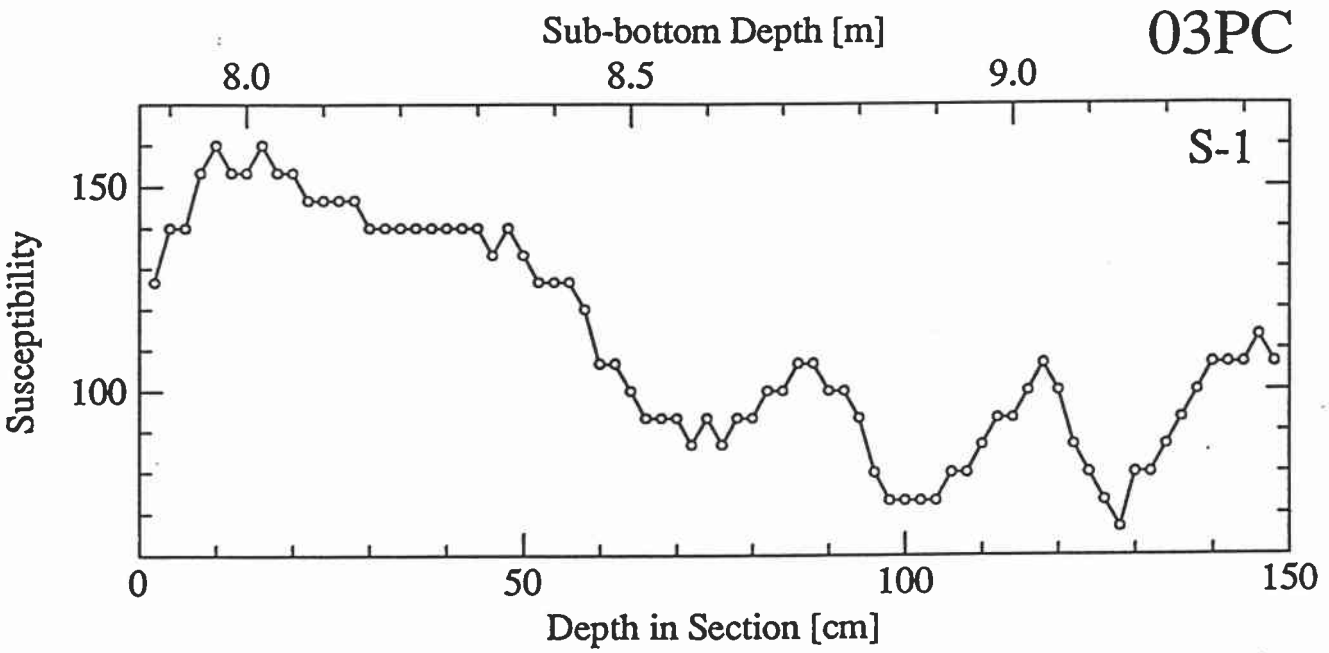
Sub-bottom Depth [m]
8.0
8.5
9.0
03PC
S-1
Susceptibility
150
100
0
50
100
150
Depth in Section [cm]

VNTR01-04PC

Piston core 04 was taken on 6-Sep-1989 (5.349°N, 110.080°W, 3855 m water depth). The core is 8.27 m long, consisting of calcareous pelagic ooze. After the data selection we use 408 susceptibility determinations (range: 26.7 to 146.7, arithmetic mean: 78.5 (all 10^{-6} unitless SI)). The downcore susceptibility is shown in Figure 20, and Figure 21 shows details of individual measurements by sections.

Data selection. The measurements seem to be smooth across all the section boundaries and no data were deleted.

Chronology. Table 11 shows age-depth correlations, and the sedimentation rate is estimated to be about 1.1 cm/ky. It is possible that this core penetrates the Brunhes/Matuyama boundary.

TABLE 11. Age-depth estimates from susceptibility correlations of 04PC

Piston Core	Event Name	Event Age (ka)	Position of Event Section (S-cm)	Position of Event Depth (m)	Sedimentation Rate (from top) (cm/ky)	Core Length (m)	Bottom Age (ka)
			Estimates Made During the Cruise:				
04	6.0	128		1.43	1.1		
			Estimates of this Report:				
04	5.0	74	5-17	0.87	1.18		
04	6.0	130	5-73	1.43	1.10	8.27	700–800

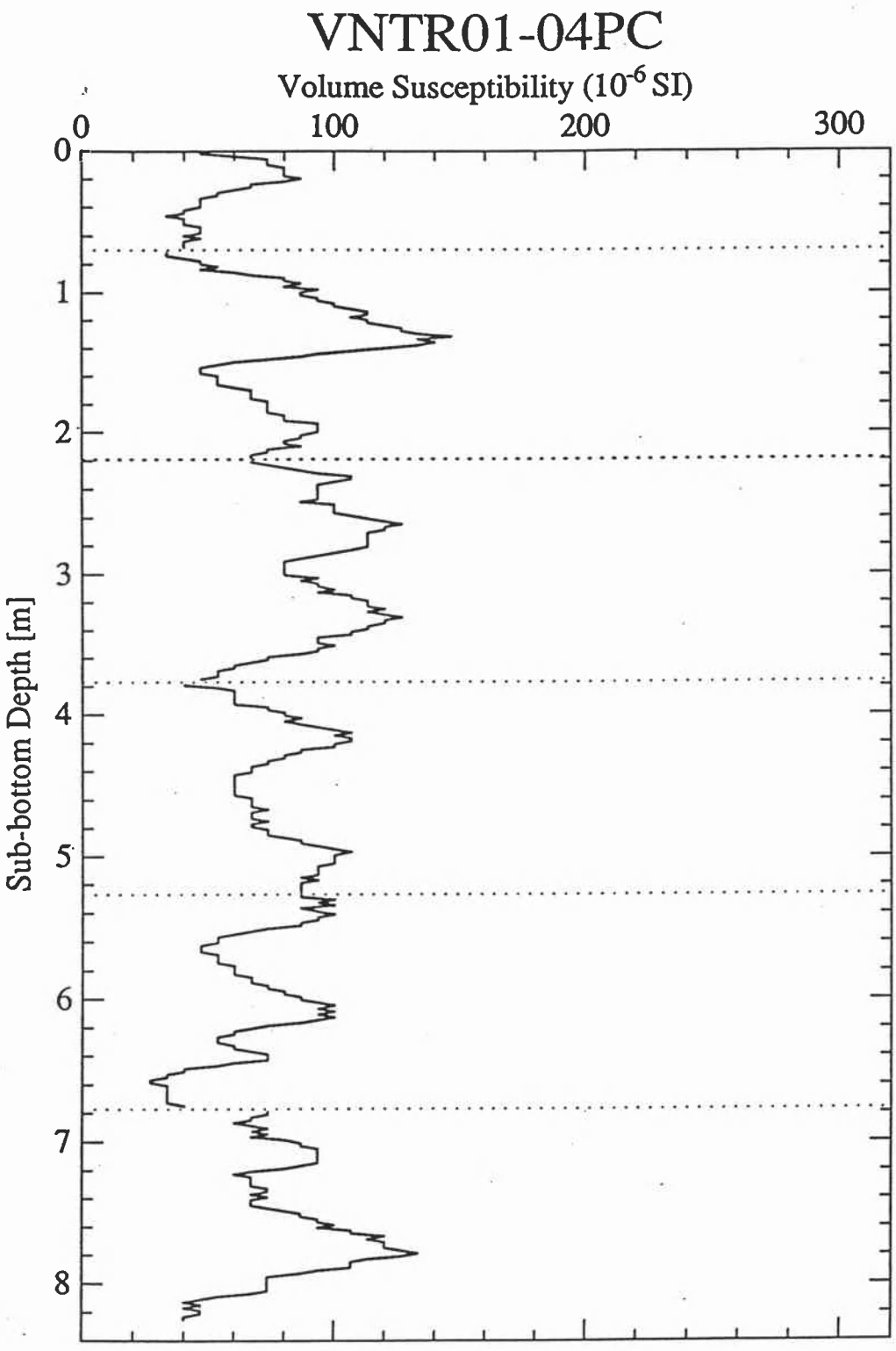

Figure 20. The downhole susceptibility in core VNTR01-04PC (5°N, 110°W). Section boundaries are shown by dotted lines.

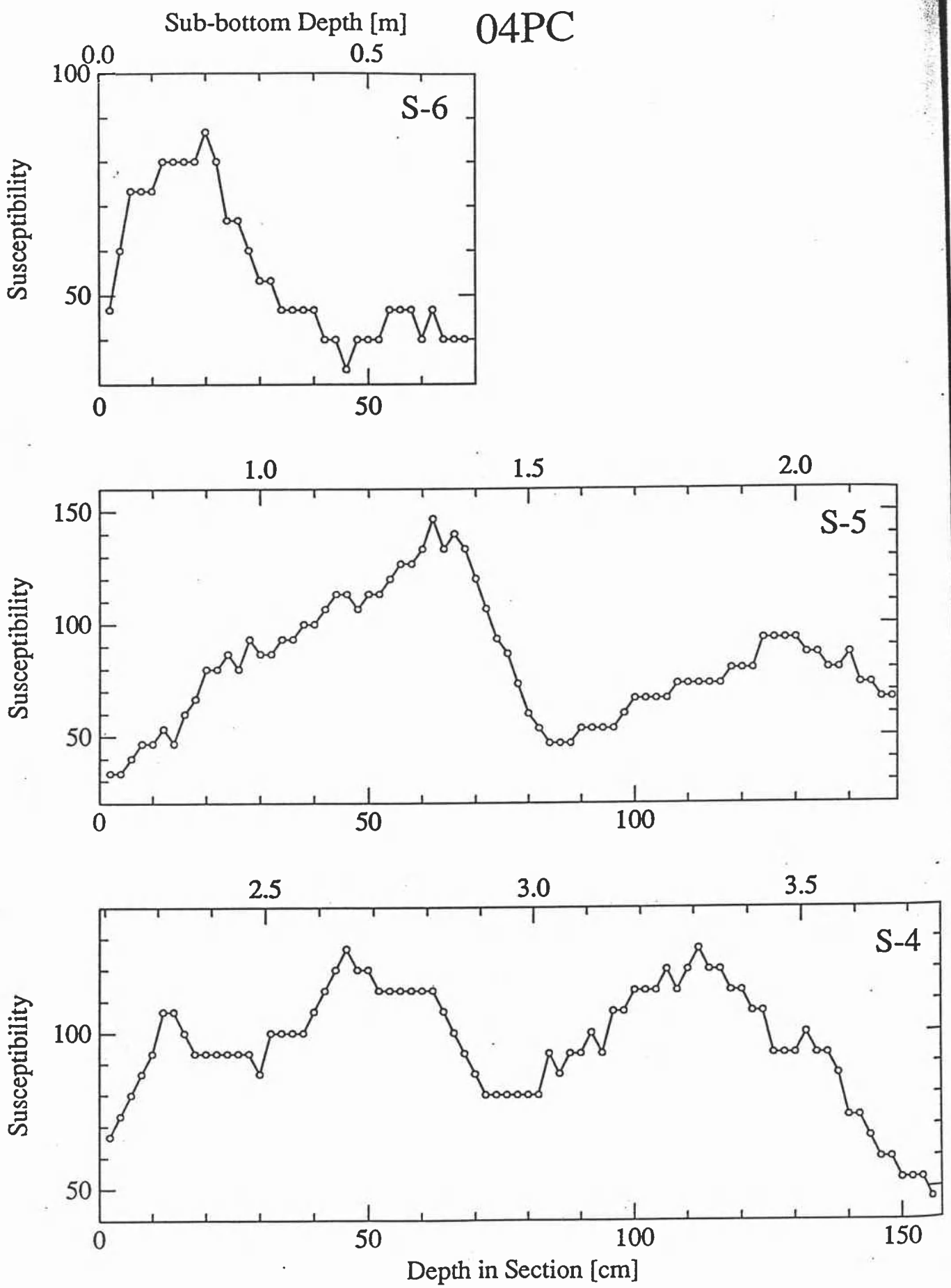

Figure 21. Details of the susceptibility data in core VNTR01-04PC by sections.

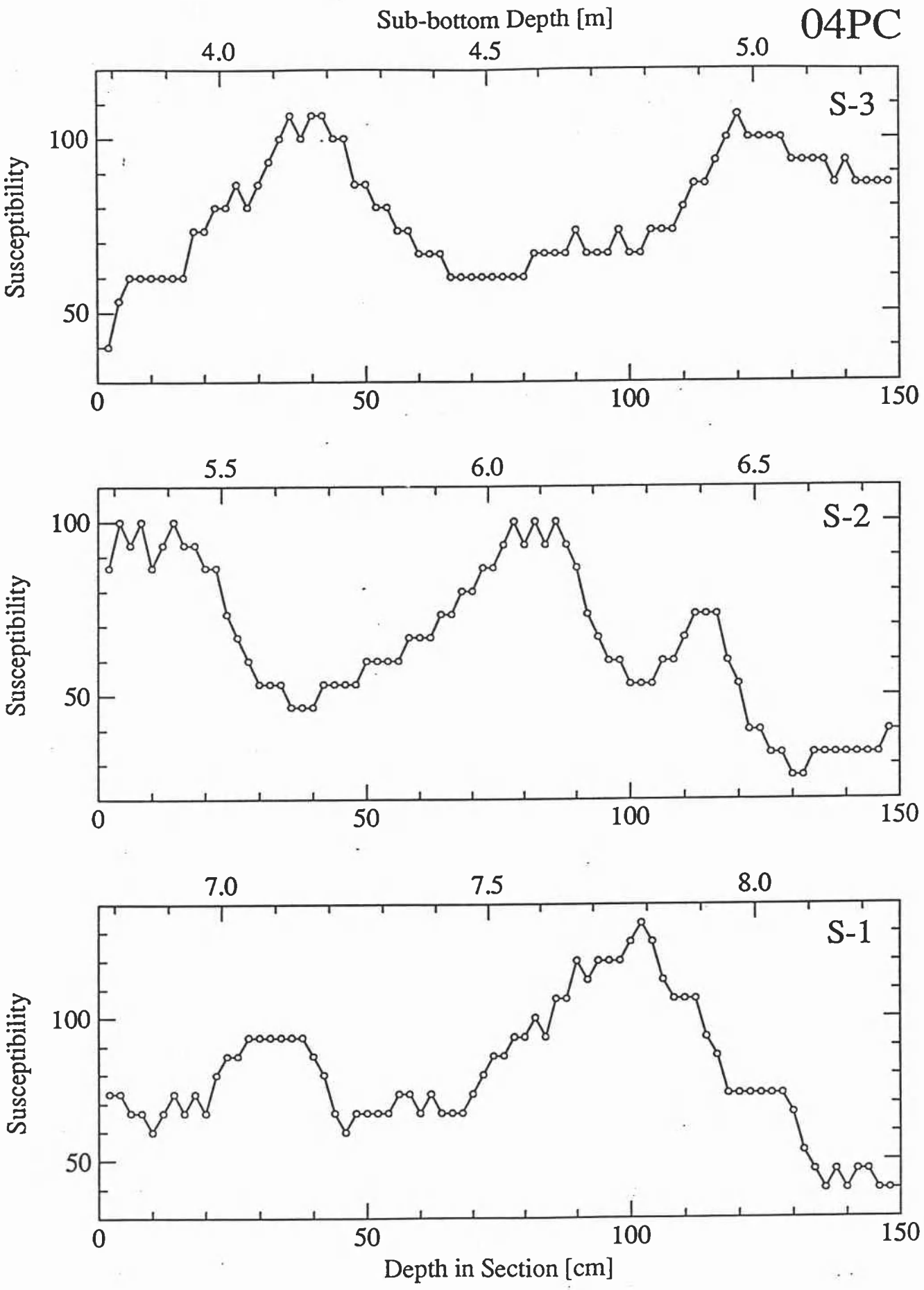
04PC
Sub-bottom Depth [m]
4.0
4.5
5.0
S-3
Susceptibility
100
50
0
50
100
150
5.5
6.0
6.5
S-2
Susceptibility
100
50
0
50
100
150
7.0
7.5
8.0
S-1
Susceptibility
100
50
0
50
100
150
Depth in Section [cm]

VNTR01-05PC

Coring for piston core 05 was attempted on 7 to 8-Sep-1989 (2.757°N, 110.584°W, 3764 m water depth), but the piston corer did not trip and this core is not considered in this report. Piston core 06 was subsequently taken from the same site.

VNTR01-06PC

Piston core 06 was taken on 8-Sep-1989 (2.758°N, 110.573°W, 3765 m water depth). The core is 7.43 m long, consisting of calcareous pelagic ooze. After the data selection we use 364 susceptibility determinations (range: 9.3 to 50.7, arithmetic mean: 26.7 (all 10^{-6} unitless SI)). The downcore susceptibility is shown in Figure 22, and Figure 23 shows details of individual measurements by sections.

TABLE 12. Age-depth estimates from susceptibility correlations of 06PC

Piston Core	Event Name	Event Age (ka)	Position of Event Section (S-cm)	Position of Event Depth (m)	Sedimentation Rate (from top) (cm/ky)	Core Length (m)	Bottom Age (ka)
			Estimates Made During the Cruise:				
06	6.0	128		2.20	1.7		
			Estimates of this Report:				
06	5.1	79	4-34	1.69	2.14		
06	5.2	91	4-45	1.80	1.98		
06	5.3	99	4-60	1.95	1.97		
06	5.4	111	4-66	2.01	1.81		
06	5.5	124	4-78	2.13	1.72		
06	6.0	130	4-85	2.20	1.69		
06	7.0	190	4-146	2.81	1.48		
06	8.4	266	3-94	3.87	1.45		
06	8.5	289	3-122	4.15	1.44		
06	9.1	310	2-26	4.69	1.51		
06	9.2	320	2-38	4.81	1.50		
06	9.3	331	2-53	4.96	1.50		
06	10.0	339	2-61	5.04	1.49		
06	11.3	405	2-122	5.65	1.40		
06	12.2	434	1-44	6.37	1.47		
06	12.4	471	1-69	6.62	1.41		
06	13.0	478	1-90	6.83	1.43		
06	13.2	513	1-118	7.11	1.39		
06	14.2	538	1-143	7.36	1.37	7.43	540–550

Data selection. The section boundary S-4/S-3 had a strong spike originating mainly from the bottom of S-4 which has anomalously high values, and top of S-3 starts in rather low values. From analysis of the shape of the spike in S-4 it is estimated that its source is within 1 cm of the bottom and might be metallic contamination on the bottom cap. Therefore, two values were deleted from the bottom (S-4: 154 cm and 156 cm). The low values in the top of S-3 are possibly true but to be on the safe side one value was deleted (S-3: 2 cm).

Chronology. The susceptibility in piston core 06 has straightforward correlation to the oxygen isotope timescale. Based on the correlations shown in Table 12, the bottom age is about 540 ka, and the sedimentation rate is on the order of 1.4 cm/ky to 2.0 cm/ky. The most serious mismatch is an extra spike at about 420 ka. The method of *Martinson et al.* [1982] was used to obtain a smooth depth-age mapping function and the results are shown in Table 13 and Figures 5 and 6.

TABLE 13. Depth-Age mapping function from inverse correlations of susceptibility in 06PC and the oxygen isotope timescale

Depth (m)	Age (ka)	Depth (m)	Age (ka)	Depth (m)	Age (ka)	Depth (m)	Age (ka)
0.00	22.0	2.00	104.1	4.00	278.6	6.00	422.2
0.10	24.2	2.10	115.0	4.10	282.9	6.10	426.6
0.20	26.5	2.20	126.7	4.20	287.0	6.20	431.1
0.30	28.8	2.30	138.4	4.30	291.1	6.30	436.0
0.40	31.1	2.40	149.5	4.40	295.3	6.40	441.4
0.50	33.4	2.50	159.8	4.50	299.6	6.50	447.5
0.60	35.9	2.60	169.4	4.60	304.3	6.60	454.9
0.70	38.4	2.70	178.5	4.70	309.5	6.70	463.7
0.80	41.1	2.80	187.6	4.80	315.5	6.80	474.4
0.90	43.9	2.90	196.9	4.90	322.7	6.90	486.6
1.00	46.9	3.00	206.5	5.00	331.6	7.00	499.3
1.10	50.1	3.10	216.3	5.10	343.1	7.10	511.3
1.20	53.6	3.20	226.0	5.20	357.0	7.20	521.9
1.30	57.4	3.30	235.2	5.30	371.6	7.30	531.3
1.40	61.7	3.40	243.7	5.40	384.3	7.40	540.0
1.50	66.5	3.50	251.3	5.50	394.1		
1.60	72.0	3.60	258.0	5.60	401.7		
1.70	78.3	3.70	263.9	5.70	407.8		
1.80	85.7	3.80	269.3	5.80	413.0		
1.90	94.3	3.90	274.1	5.90	417.8		

Note that discrepancies can occur between Tables 12 and 13, because the mapping function in Table 13 is constrained to vary smoothly and depends on all the data points, whereas Table 12 shows discrete manual picks which depend mainly on position of highs and lows.

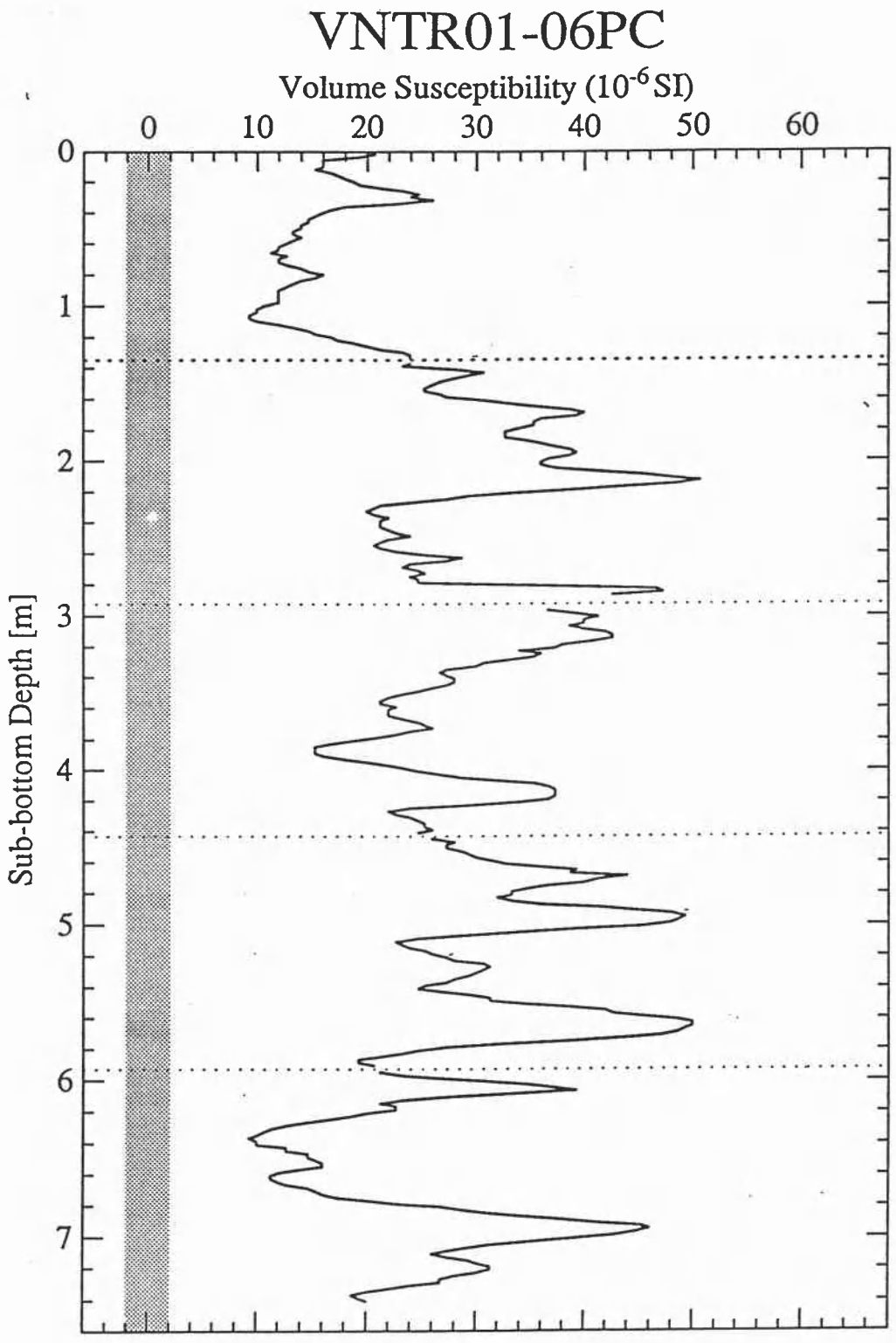

Figure 22. The downhole susceptibility in core VNTR01-06PC (3°N, 111°W). Section boundaries are shown by dotted lines and the approximate noise level by the shaded zero line.

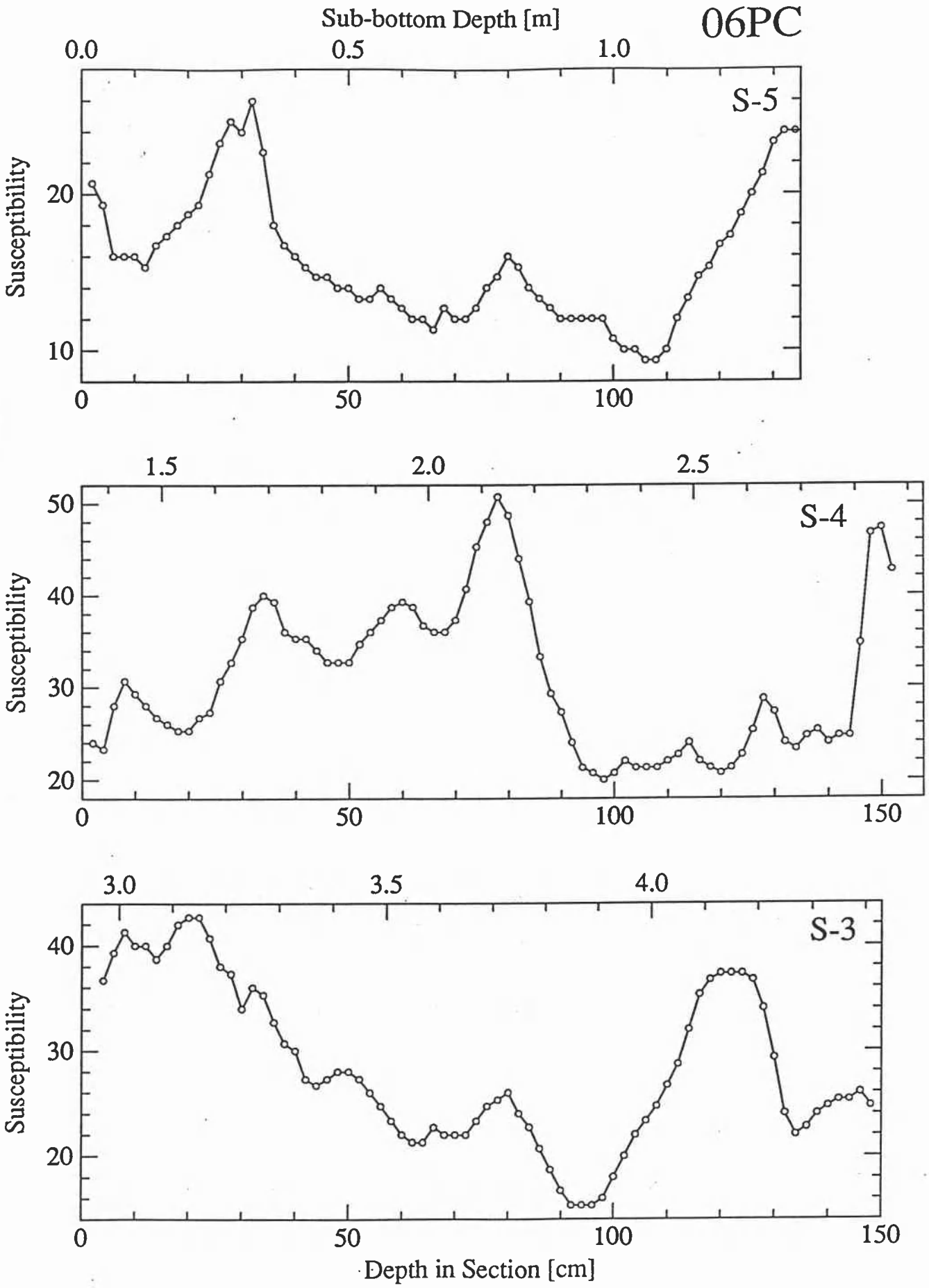

Figure 23. Details of the susceptibility data in core VNTR01-06PC by sections.

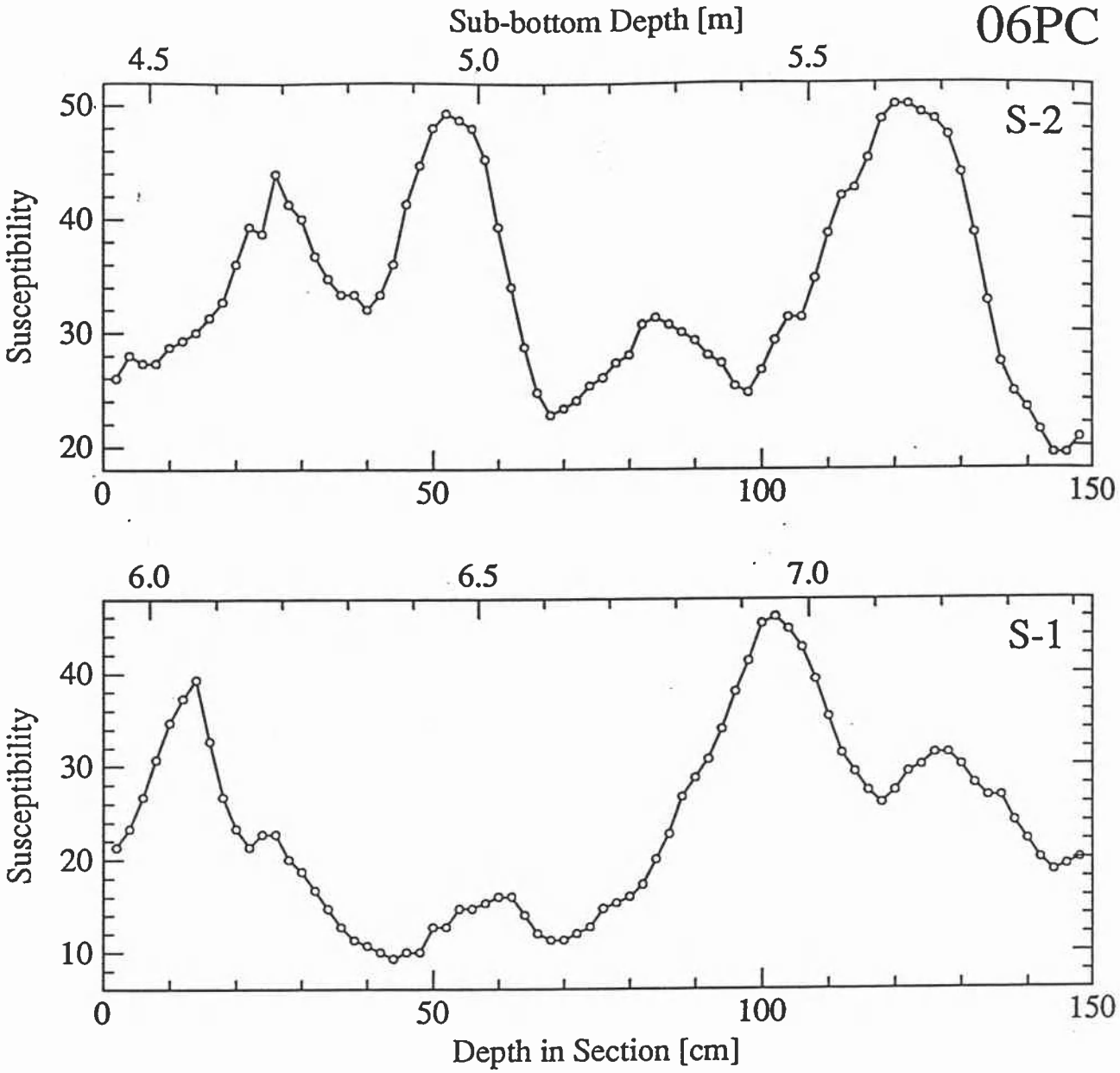
06PC
Sub-bottom Depth [m]
4.5
5.0
5.5
S-2
Susceptibility
50
40
30
20
0
50
100
150
6.0
6.5
7.0
S-1
Susceptibility
40
30
20
10
0
50
100
150
Depth in Section [cm]

VNTR01-07PC

Piston core 07 was taken on 8 to 9-Sep-1989 (1.019°N, 110.568°W, 3775 m water depth). The core is 7.42 m long, consisting of calcareous pelagic ooze. After the data selection we use 168 susceptibility determinations (range: –2.7 to 24.7, arithmetic mean: 8.1 (all 10^{-6} unitless SI)). The downcore susceptibility is shown in Figure 24, and Figure 25 shows details of individual measurements by sections. Below 3 m the measurements were only made every 10 cm.

Data selection. The measurements seem to be smooth across all the section boundaries and no data were deleted.

Chronology. Table 14 shows age-depth correlations, and the sedimentation rate is estimated to be about 1.2 to 1.6 cm/ky. The susceptibility below 2 m is very low and might represent active chemical processes in the sediment. It is therefore possible that the boundary correlated here to oxygen isotope event 6.0 is instead a chemical boundary.

TABLE 14. Age-depth estimates from susceptibility correlations of 07PC

Piston Core	Event Name	Event Age (ka)	Position of Event Section (S-cm)	Position of Event Depth (m)	Sedimentation Rate (from top) (cm/ky)	Core Length (m)	Bottom Age (ka)
			Estimates Made During the Cruise:				
07	6.0	128		2.07	1.6		
			Estimates of this Report:				
07	5.0	74	5-92	0.92	1.24		
07	6.0	130	4-72	2.07	1.59	7.42	400–600 ?

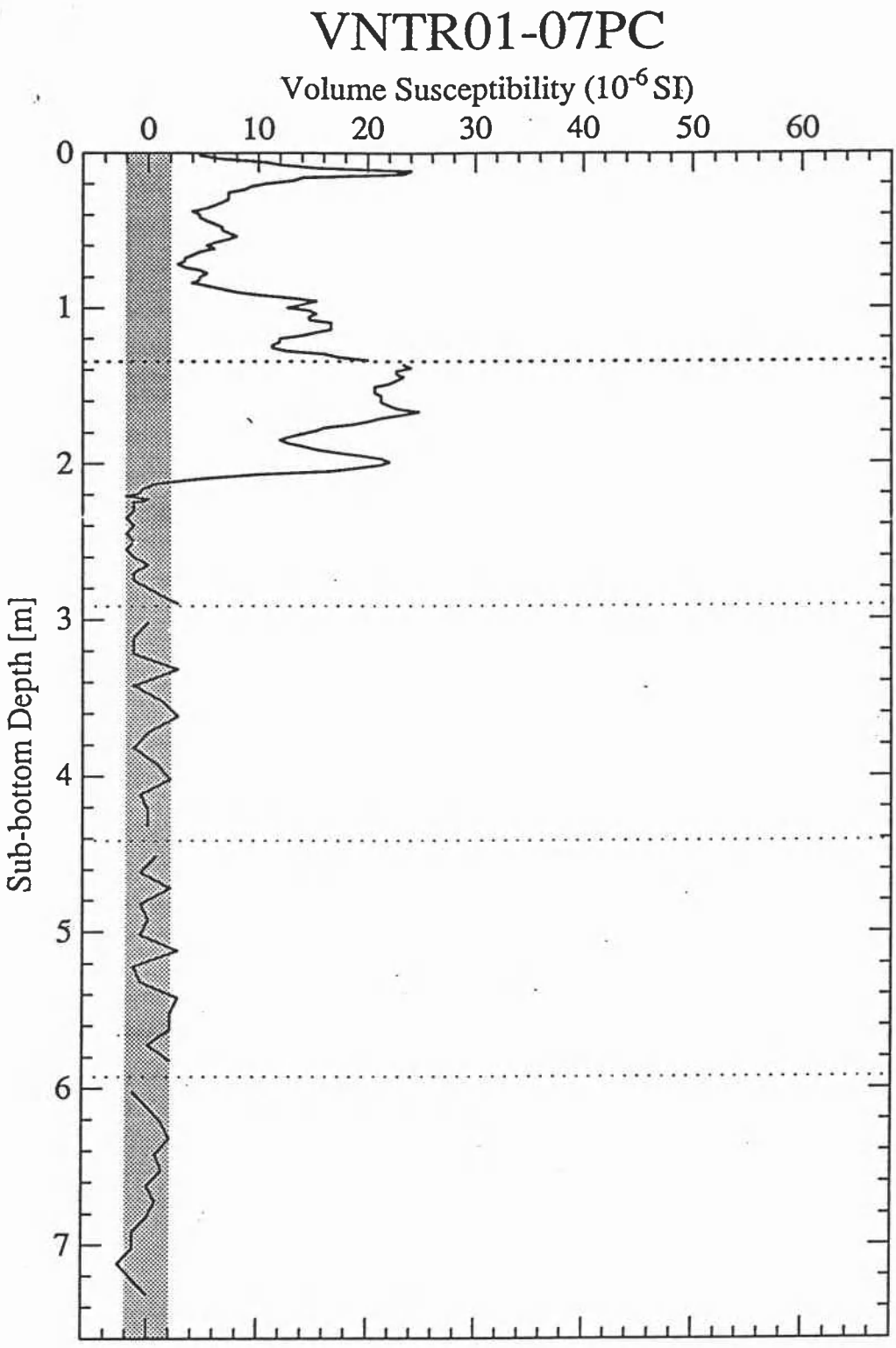

Figure 24. The downhole susceptibility in core VNTR01-07PC (1°N, 111°W). Section boundaries are shown by dotted lines and the approximate noise level by the shaded zero line.

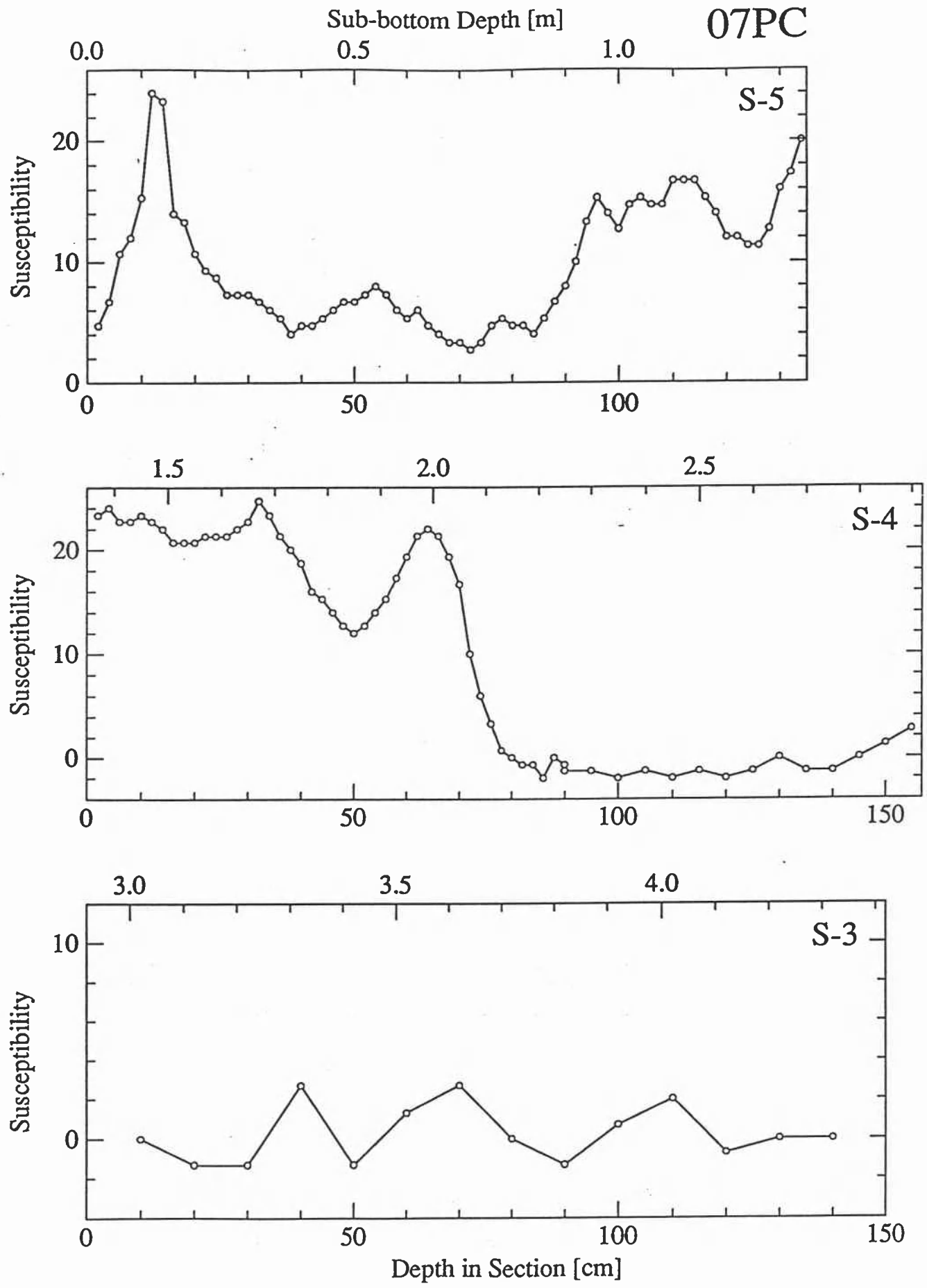

Figure 25. Details of the susceptibility data in core VNTR01-07PC by sections.

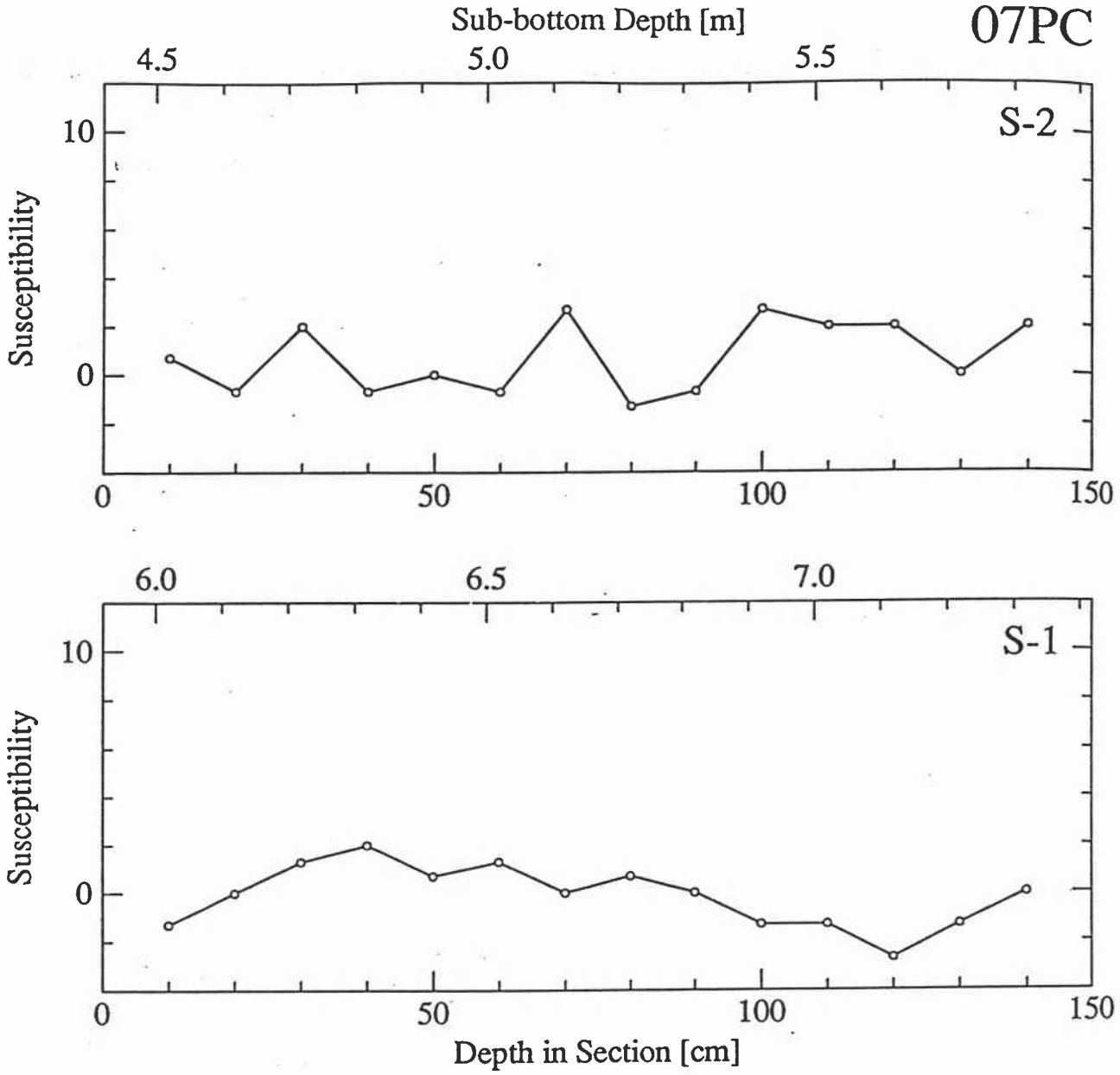
07PC
Sub-bottom Depth [m]
4.5
5.0
5.5
S-2
Susceptibility
10
0
0
50
100
150
6.0
6.5
7.0
S-1
Susceptibility
10
0
0
50
100
150
Depth in Section [cm]

VNTR01-08PC

Piston core 08 was taken on 9-Sep-1989 (0.039°N, 110.476°W, 3800 m water depth). The core is 8.69 m long, consisting of calcareous pelagic ooze. After the data selection we use 198 susceptibility determinations (range: –4.7 to 65.3, arithmetic mean: 6.9 (all 10^{-6} unitless SI)). The downcore susceptibility is shown in Figure 26, and Figure 27 shows details of individual measurements by sections. Below 3 m the measurements were only made every 10 cm.

Data selection. A minor spike at the top of section 5 was deleted (S-5: 2 cm and 4 cm). Furthermore the top 3 cm fell out of the top of section 4, and were put back in and may be disturbed. The susceptibility of the top of section 4 shows signs of possible metallic contaminations with a spike centered at 3 cm. Therefore three data were deleted (S-4: 2 cm, 4 cm and 6 cm).

Chronology. Table 15 shows age-depth correlations, and the sedimentation rate is estimated to be about 2.0 cm/ky.

TABLE 15. Age-depth estimates from susceptibility correlations of 08PC

Piston Core	Event Name	Event Age (ka)	Position of Event Section (S-cm)	Position of Event Depth (m)	Sedimentation Rate (from top) (cm/ky)	Core Length (m)	Bottom Age (ka)
			Estimates Made During the Cruise:				
08	6.0	128		2.67	2.1		
			Estimates of this Report:				
08	5.0	74	5-37	1.48	2.00		
08	6.0	130	4-6	2.67	2.05	8.69	400–600 ?

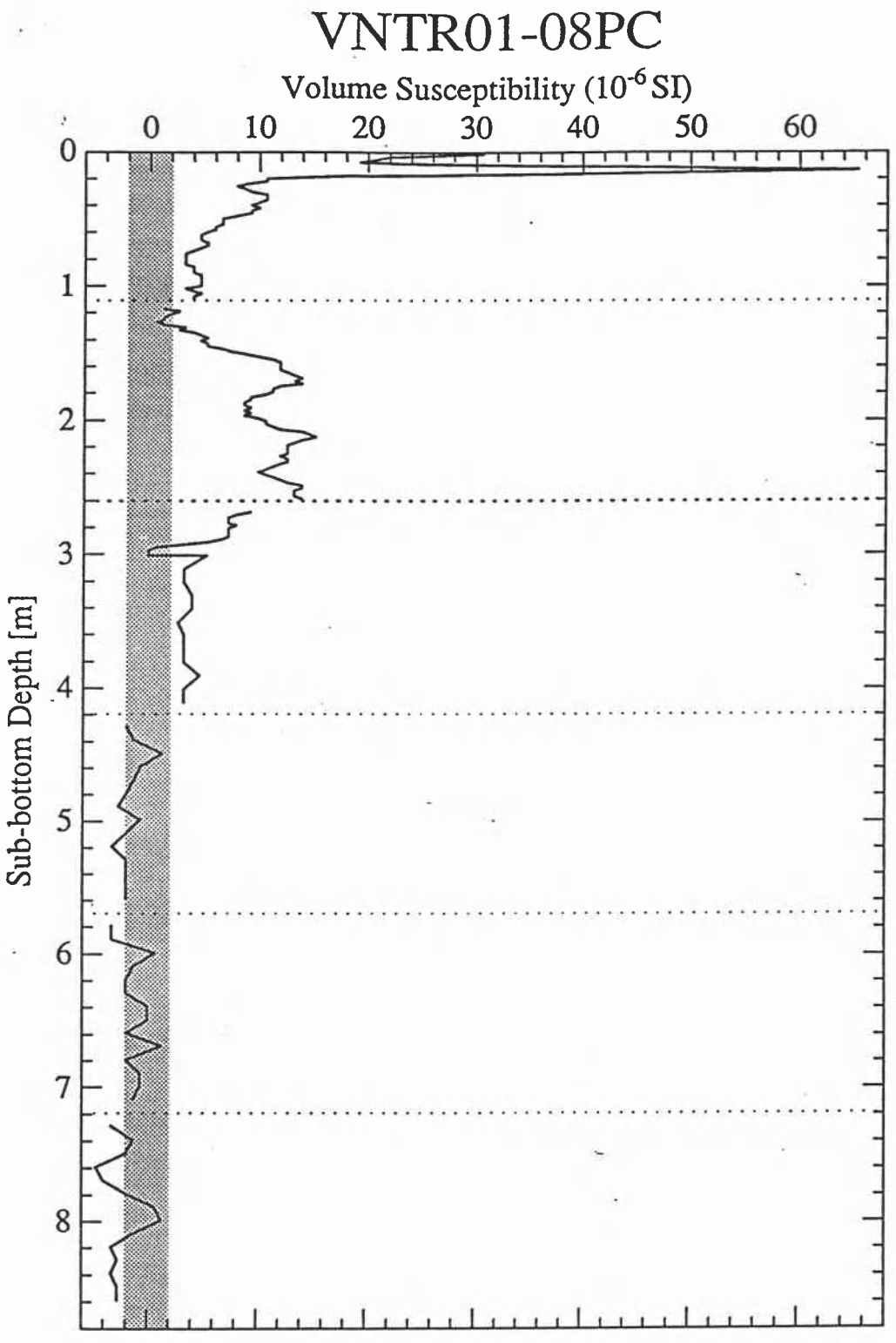

Figure 26. The downhole susceptibility in core VNTR01-08PC (0°N, 110°W). Section boundaries are shown by dotted lines and the approximate noise level by the shaded zero line.

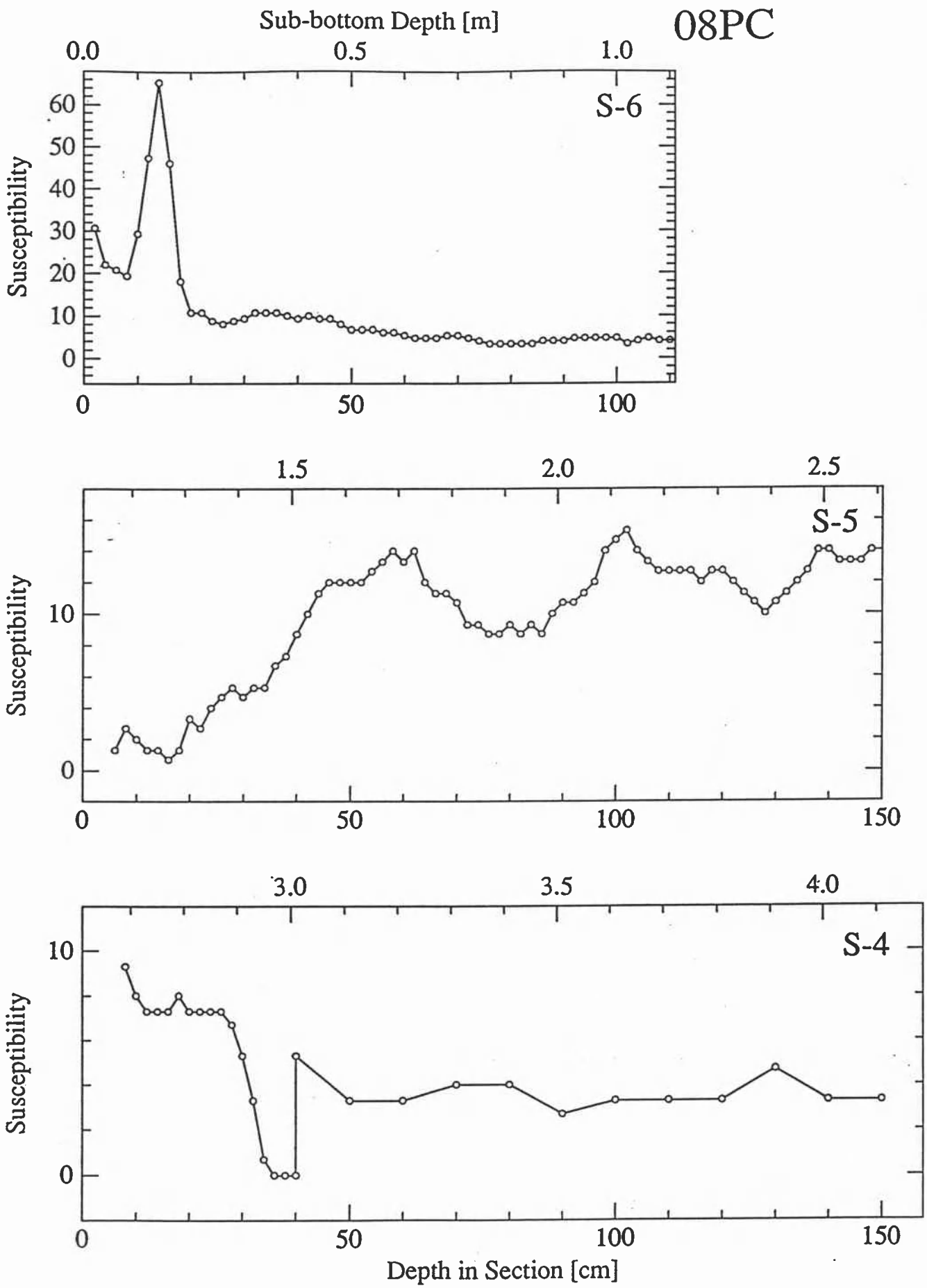

Figure 27. Details of the susceptibility data in core VNTR01-08PC by sections.

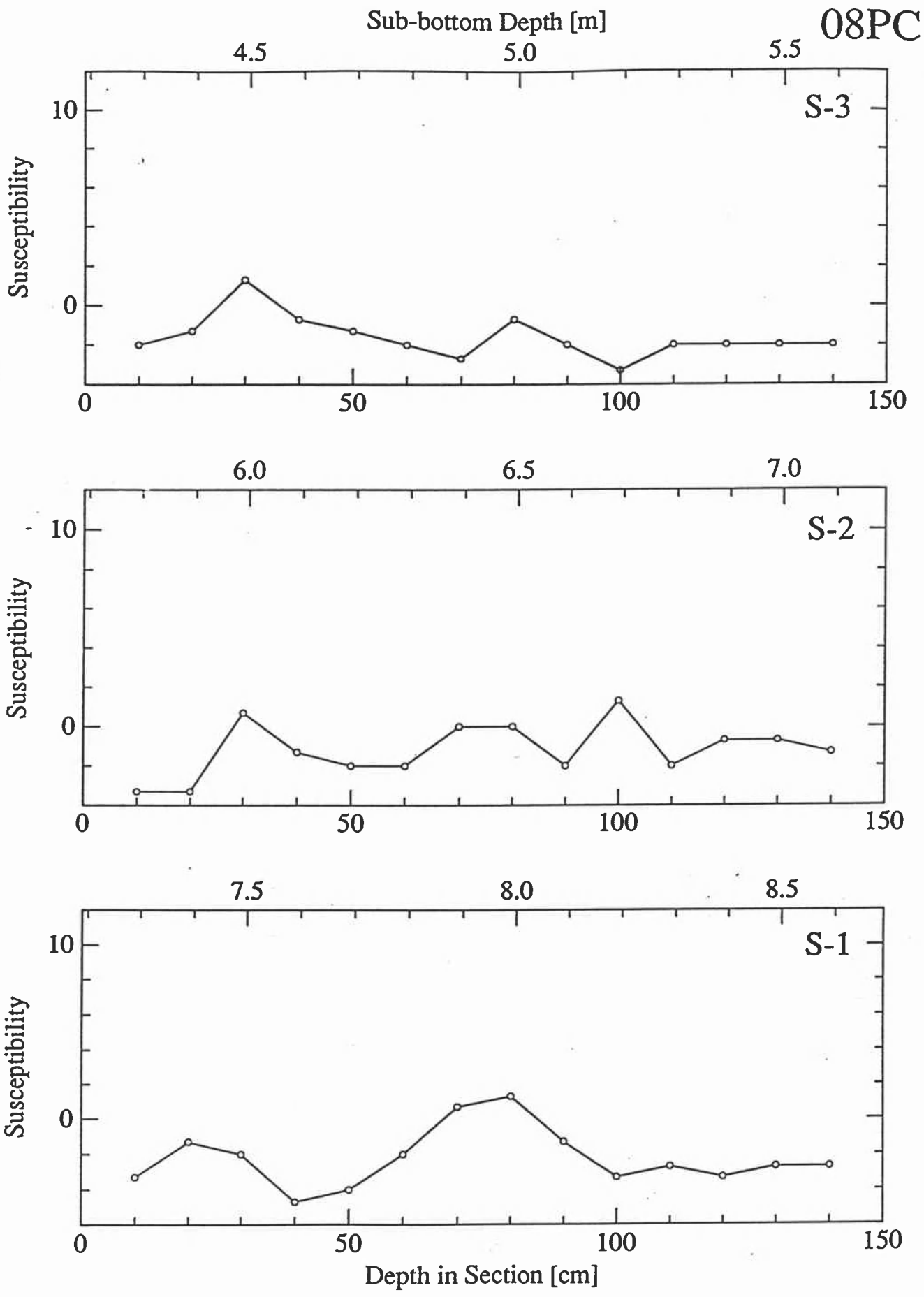
08PC
Sub-bottom Depth [m]
4.5
5.0
5.5
S-3
10
0
Susceptibility
0
50
100
150
6.0
6.5
7.0
S-2
10
0
Susceptibility
0
50
100
150
7.5
8.0
8.5
S-1
10
0
Susceptibility
0
50
100
150
Depth in Section [cm]

VNTR01-09PC

Piston core 09 was taken on 10-Sep-1989 (3.004°S, 110.491°W, 3860 m water depth). The core is 7.79 m long, consisting of calcareous pelagic ooze. After the data selection we use 359 susceptibility determinations (range: –2.7 to 52.7, arithmetic mean: 14.8 (all 10^{-6} unitless SI)). The downcore susceptibility is shown in Figure 28, and Figure 29 shows details of individual measurements by sections.

Data selection. Steps between section boundaries S-3/S-2 and S-2/S-1 were fixed by deleting five data points (S-2: 2 cm, 4 cm and 148 cm, S-1: 2 cm and 4 cm).

Chronology. Table 16 shows age-depth correlations, and the sedimentation rate is estimated to be about 1.7 cm/ky.

TABLE 16. Age-depth estimates from susceptibility correlations of 09PC

Piston Core	Event Name	Event Age (ka)	Position of Event Section (S-cm)	Position of Event Depth (m)	Sedimentation Rate (from top) (cm/ky)	Core Length (m)	Bottom Age (ka)
			Estimates Made During the Cruise:				
09	6.0	128		2.25	1.8		
			Estimates of this Report:				
09	6.0	130	4-53	2.25	1.73	7.79	300–500 ?

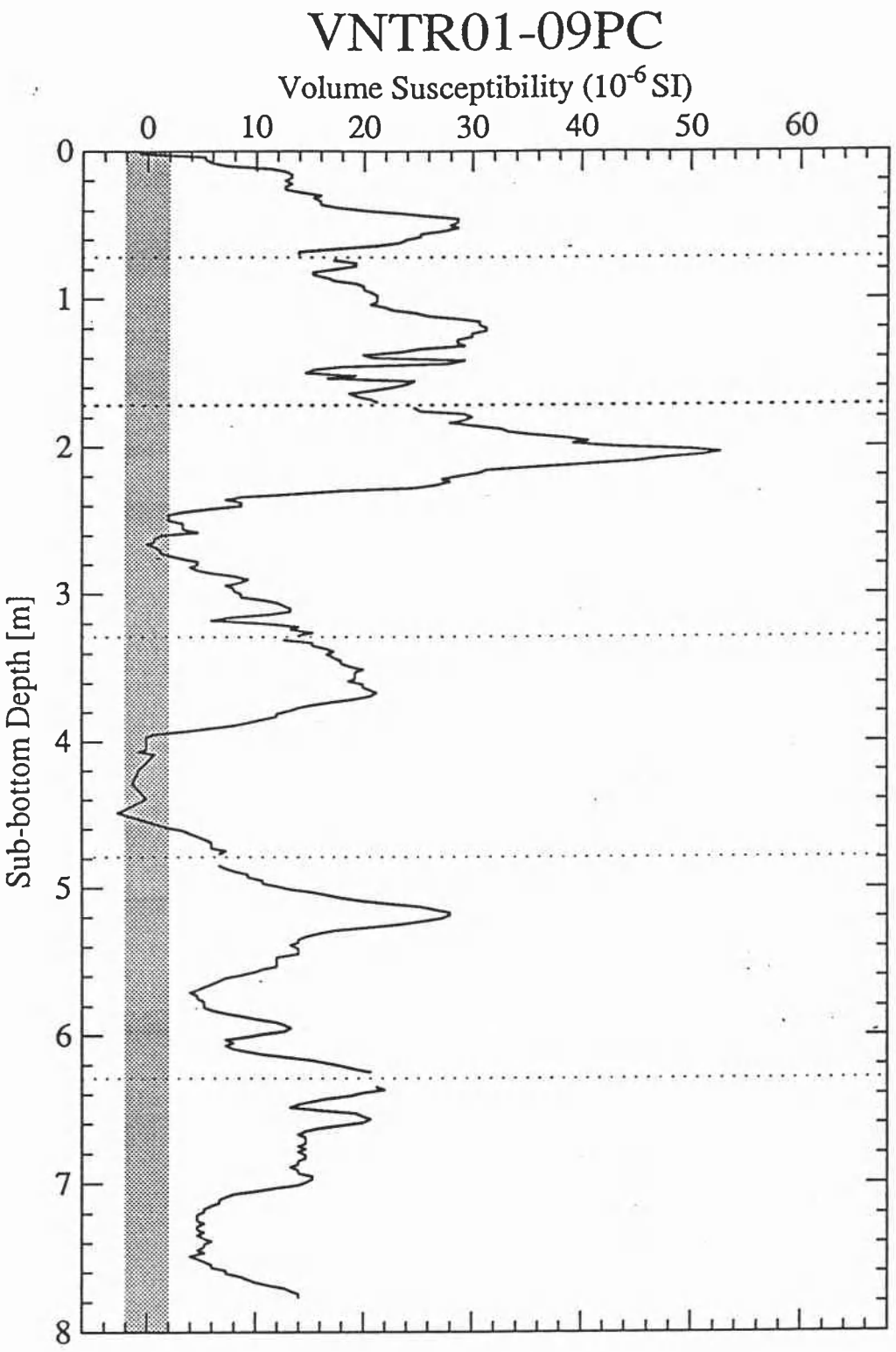

Figure 28. The downhole susceptibility in core VNTR01-09PC (3°S, 110°W). Section boundaries are shown by dotted lines and the approximate noise level by the shaded zero line.

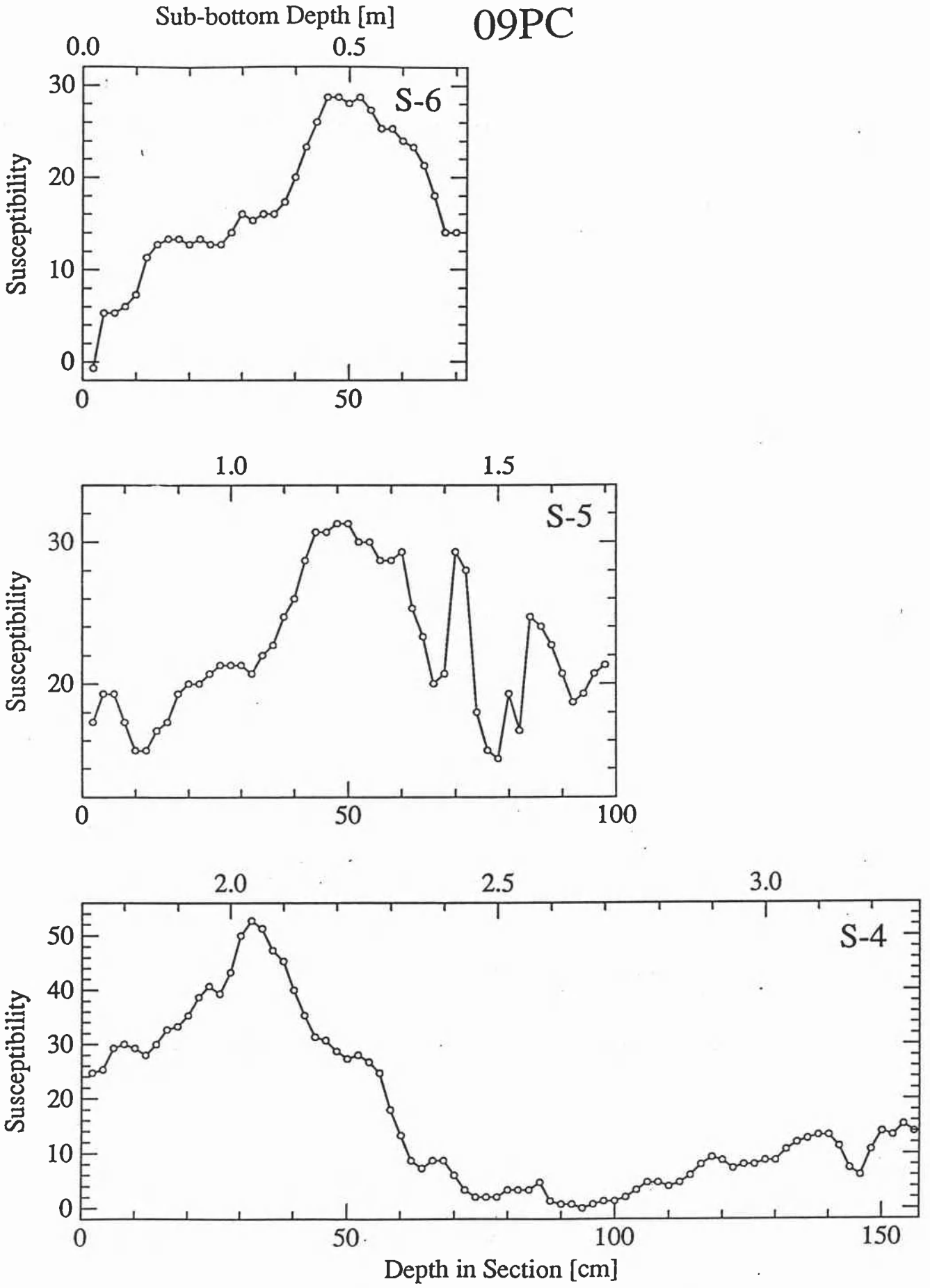

Figure 29. Details of the susceptibility data in core VNTR01-09PC by sections.

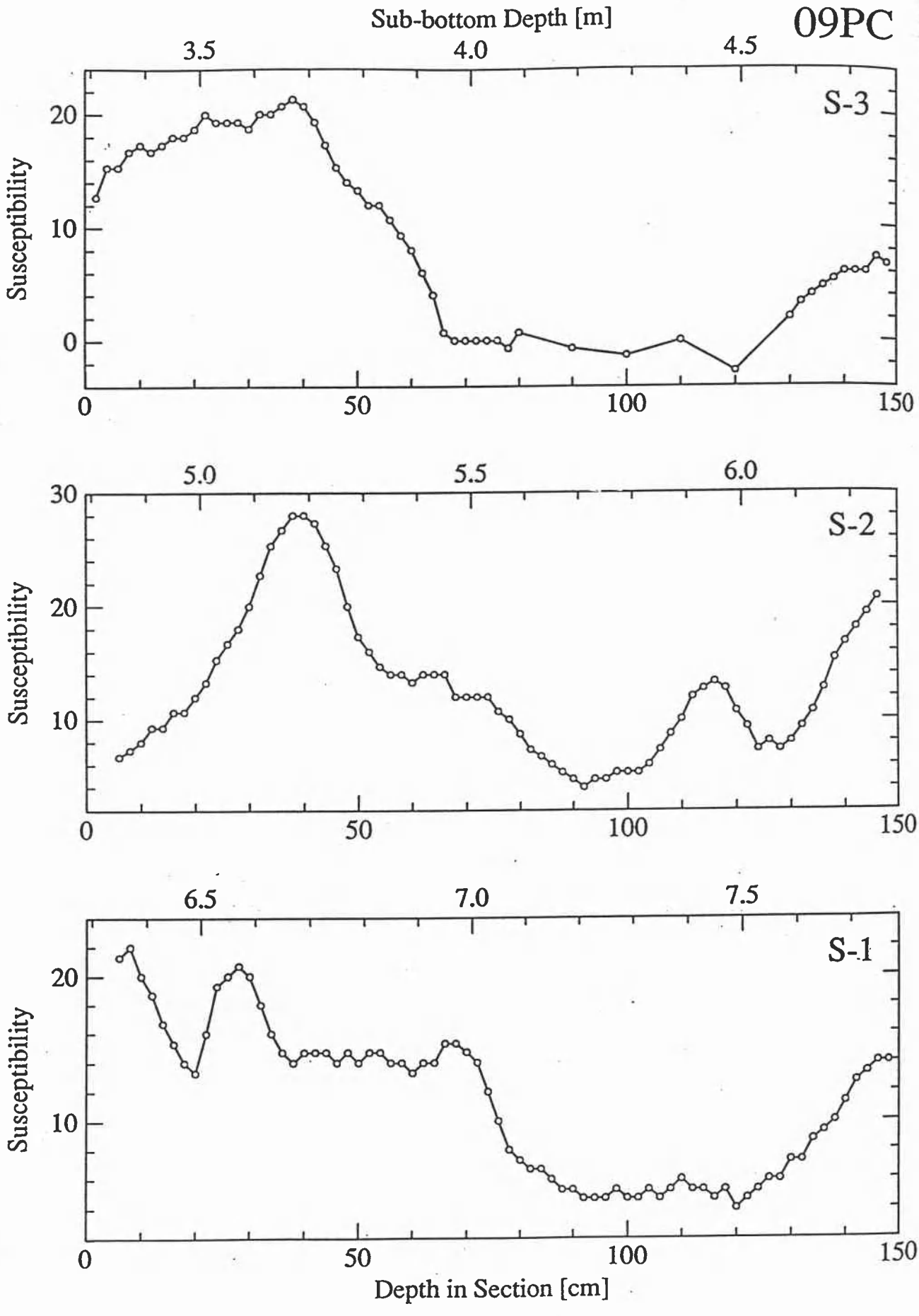
09PC
Sub-bottom Depth [m]
3.5
4.0
4.5
S-3
Susceptibility
20
10
0
0
50
100
150
5.0
5.5
6.0
S-2
30
20
10
6.5
7.0
7.5
S-1
Depth in Section [cm]

VNTR01-10PC

Piston core 10 was taken on 13-Sep-1989 (4.507°S, 102.015°W, 3405 m water depth). The core is 9.45 m long, consisting of calcareous pelagic ooze. After the data selection we use 462 susceptibility determinations (range: 2.7 to 53.3, arithmetic mean: 20.0 (all 10^{-6} unitless SI)). The downcore susceptibility is shown in Figure 30, and Figure 31 shows details of individual measurements by sections.

Data selection. Steps between section boundary S-7/S-6 and a spike at S-2/S-1 were fixed by deleting four data points (S-6: 2 cm and 4 cm, S-2: 142 cm, S-1: 2 cm).

Chronology. Table 17 shows age-depth correlations, and the sedimentation rate is estimated to be about 2.6 cm/ky.

TABLE 17. Age-depth estimates from susceptibility correlations of 10PC

Piston Core	Event Name	Event Age (ka)	Position of Event Section (S-cm)	Position of Event Depth (m)	Sedimentation Rate (from top) (cm/ky)	Core Length (m)	Bottom Age (ka)
			Estimates Made During the Cruise:				
10	6.0	128		3.38	2.6		300–400
			Estimates of this Report:				
10	6.0	130	4-0	3.38	2.60	9.45	300–500 ?

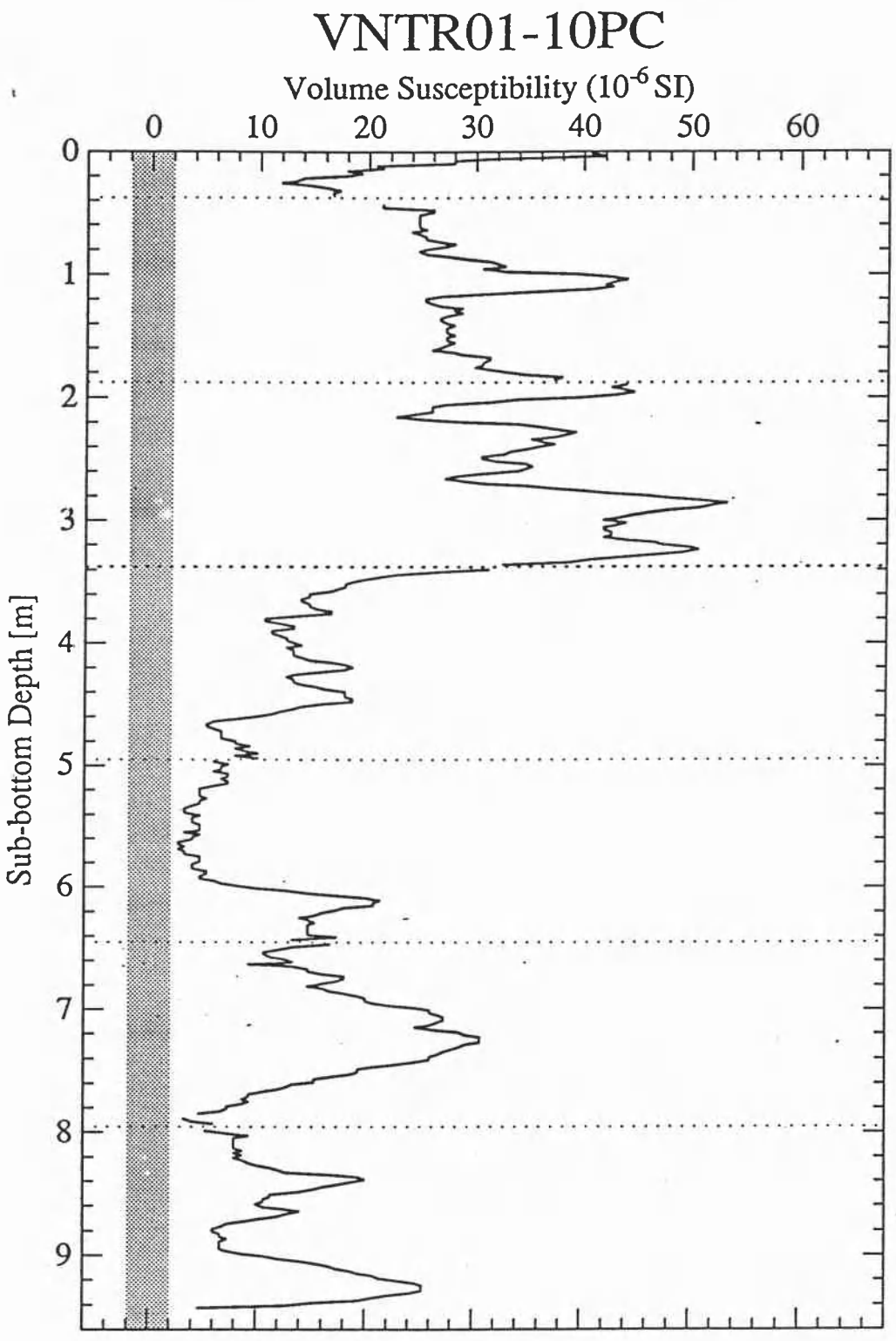

Figure 30. The downhole susceptibility in core VNTR01-10PC (5°S, 102°W). Section boundaries are shown by dotted lines and the approximate noise level by the shaded zero line.

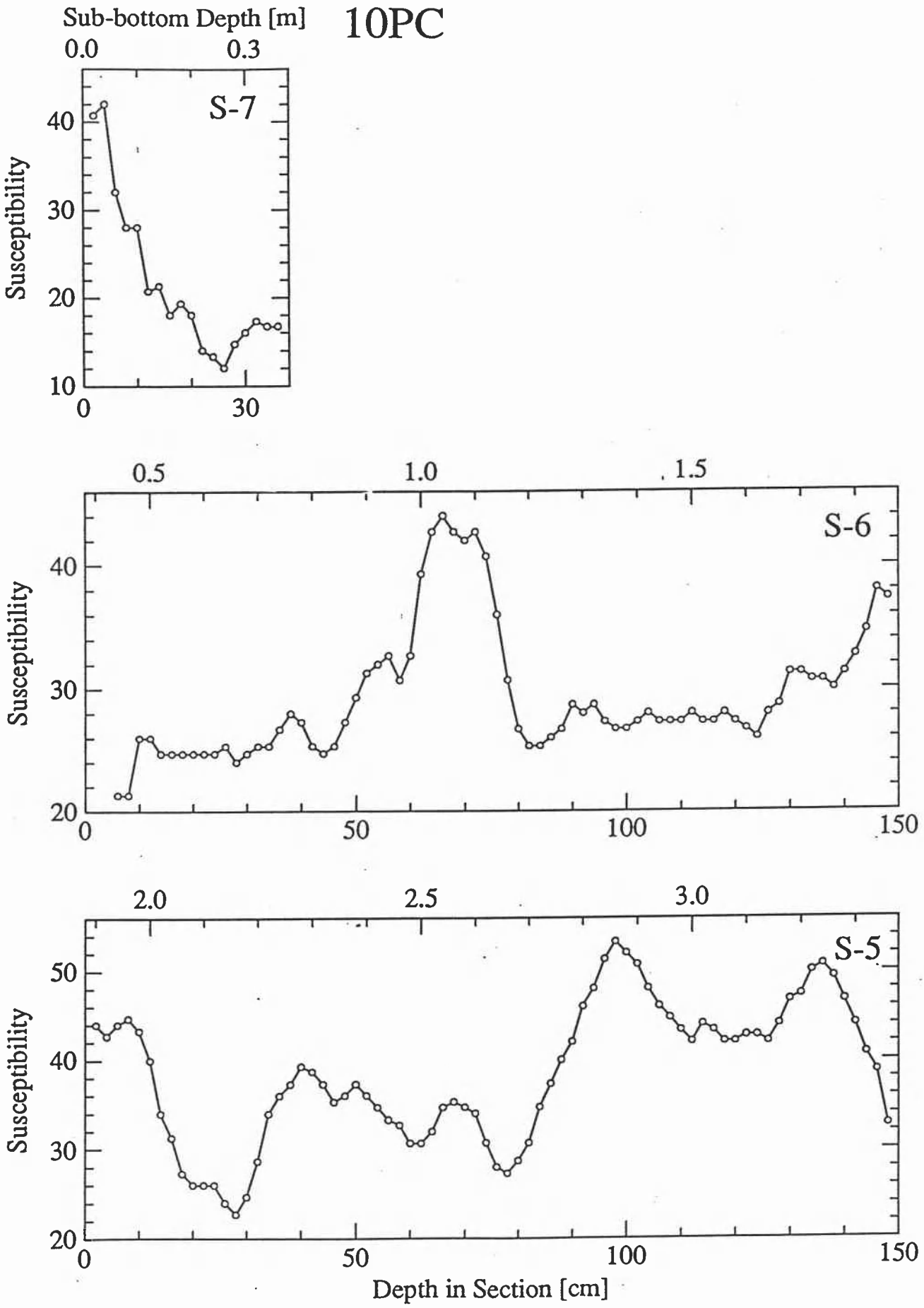

Figure 31. Details of the susceptibility data in core VNTR01-10PC by sections.

10PC

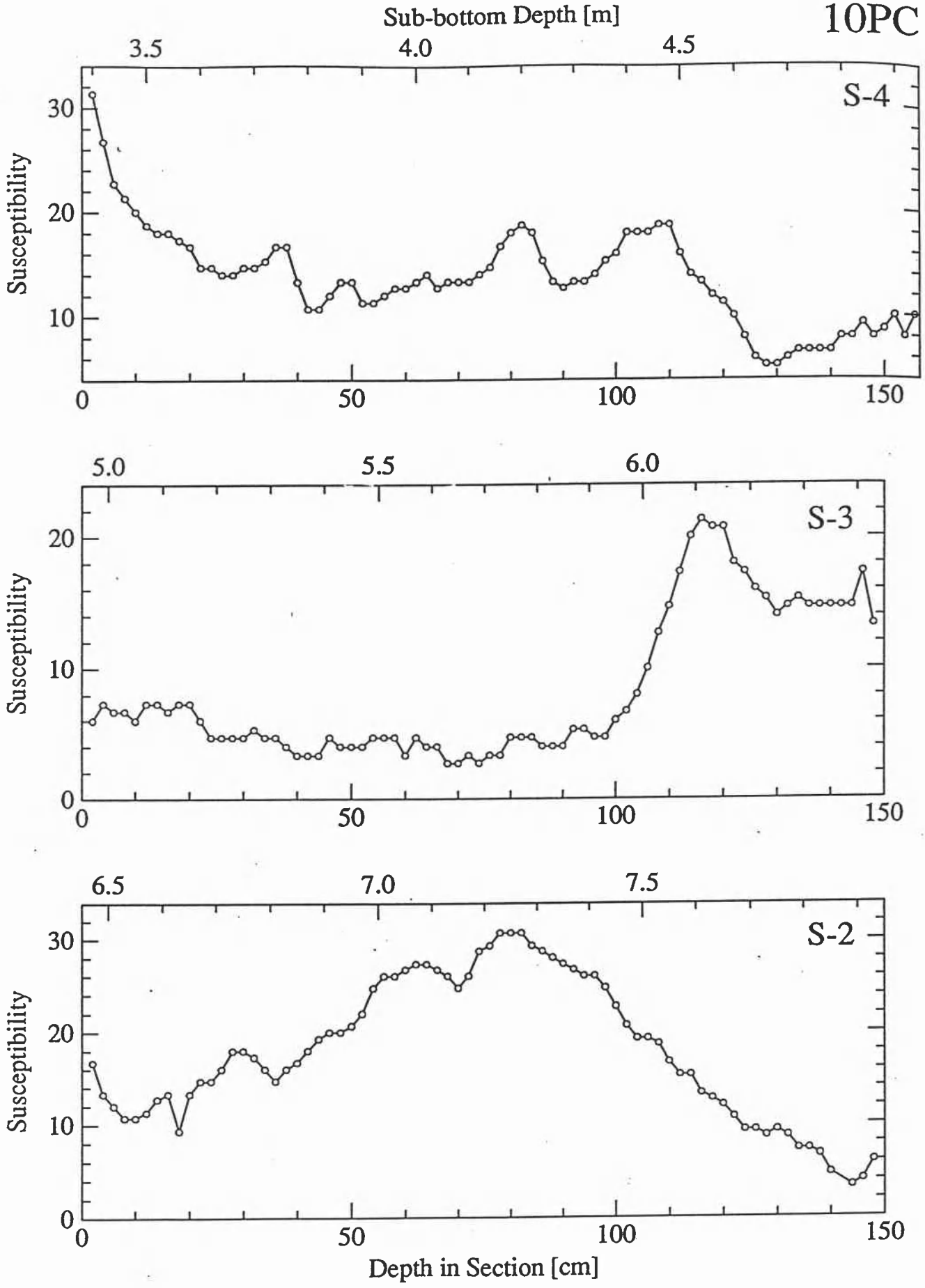
Sub-bottom Depth [m]
3.5
4.0
4.5
S-4
Susceptibility
30
20
10
0
50
100
150
5.0
5.5
6.0
S-3
Susceptibility
20
10
0
50
100
150
6.5
7.0
7.5
S-2
Susceptibility
30
20
10
0
50
100
150
Depth in Section [cm]

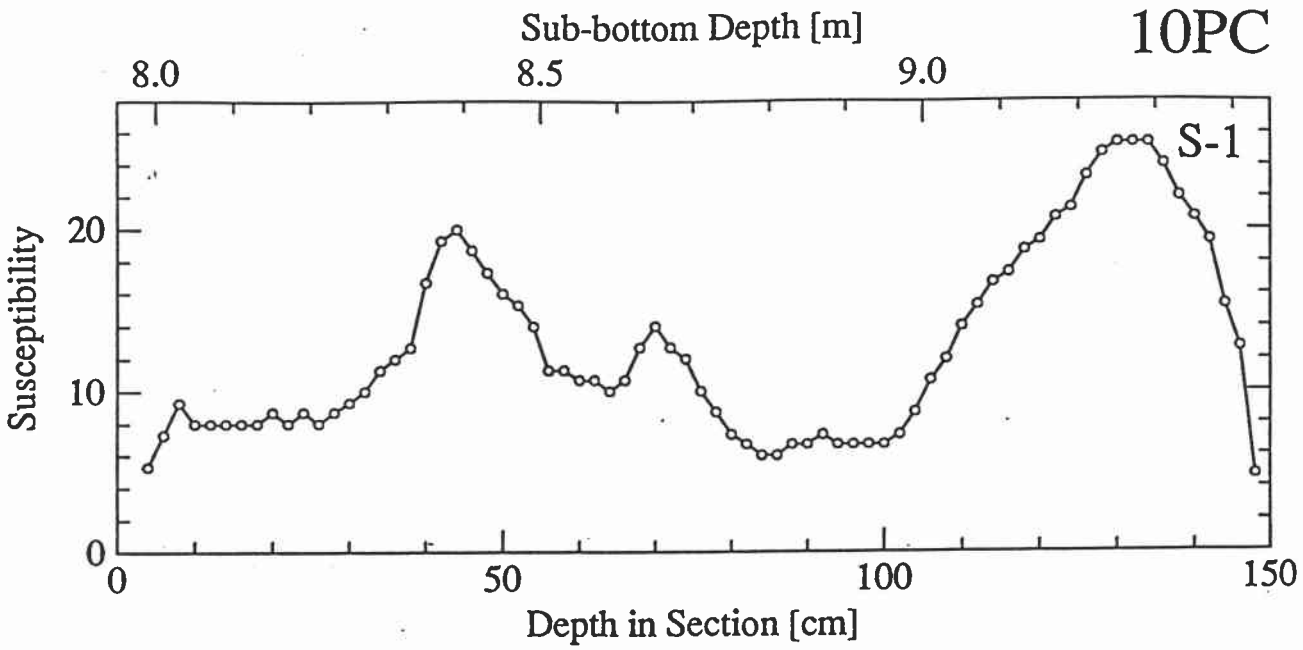
10PC
Sub-bottom Depth [m]
8.0
8.5
9.0
S-1
Susceptibility
20
10
0
0
50
100
150
Depth in Section [cm]

VNTR01-11PC

Piston core 11 was taken on 16 to 17-Sep-1989 (0.131°N, 95.340°W, 3345 m water depth). The core is 11.50 m long, consisting of calcareous pelagic ooze. After the data selection we use 566 susceptibility determinations (range: –0.7 to 43.3, arithmetic mean: 15.1 (all 10^{-6} unitless SI)). The downcore susceptibility is shown in Figure 32, and Figure 33 shows details of individual measurements by sections.

Data selection. Spikes at section boundaries S-6/S-5 and S-5/S-4 were fixed by deleting two data points (S-6: 148 cm, S-4: 2 cm).

Chronology. Table 18 shows age-depth correlations, and the sedimentation rate is estimated to be about 2.1 to 2.8 cm/ky. The chronology of core RC13-110 (0.10°N, 95.65°W), located 35 km west of 11PC, helped in dating 11PC. The susceptibility of 11PC shows similar long term features as the non-carbonate content in RC13-110. Furthermore, some humps in the eolian content of RC13-110 are seen in the susceptibility of 11PC.

TABLE 18. Age-depth estimates from susceptibility correlations of 11PC

Piston Core	Event Name	Event Age (ka)	Position of Event Section (S-cm)	Position of Event Depth (m)	Sedimentation Rate (from top) (cm/ky)	Core Length (m)	Bottom Age (ka)
			Estimates Made During the Cruise:				
11	6.0	128		3.30	2.6		
11	10.0	338		7.48	2.2		
11	12.0	426		9.28	2.2		500–550
			Estimates of this Report:				
11	5.0	74	7-110	2.06	2.78		
11	6.0	130	6-84	3.30	2.54		
11	9.3	331	3-28	7.28	2.20		
11	11.3	405	2-62	9.12	2.25		
11	13.11	481	1-0	10.00	2.08	11.50	540–560

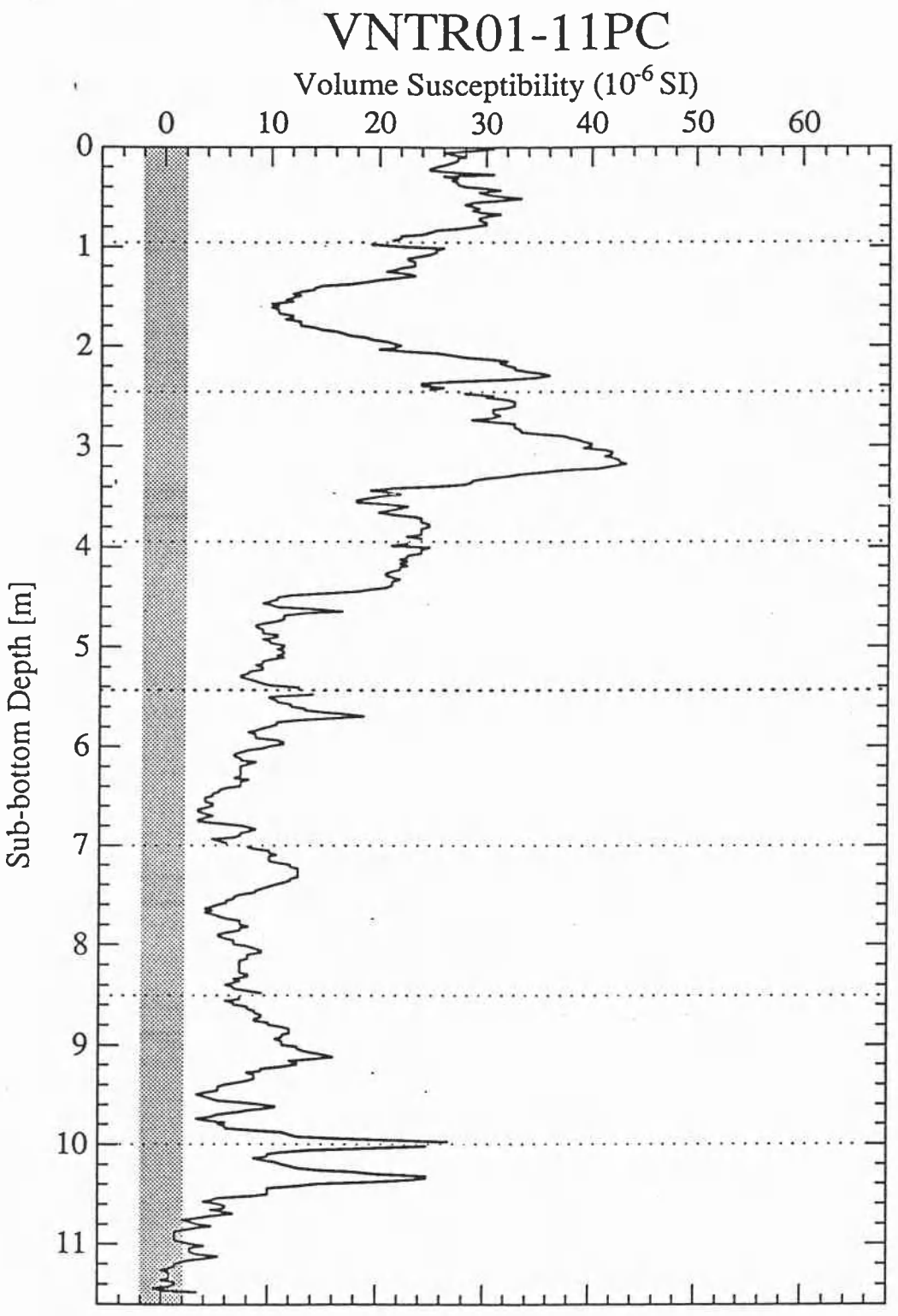

Figure 32. The downhole susceptibility in core VNTR01-11PC (0°N, 95°W). Section boundaries are shown by dotted lines and the approximate noise level by the shaded zero line.

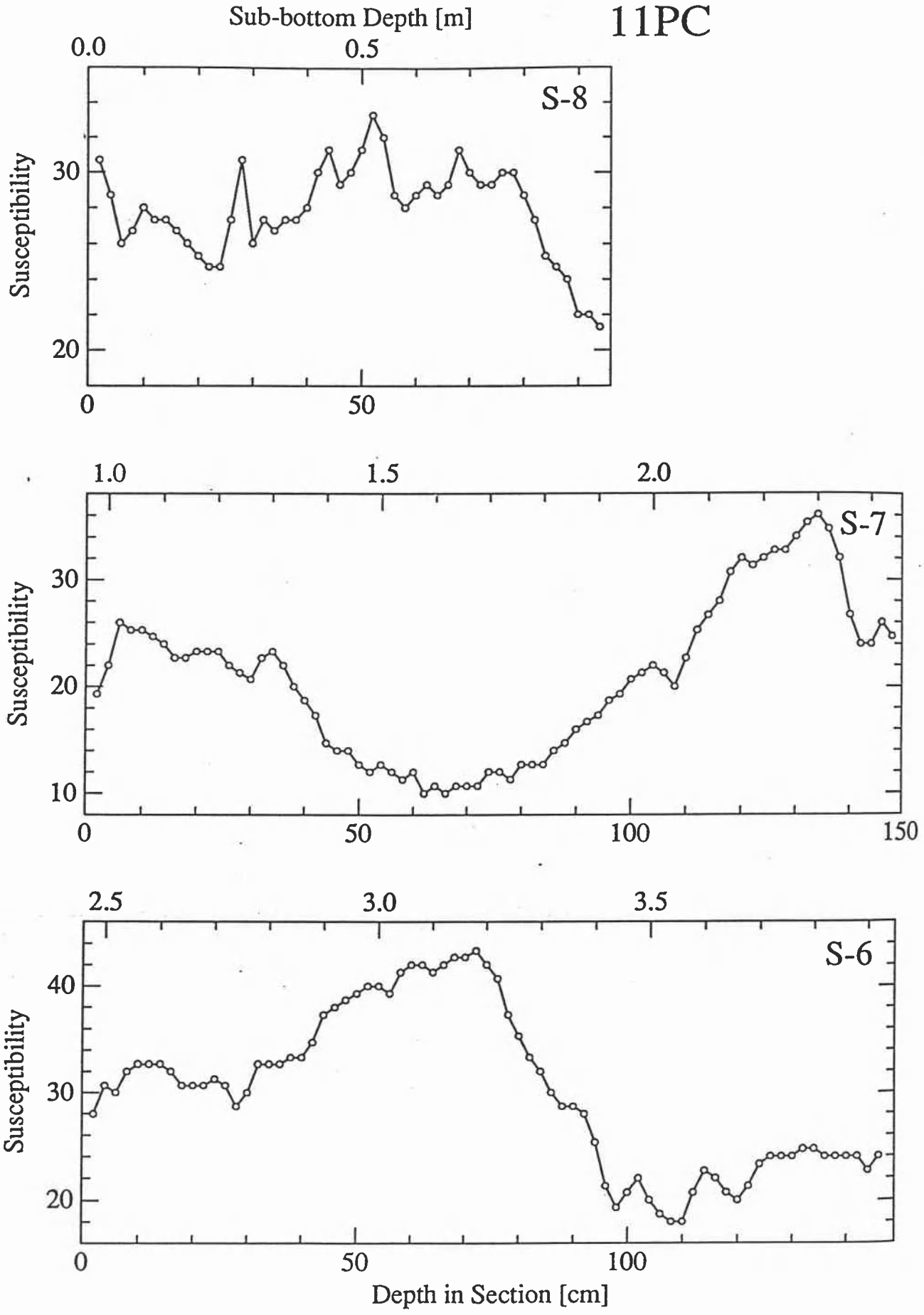

Figure 33. Details of the susceptibility data in core VNTR01-11PC by sections.

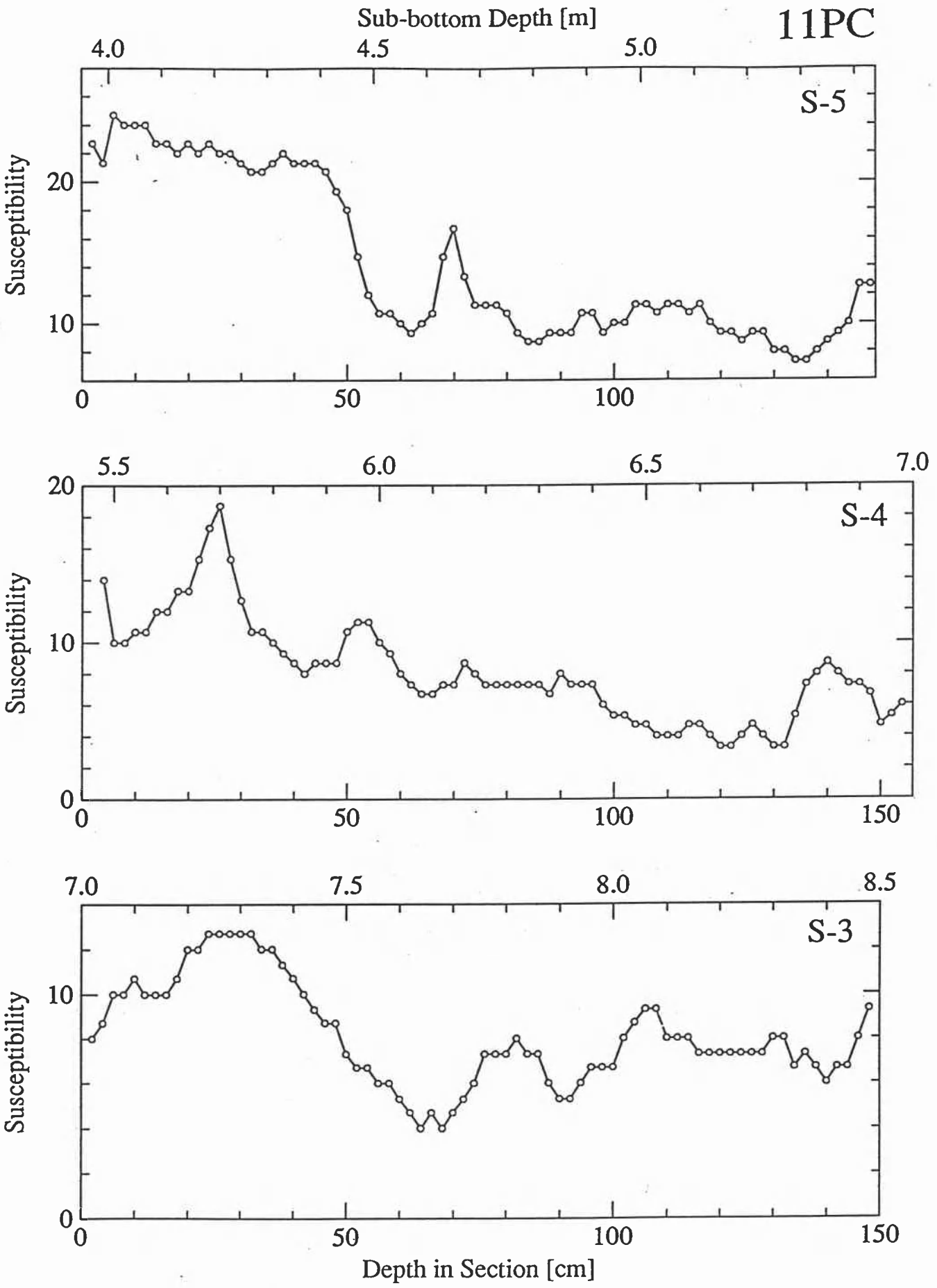
11PC
Sub-bottom Depth [m]
4.0
4.5
5.0
S-5
Susceptibility
20
10
0
50
100
5.5
6.0
6.5
7.0
S-4
Susceptibility
20
10
0
50
100
150
7.0
7.5
8.0
8.5
S-3
Susceptibility
10
0
50
100
150
Depth in Section [cm]

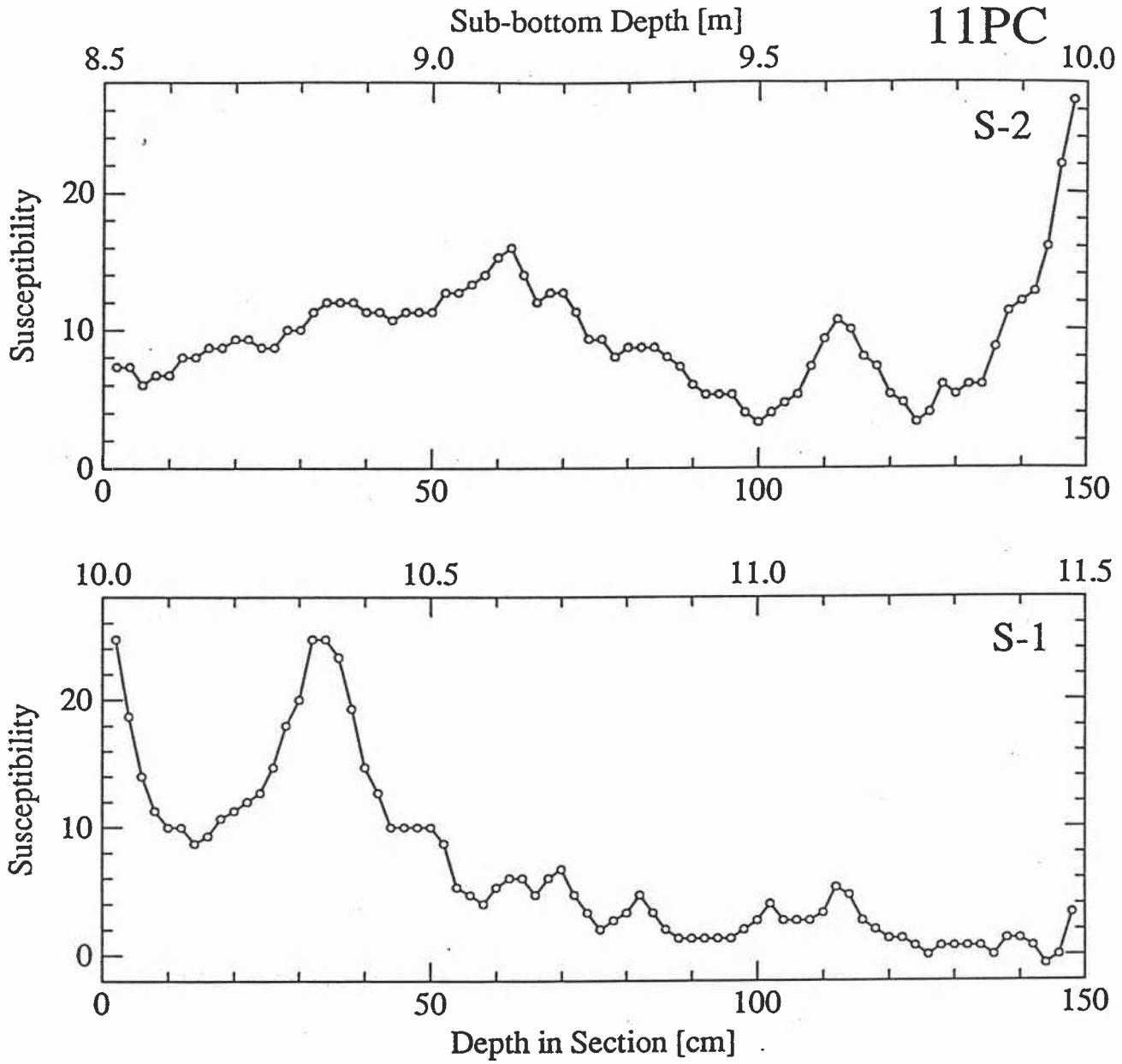
11PC
Sub-bottom Depth [m]
8.5
9.0
9.5
10.0
S-2
Susceptibility
20
10
0
0
50
100
150
10.0
10.5
11.0
11.5
S-1
Susceptibility
20
10
0
0
50
100
150
Depth in Section [cm]

VNTR01-12PC

Piston core 12 was taken on 18-Sep-1989 (3.015°S, 95.082°W, 3535 m water depth). The core is 8.06 m long, consisting of calcareous pelagic ooze. After the data selection we use 397 susceptibility determinations (range: –0.7 to 21.3, arithmetic mean: 8.6 (all 10^{-6} unitless SI)). The downcore susceptibility is shown in Figure 34, and Figure 35 shows details of individual measurements by sections.

Data selection. The measurements seem to be smooth across all the section boundaries and no data were deleted.

Chronology. Table 19 shows age-depth correlations, and the sedimentation rate is estimated to be on the order of 1.2 cm/ky.

TABLE 19. Age-depth estimates from susceptibility correlations of 12PC

Piston Core	Event Name	Event Age (ka)	Position of Event Section (S-cm)	Position of Event Depth (m)	Sedimentation Rate (from top) (cm/ky)	Core Length (m)	Bottom Age (ka)
			Estimates Made During the Cruise:				
12	6.0	128		1.58	1.2		
12	12.0	426		5.08	1.2		600–700
			Estimates of this Report:				
12	5.0	74	5-18	0.60	0.81		
12	6.0	130	5-116	1.58	1.22	8.06	500-800 ?

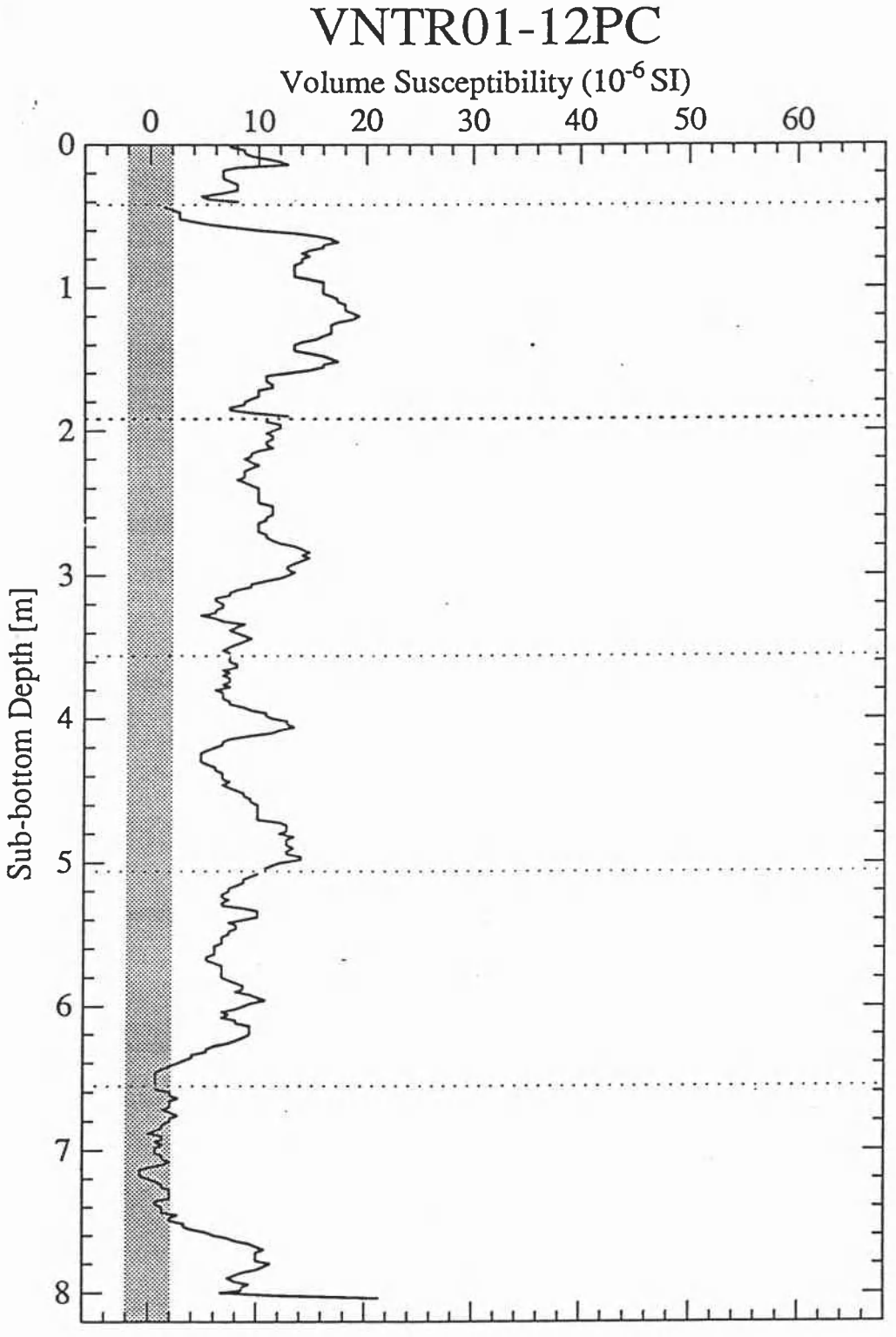

Figure 34. The downhole susceptibility in core VNTR01-12PC (3°S, 95°W). Section boundaries are shown by dotted lines and the approximate noise level by the shaded zero line.

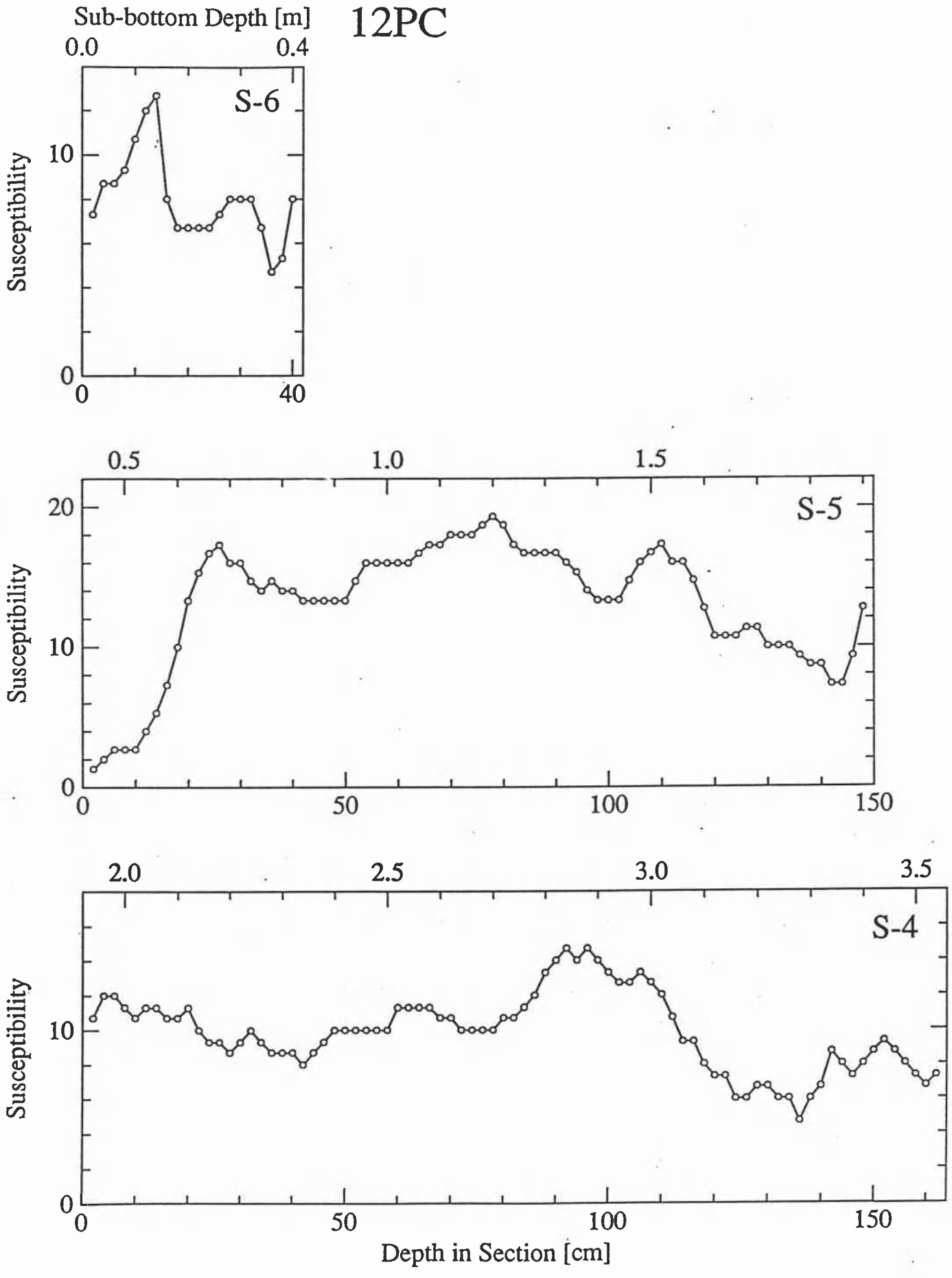

Figure 35. Details of the susceptibility data in core VNTR01-12PC by sections.

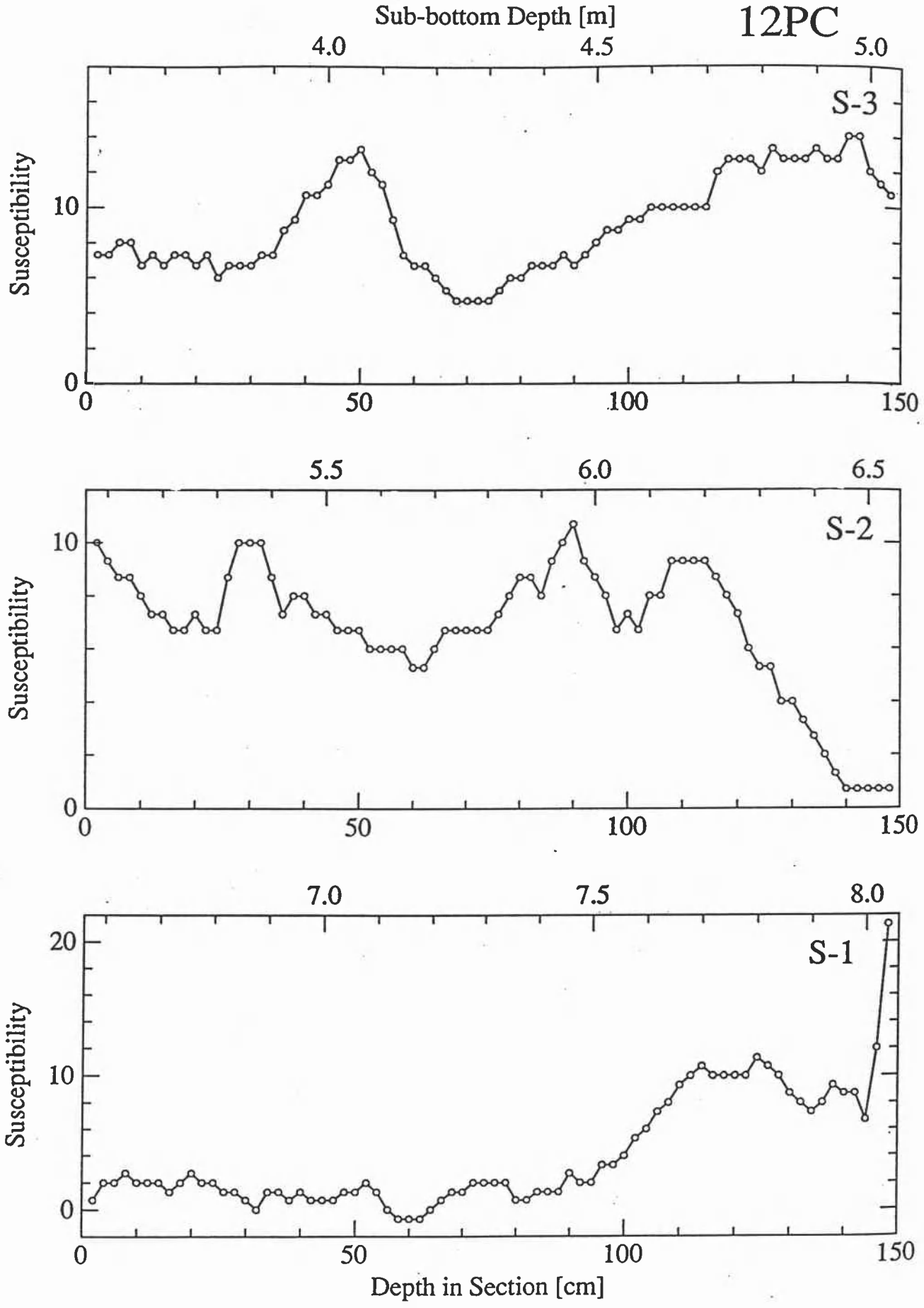
12PC
Sub-bottom Depth [m]
4.0
4.5
5.0
S-3
Susceptibility
10
0
0
50
100
150
5.5
6.0
6.5
S-2
Susceptibility
10
0
0
50
100
150
7.0
7.5
8.0
S-1
Susceptibility
20
10
0
0
50
100
150
Depth in Section [cm]

VNTR01-13PC

Piston core 13 was taken on 20-Sep-1989 (3.100°S, 90.825°W, 3304 m water depth). The core is 9.24 m long, consisting of calcareous pelagic ooze. After the data selection we use 454 susceptibility determinations (range: –3.3 to 22.7, arithmetic mean: 7.6 (all 10^{-6} unitless SI)). The downcore susceptibility is shown in Figure 36, and Figure 37 shows details of individual measurements by sections.

Data selection. A spike at section boundary S-4/S-3 was fixed by deleting one data point (S-3: 2 cm).

Chronology. Table 20 shows age-depth correlations, and the sedimentation rate is estimated to be about 0.9 cm/ky.

TABLE 20. Age-depth estimates from susceptibility correlations of 13PC

Piston Core	Event Name	Event Age (ka)	Position of Event Section (S-cm)	Position of Event Depth (m)	Sedimentation Rate (from top) (cm/ky)	Core Length (m)	Bottom Age (ka)
			Estimates Made During the Cruise:				
13	6.0	128		1.10	0.9		1000 ?
			Estimates of this Report:				
13	5.0	74	6-52	0.66	0.89		
13	6.0	130	6-94	1.08	0.83	9.24	600–1100 ?

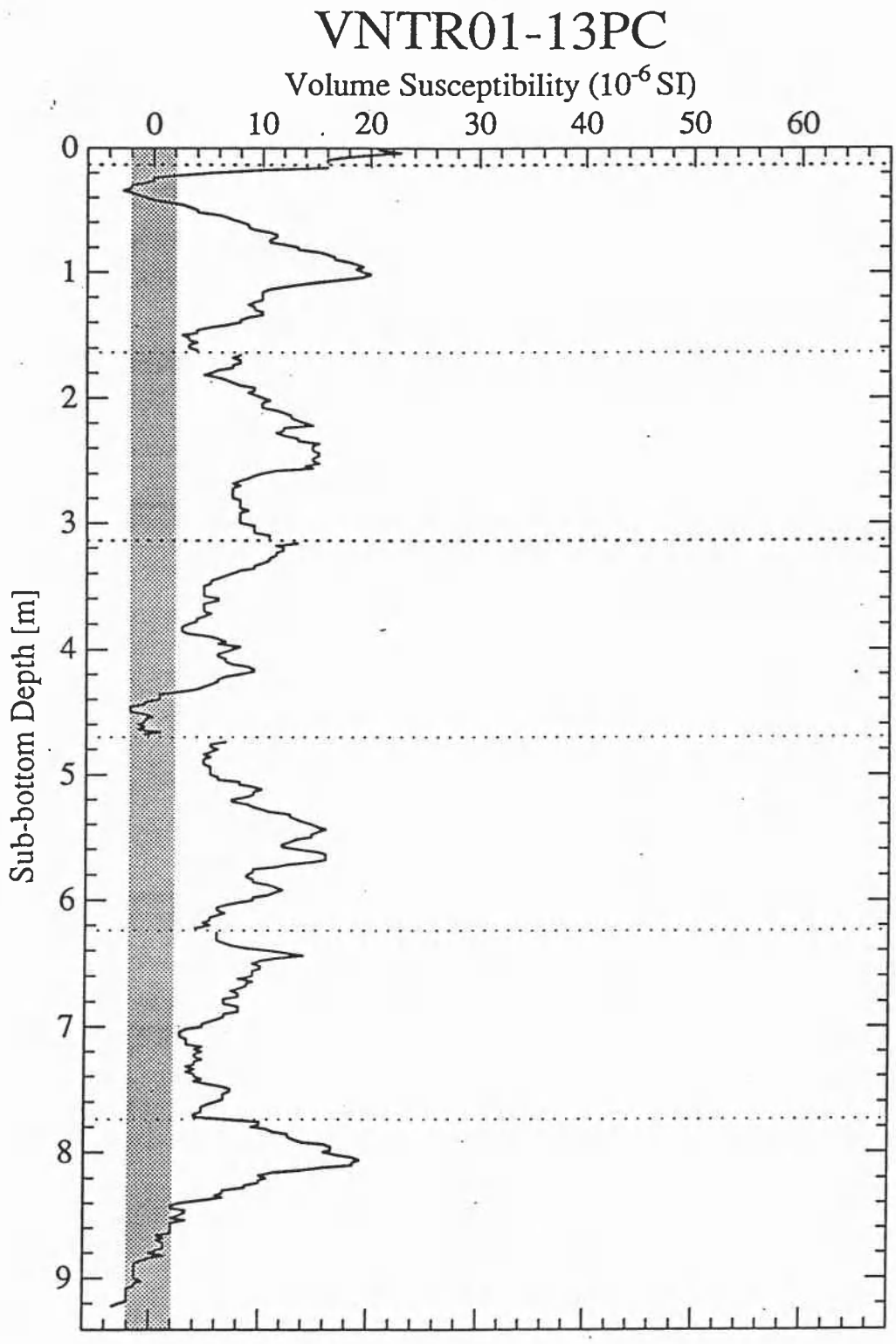

Figure 36. The downhole susceptibility in core VNTR01-13PC (3°S, 91°W). Section boundaries are shown by dotted lines and the approximate noise level by the shaded zero line.

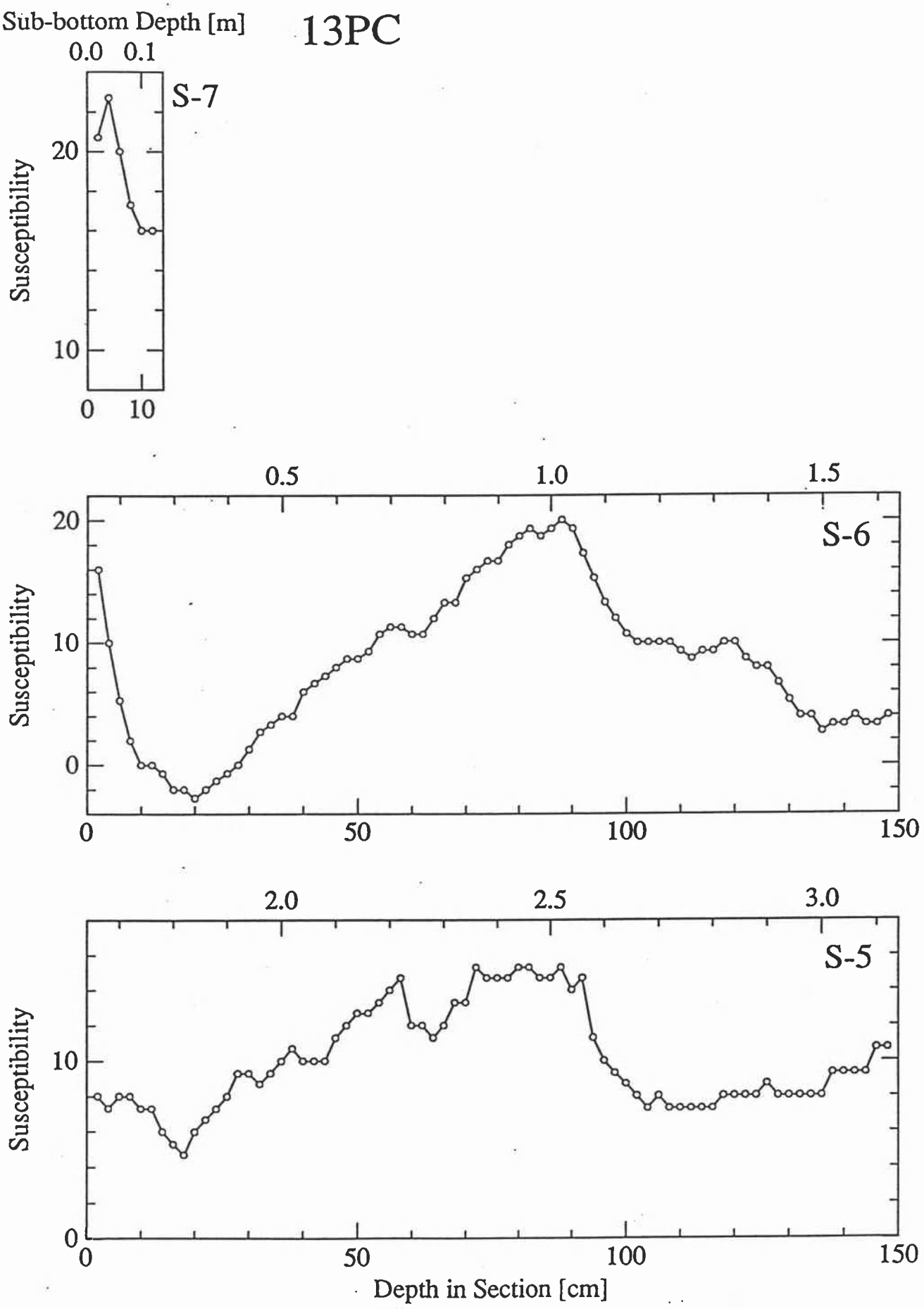

Figure 37. Details of the susceptibility data in core VNTR01-13PC by sections.

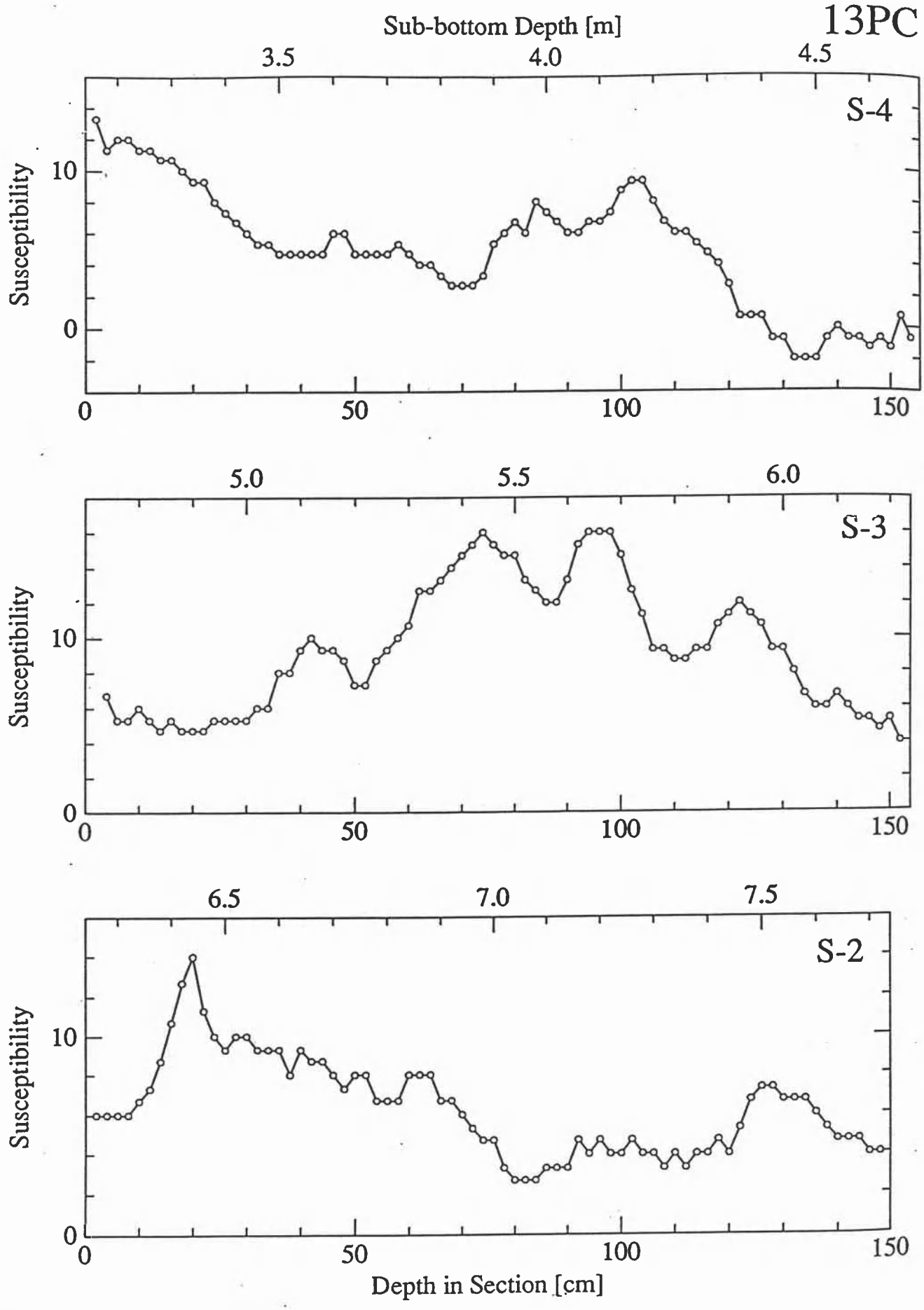
13PC
Sub-bottom Depth [m]
3.5
4.0
4.5
S-4
Susceptibility
10
0
0
50
100
150
5.0
5.5
6.0
S-3
Susceptibility
10
0
0
50
100
150
6.5
7.0
7.5
S-2
Susceptibility
10
0
0
50
100
150
Depth in Section [cm]

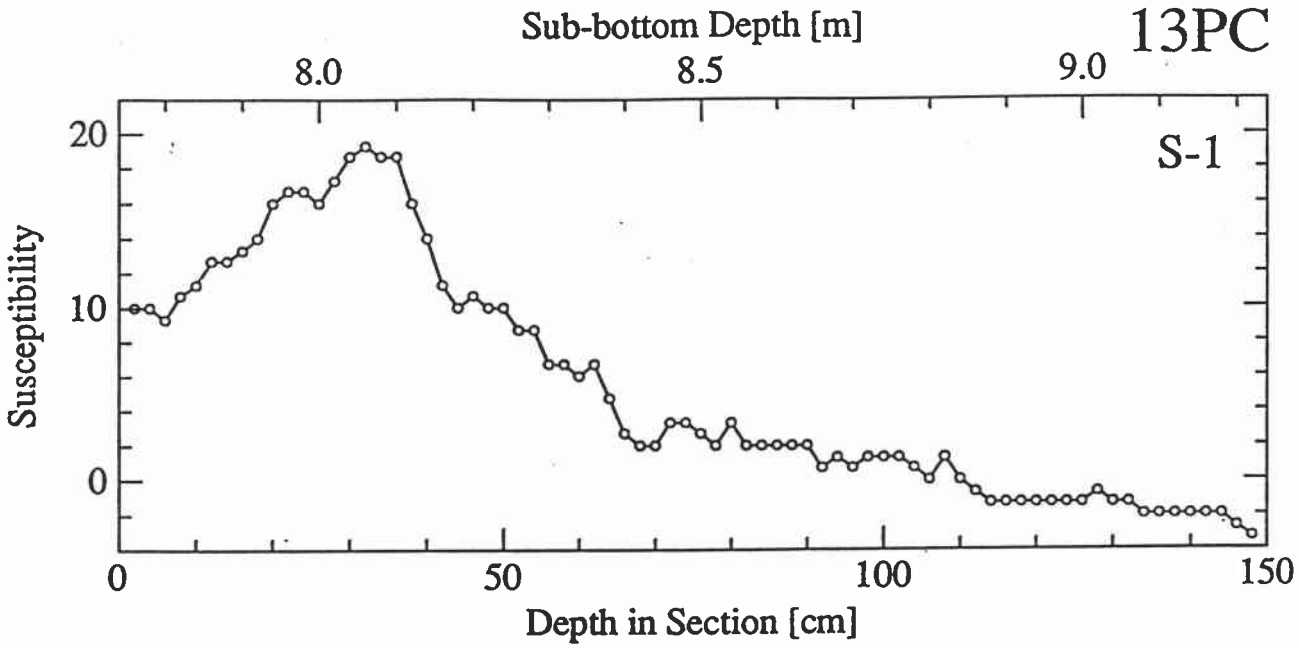
Sub-bottom Depth [m]
8.0
8.5
9.0
13PC
S-1
Susceptibility
20
10
0
0
50
100
150
Depth in Section [cm]

VNTR01-14PC

Piston core 14 was taken on 22-Sep-1989 (1.485°N, 89.862°W, 1944 m water depth). The core is 11.61 m long, consisting of foraminiferal sand. After the data selection we use 571 susceptibility determinations (range: 0.0 to 316.0, arithmetic mean: 16.4 (all 10^{-6} unitless SI)). The downcore susceptibility is shown in Figures 38 and 39, and Figure 40 shows details of individual measurements by sections.

Data selection. A spike at section boundary S-4A/S-4 was fixed by deleting one data points (S-4A: 46 cm).

Chronology. Table 21 shows age-depth correlations, and the sedimentation rate is estimated to be about 1.8 to 2.0 cm/ky. Correlations to the susceptibility of 11PC helped in assigning the age for the lower part of 14PC.

VNTR01-15PC

Coring was attempted on 22-Sep-1989 at the same site as 14PC (1.485°N, 89.862°W, 1955 m water depth), but no piston core was recovered.

TABLE 21. Age-depth estimates from susceptibility correlations of 14PC

Piston Core	Event Name	Event Age (ka)	Position of Event Section (S-cm)	Position of Event Depth (m)	Sedimentation Rate (from top) (cm/ky)	Core Length (m)	Bottom Age (ka)
			Estimates Made During the Cruise:				
14	6.0	128		2.30	1.8		
14	Ash L	256		4.62	1.8		
14	12.0	426		7.10	1.7		600–700
			Estimates of this Report:				
14	6.0	130	8-136	2.30	1.77		
14	Ash L	230	6-70	4.62	2.01		
14	13.11	481	3-119	8.89	1.85	11.61	550–650

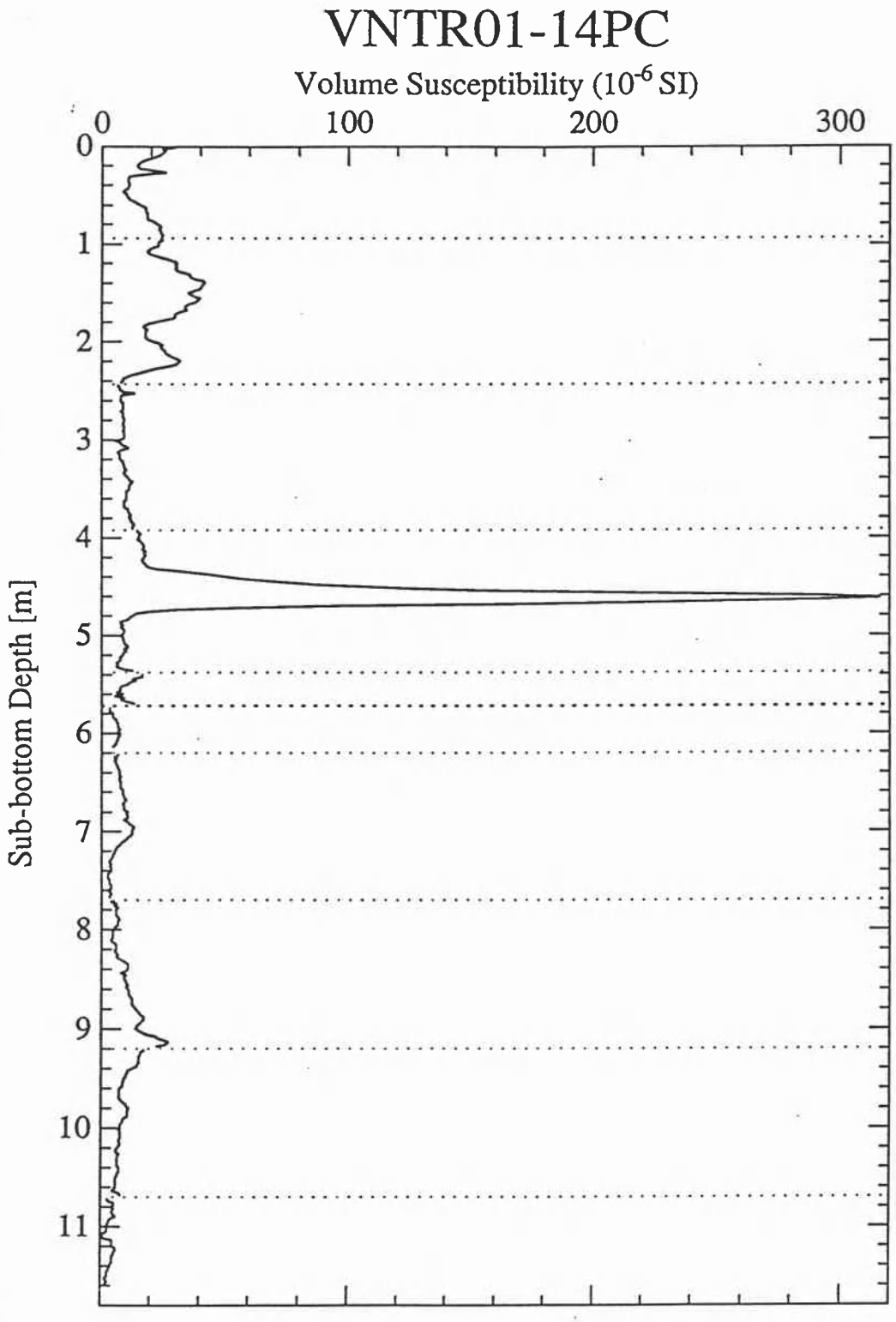

Figure 38. The downhole susceptibility in core VNTR01-14PC (1°N, 90°W). Section boundaries are shown by dotted lines.

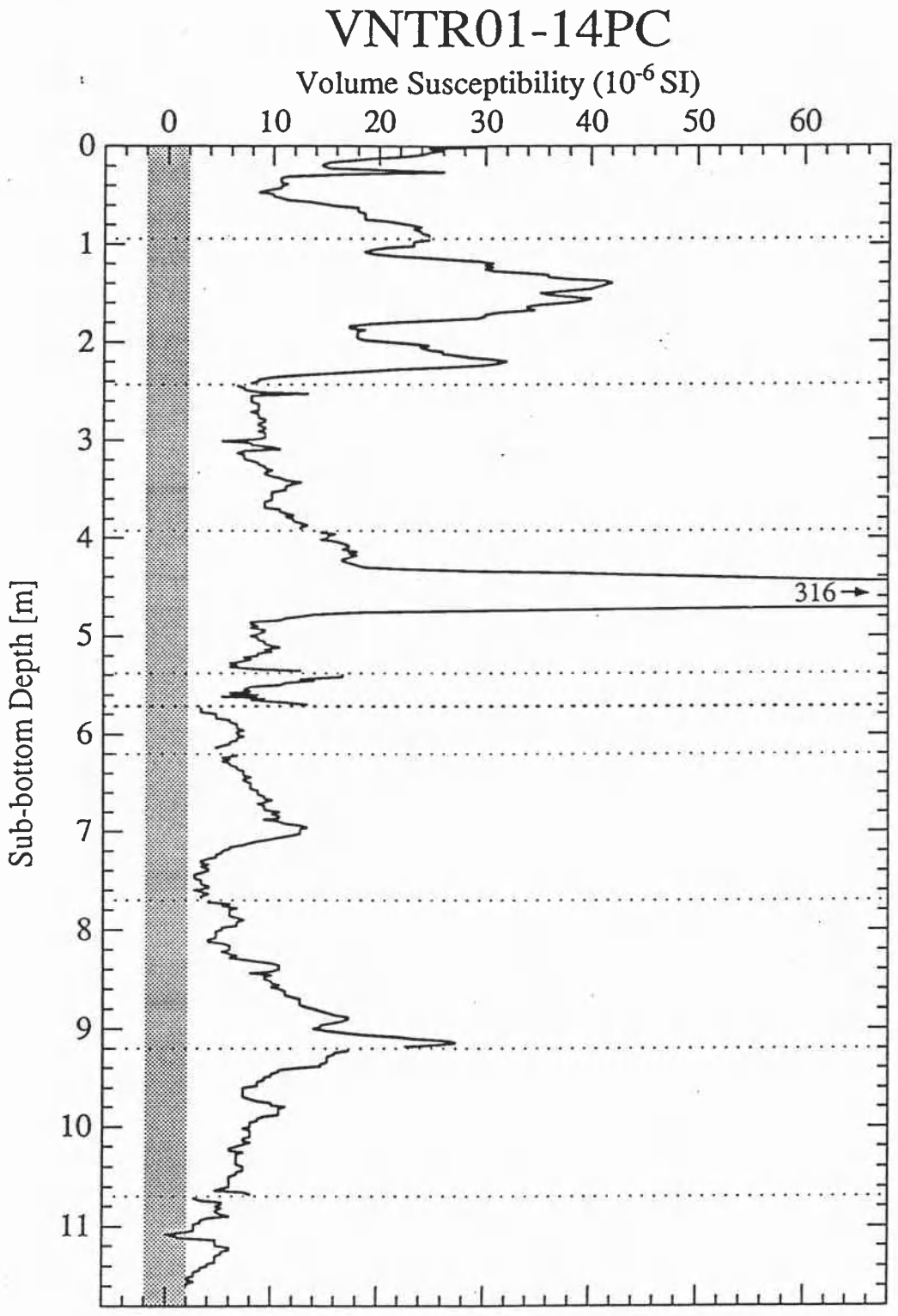

Figure 39. Blown up version of the downhole susceptibility in core VNTR01-14PC. Section boundaries are shown by dotted lines and the approximate noise level by the shaded zero line.

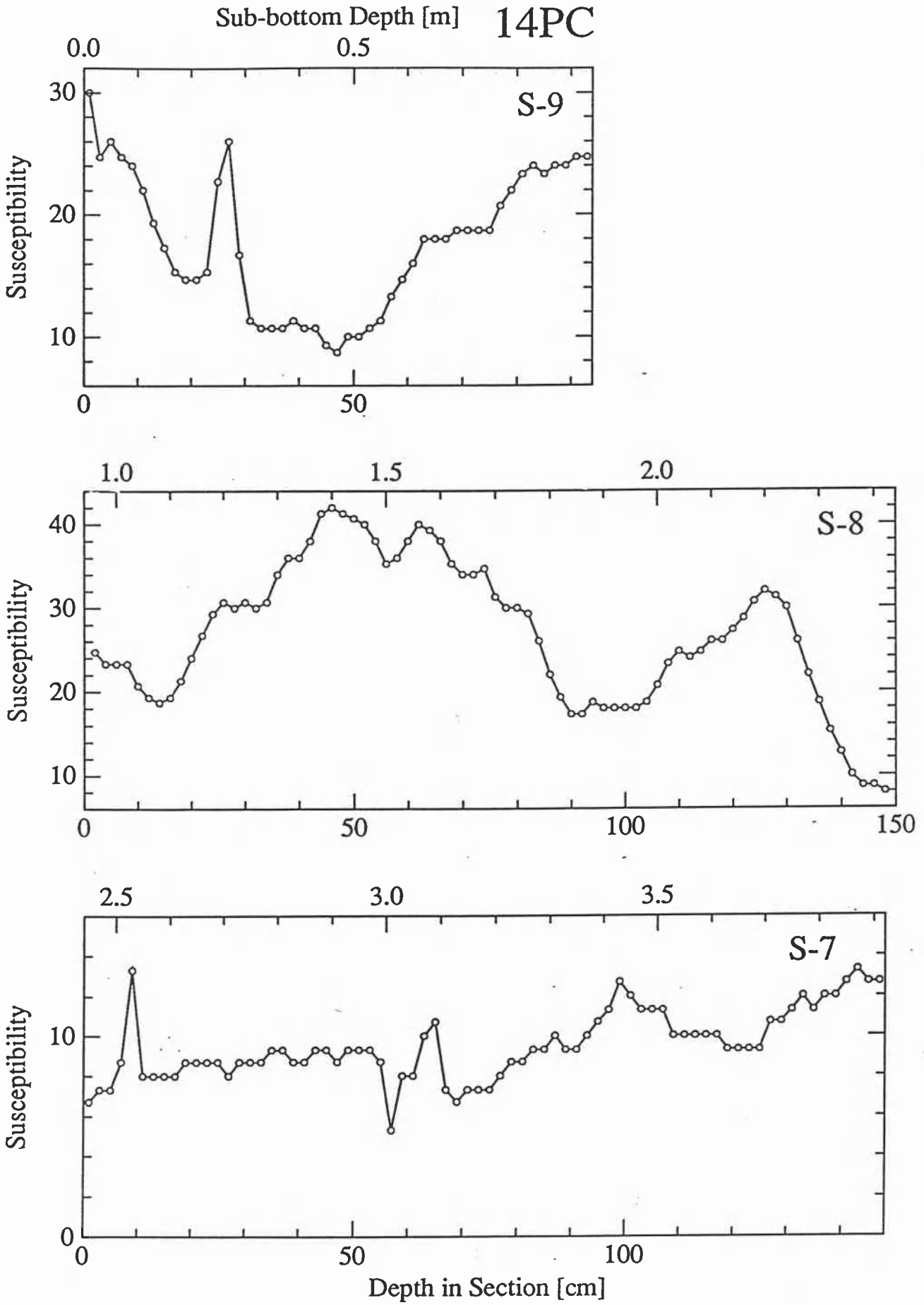

Figure 40. Details of the susceptibility data in core VNTR01-14PC by sections.

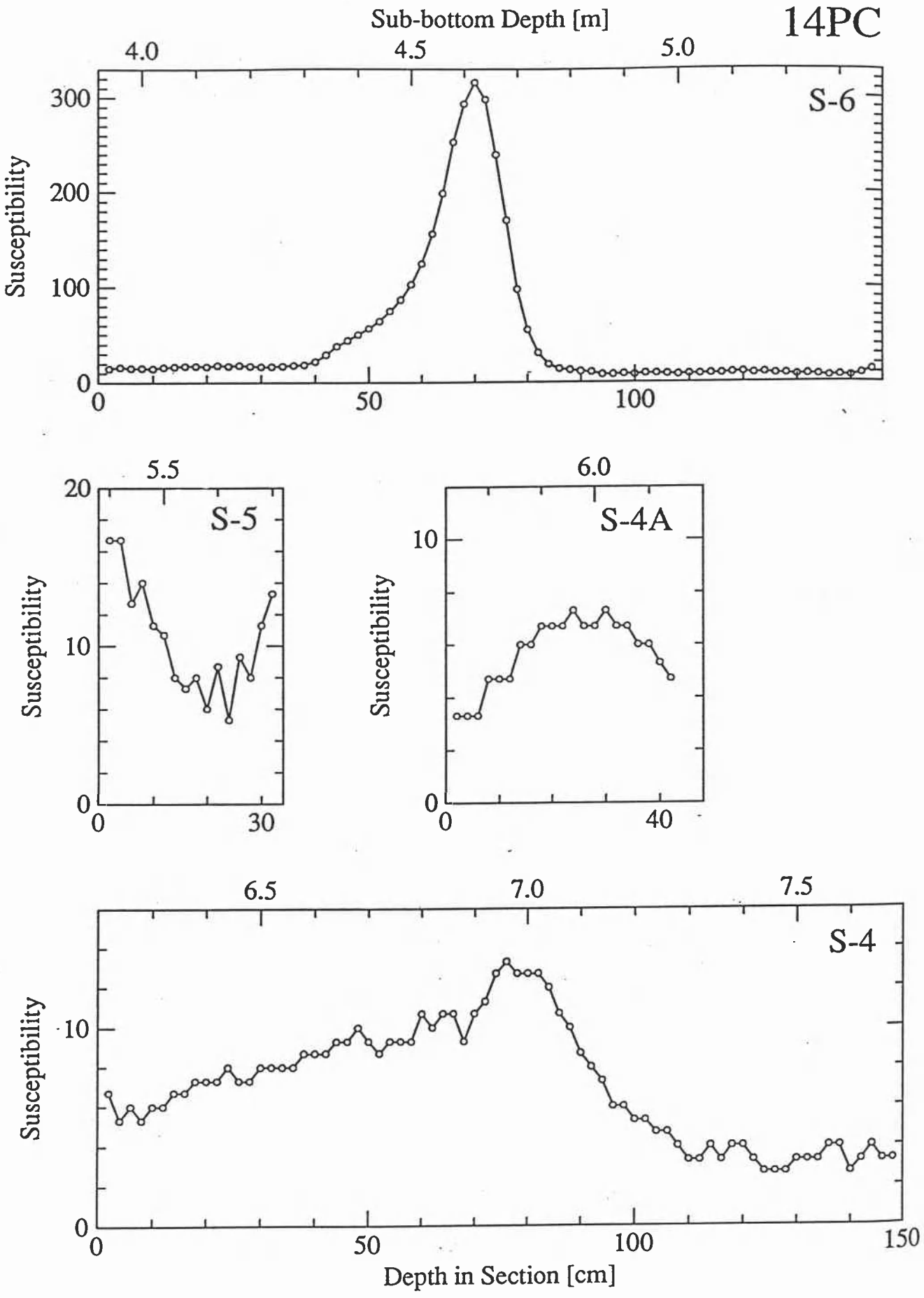
14PC
Sub-bottom Depth [m]
4.0
4.5
5.0
S-6
Susceptibility
300
200
100
0
0
50
100
5.5
S-5
20
10
0
0
30
6.0
S-4A
10
0
0
40
6.5
7.0
7.5
S-4
10
0
0
50
100
150
Depth in Section [cm]

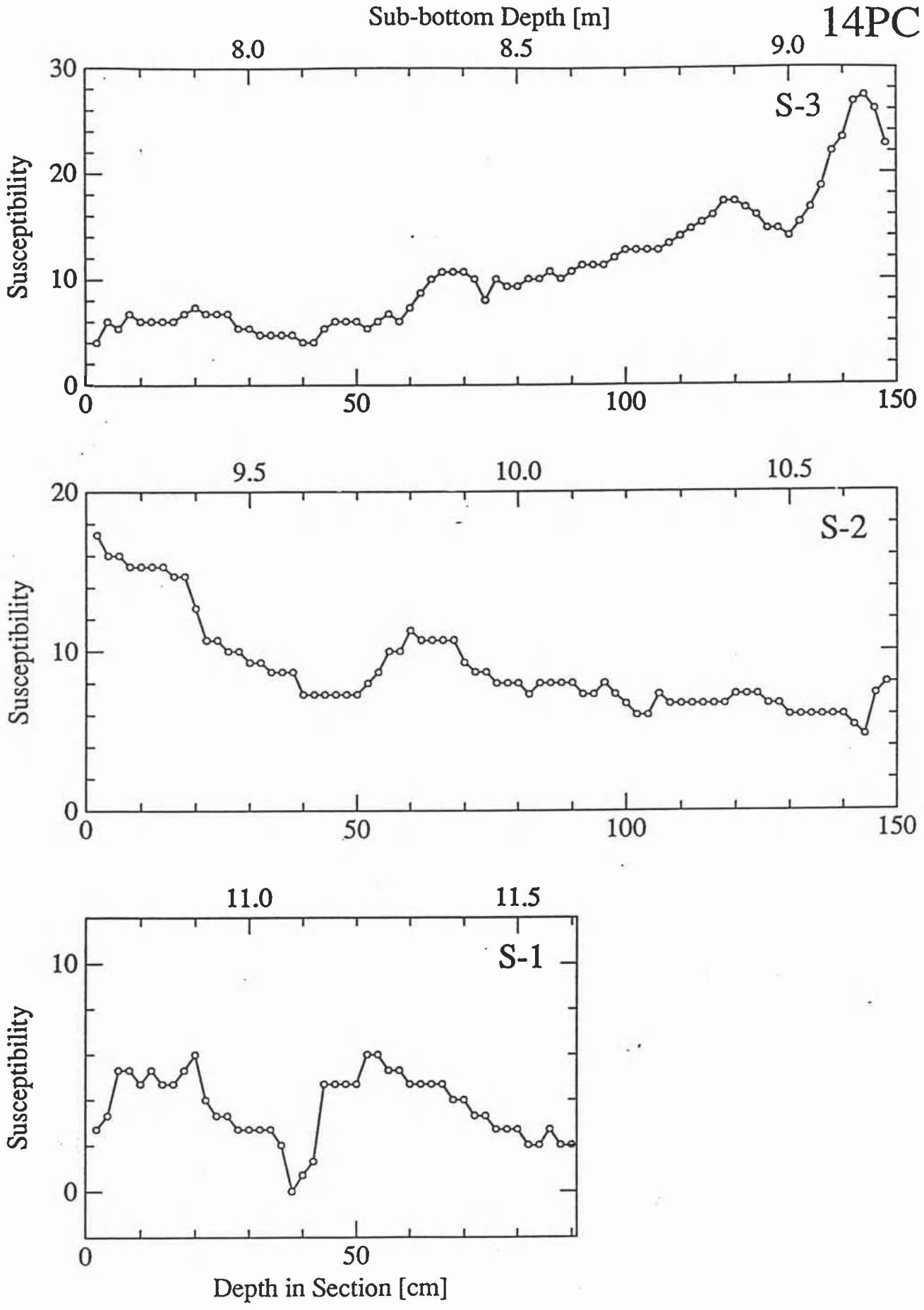
14PC
Sub-bottom Depth [m]
8.0
8.5
9.0
S-3
Susceptibility
30
20
10
0
0
50
100
150
9.5
10.0
10.5
S-2
Susceptibility
20
10
0
0
50
100
150
11.0
11.5
S-1
Susceptibility
10
0
0
50
Depth in Section [cm]

VNTR01-16PC

Piston core 16 was taken on 22-Sep-1989 (2.598°N, 89.737°W, 1546 m water depth). The core is 9.44 m long, consisting of foraminiferal sand. After the data selection we use 466 susceptibility determinations (range: –4.0 to 44.7, arithmetic mean: 3.6 (all 10^{-6} unitless SI)). The downcore susceptibility is shown in Figure 41, and Figure 42 shows details of individual measurements by sections.

Data selection. The measurements seem to be smooth across all the section boundaries and no data were deleted.

Chronology. Table 22 shows age-depth correlations, and the sedimentation rate is estimated to be about 1.6 cm/ky. Correlations to the susceptibility of 11PC helped in assigning the age for the lower part of 16PC.

TABLE 22. Age-depth estimates from susceptibility correlations of 16PC

Piston Core	Event Name	Event Age (ka)	Position of Event Section (S-cm)	Position of Event Depth (m)	Sedimentation Rate (from top) (cm/ky)	Core Length (m)	Bottom Age (ka)
			Estimates Made During the Cruise:				
16	Ash L	256		3.75	1.5		600–700
			Estimates of this Report:				
16	Ash L	230	4-45	3.75	1.63		
16	13.11	481	2-117	7.61	1.58	9.44	550–650

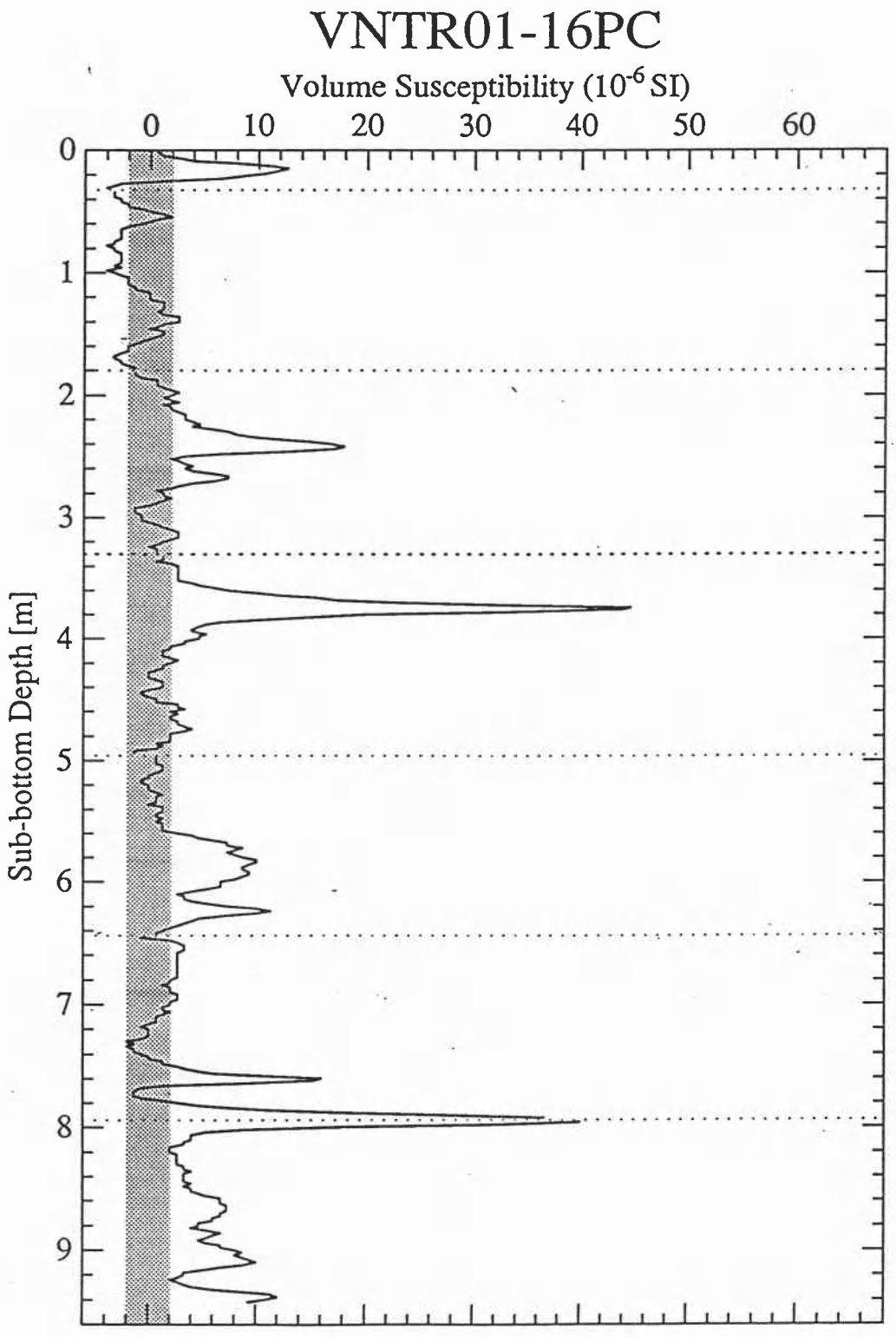

Figure 41. The downhole susceptibility in core VNTR01-16PC (3°N, 90°W). Section boundaries are shown by dotted lines and the approximate noise level by the shaded zero line.

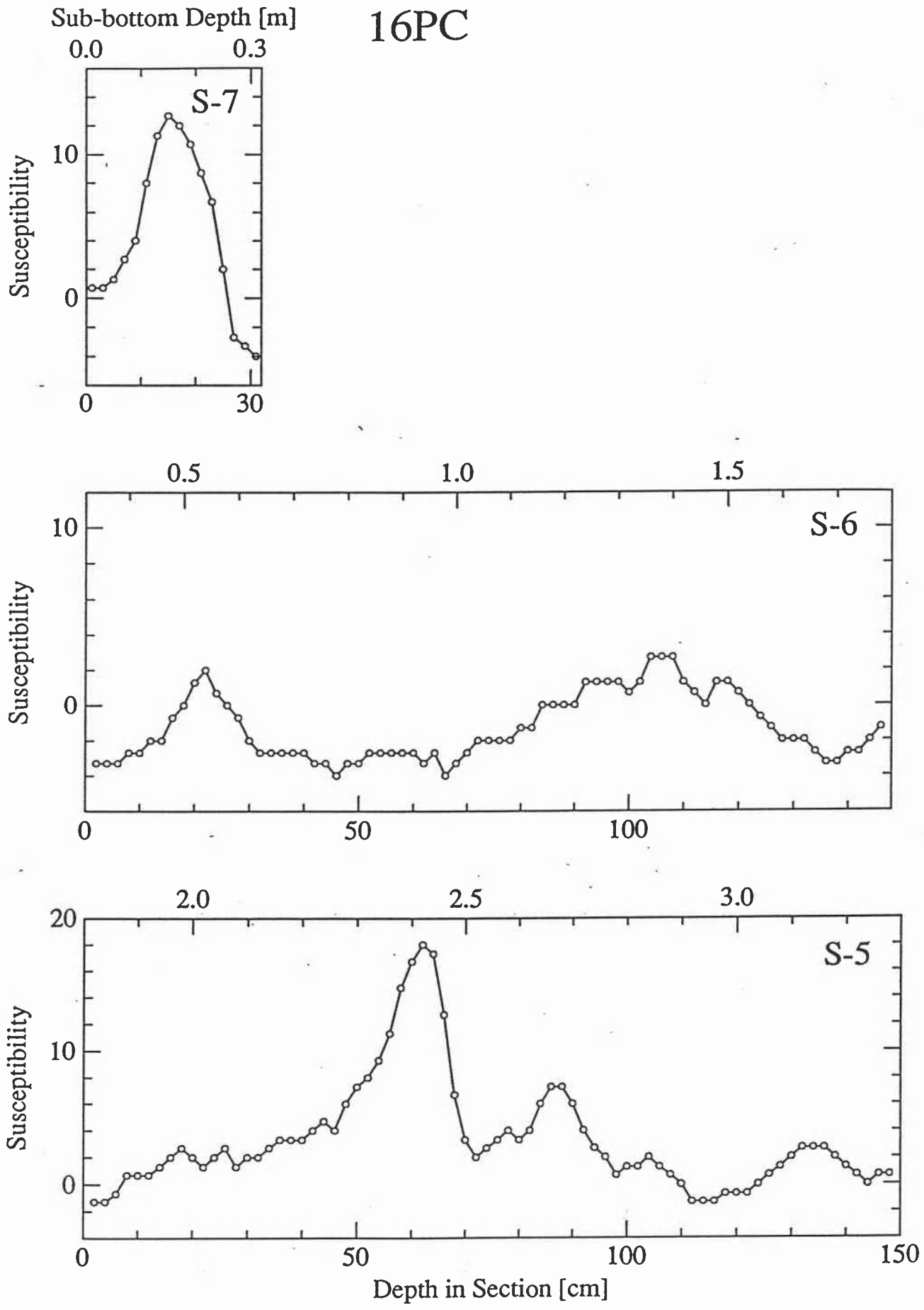

Figure 42. Details of the susceptibility data in core VNTR01-16PC by sections.

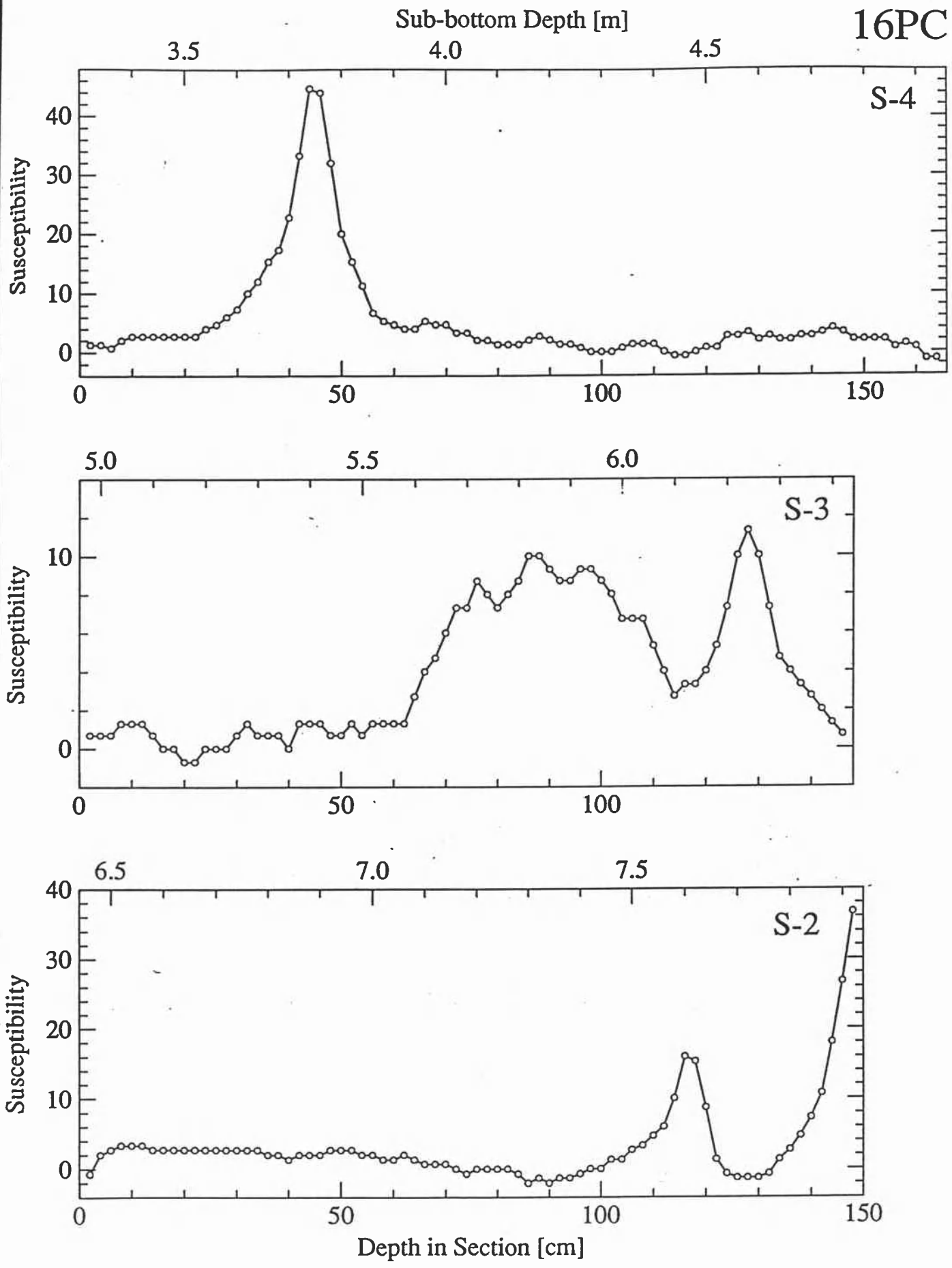
16PC
Sub-bottom Depth [m]
3.5
4.0
4.5
S-4
Susceptibility
40
30
20
10
0
0
50
100
150
5.0
5.5
6.0
S-3
Susceptibility
10
0
0
50
100
6.5
7.0
7.5
S-2
Susceptibility
40
30
20
10
0
0
50
100
150
Depth in Section [cm]

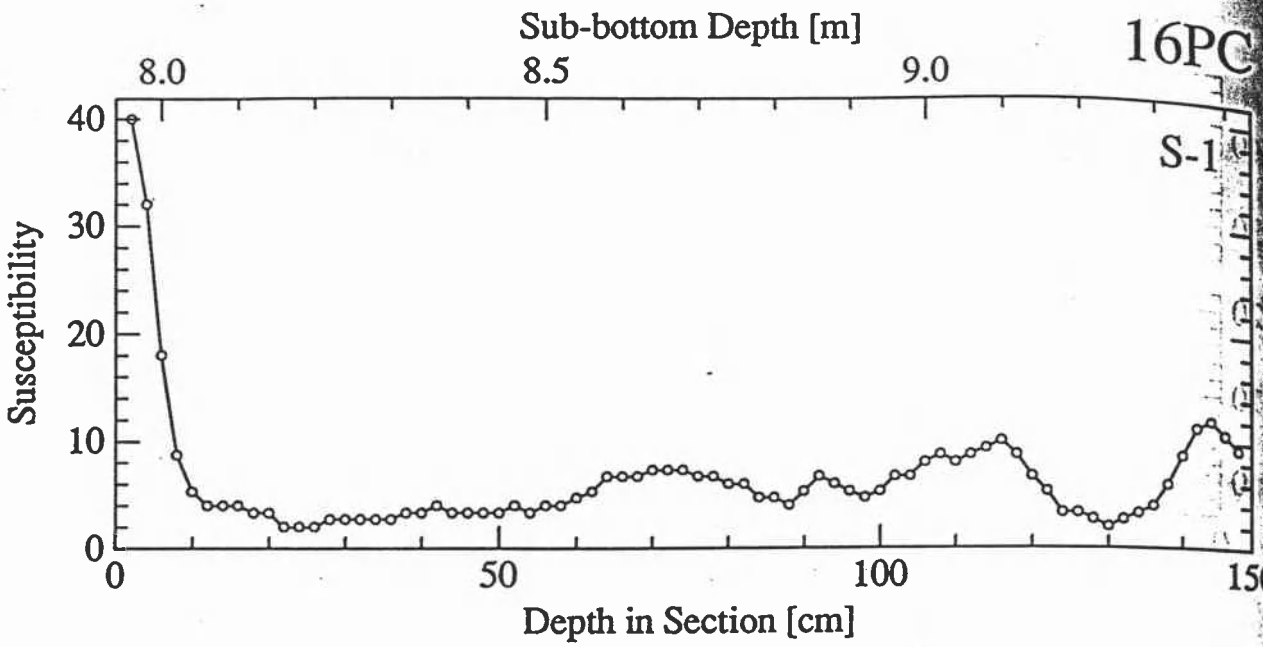
Sub-bottom Depth [m]
8.0
8.5
9.0
16PC
S-1
Susceptibility
40
30
20
10
0
0
50
100
150
Depth in Section [cm]

VNTR01-17PC

Piston core 17 was taken on 23-Sep-1989 (2.445°N, 89.325°W, 1758 m water depth). The core is 8.65 m long, consisting of foraminiferal sand. After the data selection we use 427 susceptibility determinations (range: –2.7 to 66.0, arithmetic mean: 4.9 (all 10^{-6} unitless SI)). The downcore susceptibility is shown in Figure 43, and Figure 44 shows details of individual measurements by sections.

Data selection. The measurements seem to be smooth across all the section boundaries and no data were deleted.

Chronology. Table 23 shows age-depth correlations, and the sedimentation rate is estimated to be about 1.9 cm/ky.

Correlation between 17PC and 16PC. The susceptibilities of 16PC and 17PC show very similar features, although both signals are very low and close to the noise level of the meter. The *Martinson et al.* [1982] inverse correlation method was used to find a smooth mapping function between the depth in 17PC and the depth in 16PC that maximizes the correlation. By using 17PC as a reference signal and allowing degree N=10 a correlation of r = 0.86 was obtained. The susceptibility signals in 16PC and 17PC are compared in Figure 45, and the mapping function is shown in Figure 46 and Table 24.

VNTR01-18PC

Gravity coring was attempted on a seamount on 23-Sep-1989 (3.346°N, 90.789°W, 326 m water depth), however piston coring was not tried.

TABLE 23. Age-depth estimates from susceptibility correlations of 17PC

Piston Core	Event Name	Event Age (ka)	Position of Event Section (S-cm)	Position of Event Depth (m)	Sedimentation Rate (from top) (cm/ky)	Core Length (m)	Bottom Age (ka)
			Estimates Made During the Cruise:				
17	Ash L	256		4.42	1.7		450–550
			Estimates of this Report:				
17	Ash L	230	3-32	4.42	1.92		
17	11.3	405	1-10	7.23	1.79	8.65	450–500

TABLE 24. Depth in 16PC vs. Depth in 17PC mapping function from inverse correlations

Depth in 16PC (m)	Depth in 17PC (m)	Depth in 16PC (m)	Depth in 17PC (m)	Depth in 16PC (m)	Depth in 17PC (m)	Depth in 16PC (m)	Depth in 17PC (m)
0.00	0.00	2.00	2.13	4.00	4.73	6.00	7.39
0.10	0.13	2.10	2.25	4.10	4.85	6.10	7.49
0.20	0.26	2.20	2.37	4.20	4.97	6.20	7.58
0.30	0.39	2.30	2.49	4.30	5.09	6.30	7.68
0.40	0.51	2.40	2.62	4.40	5.22	6.40	7.77
0.50	0.62	2.50	2.74	4.50	5.35	6.50	7.86
0.60	0.73	2.60	2.87	4.60	5.48	6.60	7.95
0.70	0.84	2.70	3.00	4.70	5.63	6.70	8.05
0.80	0.94	2.80	3.13	4.80	5.78	6.80	8.14
0.90	1.03	2.90	3.27	4.90	5.93	6.90	8.23
1.00	1.13	3.00	3.40	5.00	6.09	7.00	8.33
1.10	1.22	3.10	3.54	5.10	6.25	7.10	8.43
1.20	1.31	3.20	3.68	5.20	6.40	7.20	8.53
1.30	1.40	3.30	3.82	5.30	6.55	7.32	8.65
1.40	1.50	3.40	3.96	5.40	6.70		
1.50	1.59	3.50	4.09	5.50	6.83		
1.60	1.69	3.60	4.22	5.60	6.96		
1.70	1.80	3.70	4.35	5.70	7.07		
1.80	1.90	3.80	4.48	5.80	7.18		
1.90	2.02	3.90	4.60	5.90	7.29		

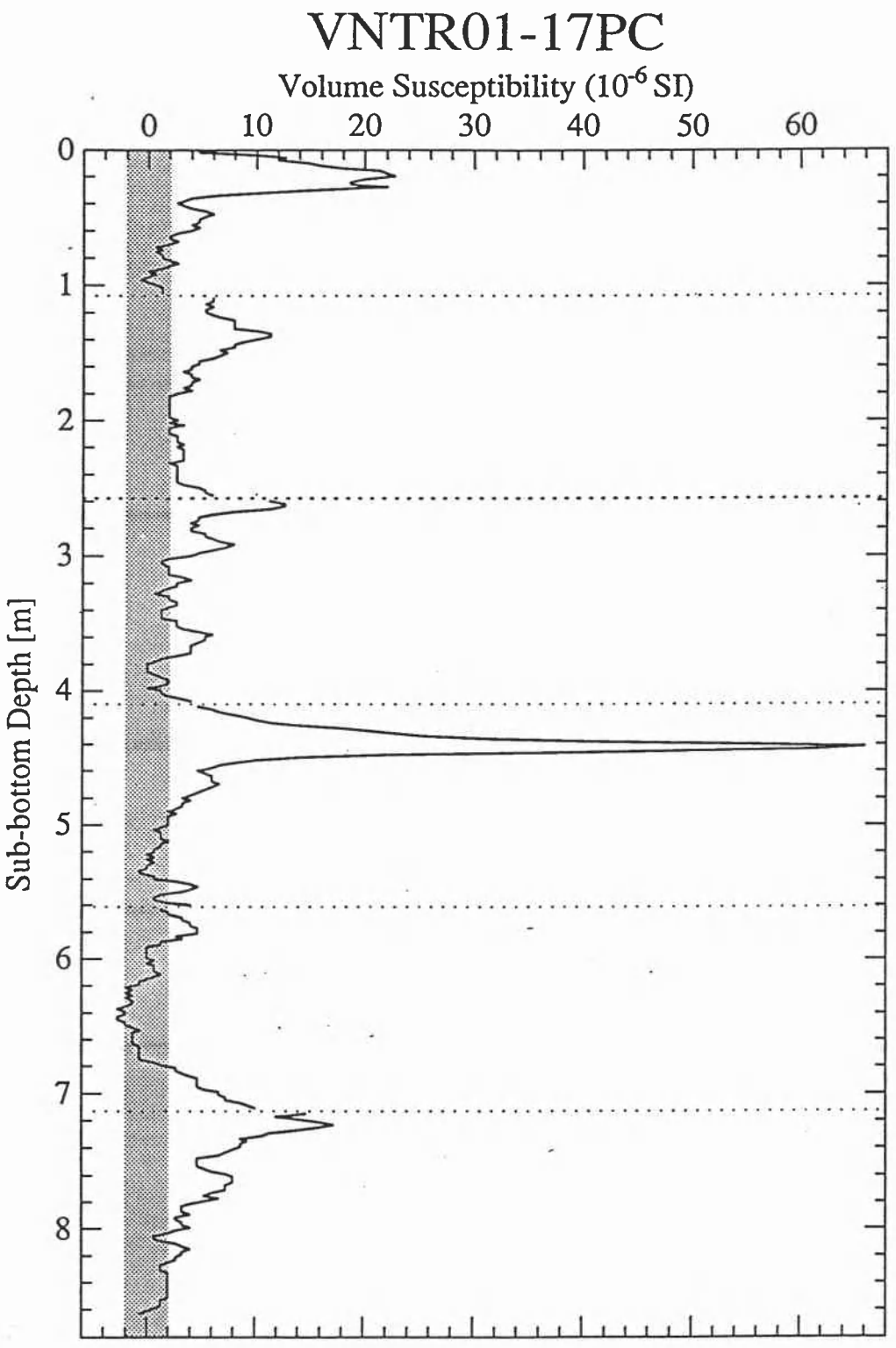

Figure 43. The downhole susceptibility in core VNTR01-17PC (2°N, 89°W). Section boundaries are shown by dotted lines and the approximate noise level by the shaded zero line.

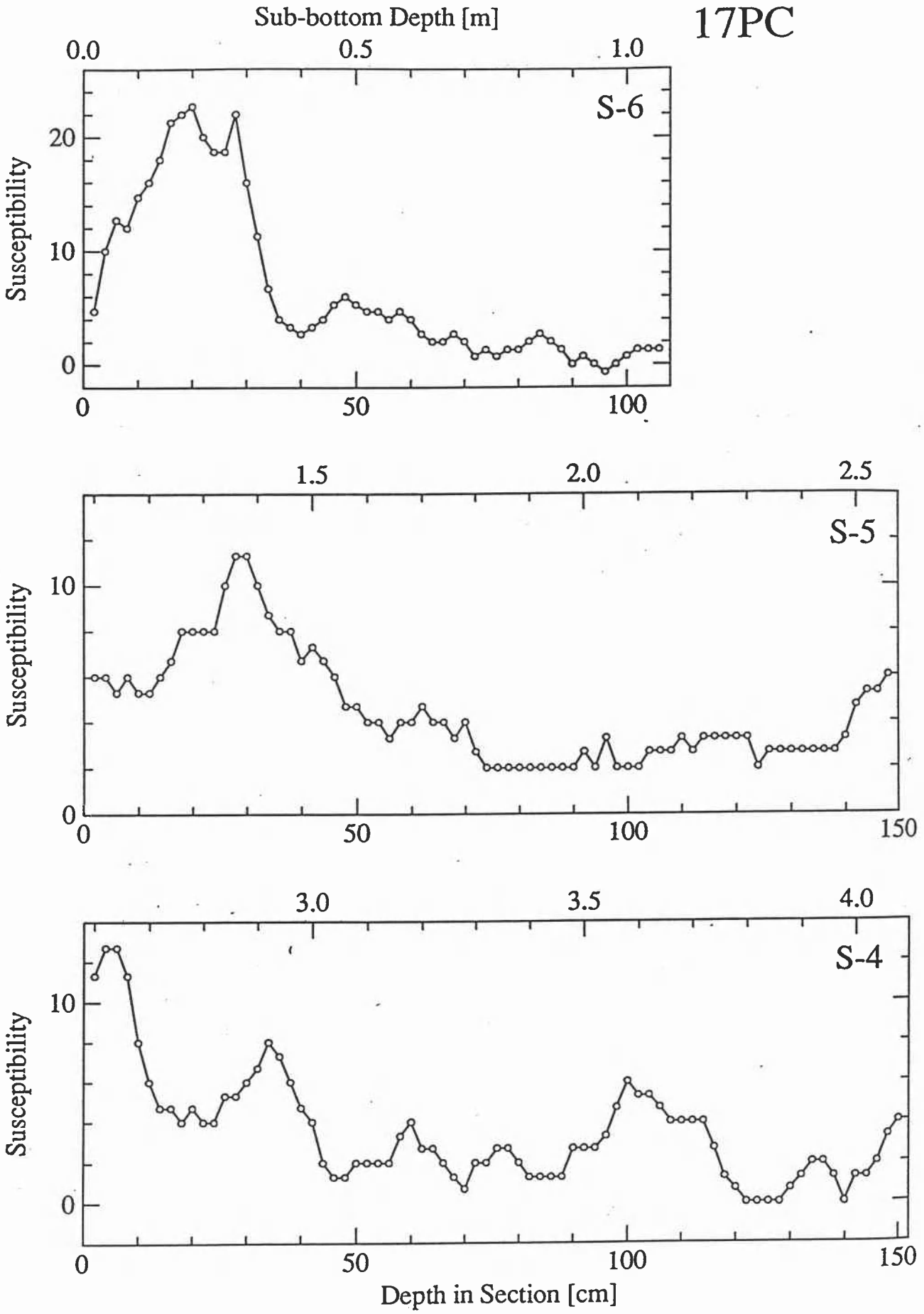

Figure 44. Details of the susceptibility data in core VNTR01-17PC by sections.

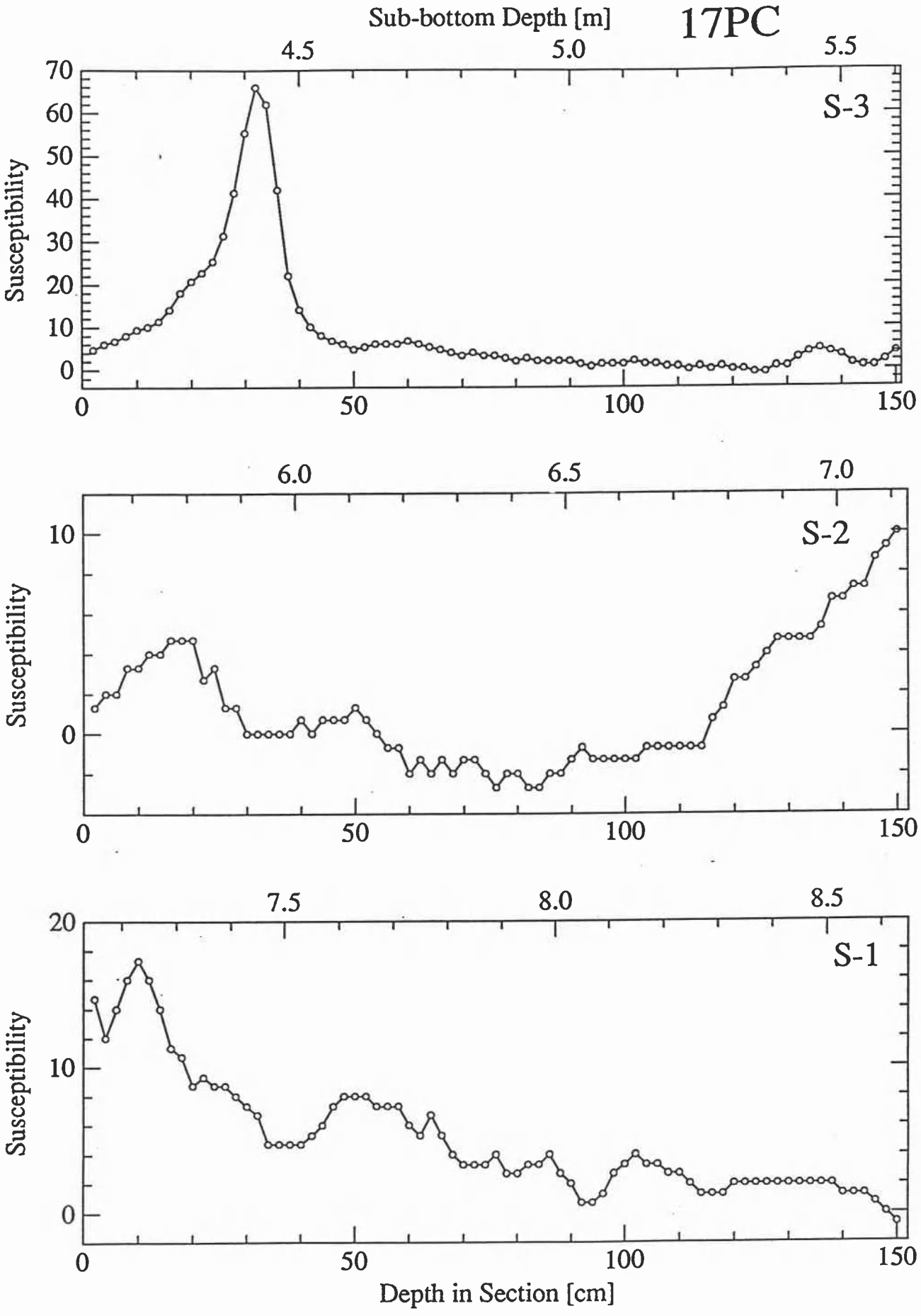
17PC
Sub-bottom Depth [m]
4.5
5.0
5.5
S-3
Susceptibility
70
60
50
40
30
20
10
0
0
50
100
150
6.0
6.5
7.0
S-2
Susceptibility
10
0
0
50
100
150
7.5
8.0
8.5
S-1
Susceptibility
20
10
0
0
50
100
150
Depth in Section [cm]

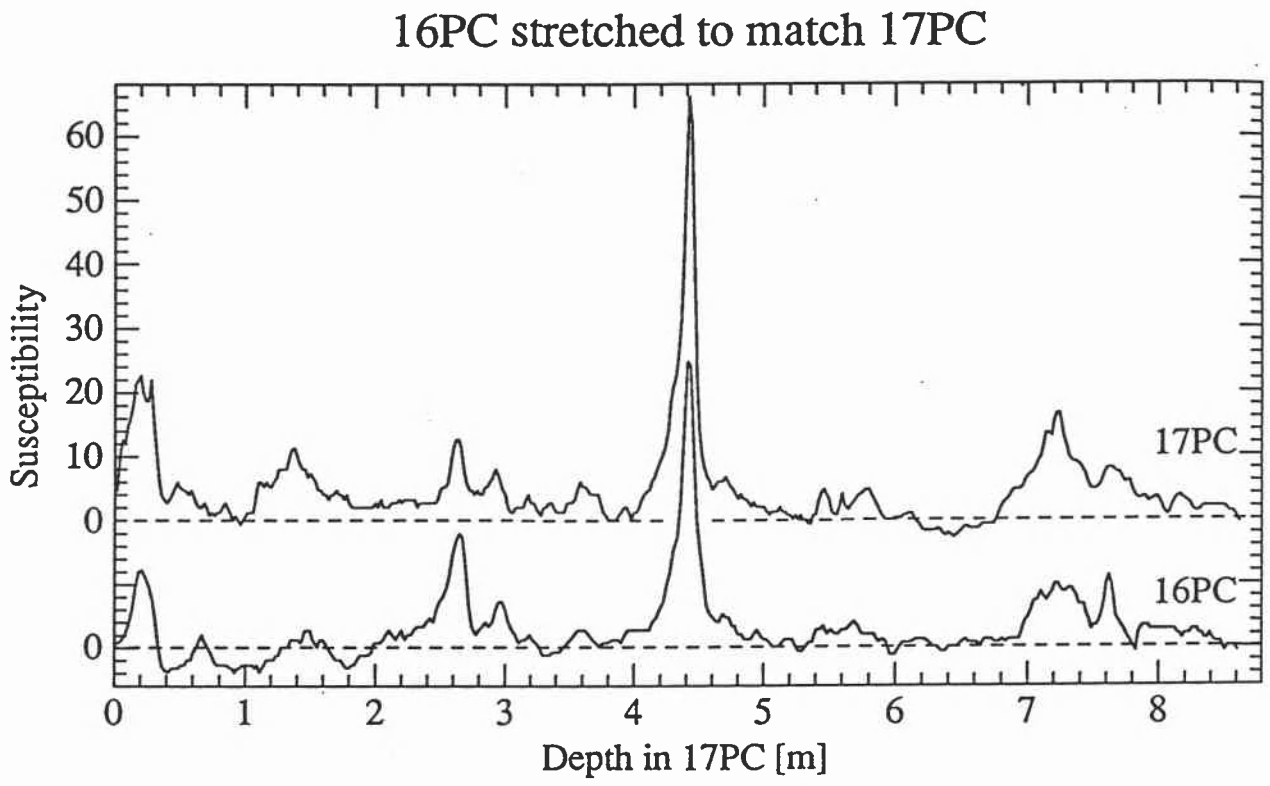

Figure 45. Correlation of the susceptibilities in cores VNTR01-16PC and VNTR01-17PC. The depth scale of 16PC was stretched and squeezed in a smooth fashion (see Figure 46) in order to maximize the correlation (r = 0.86).

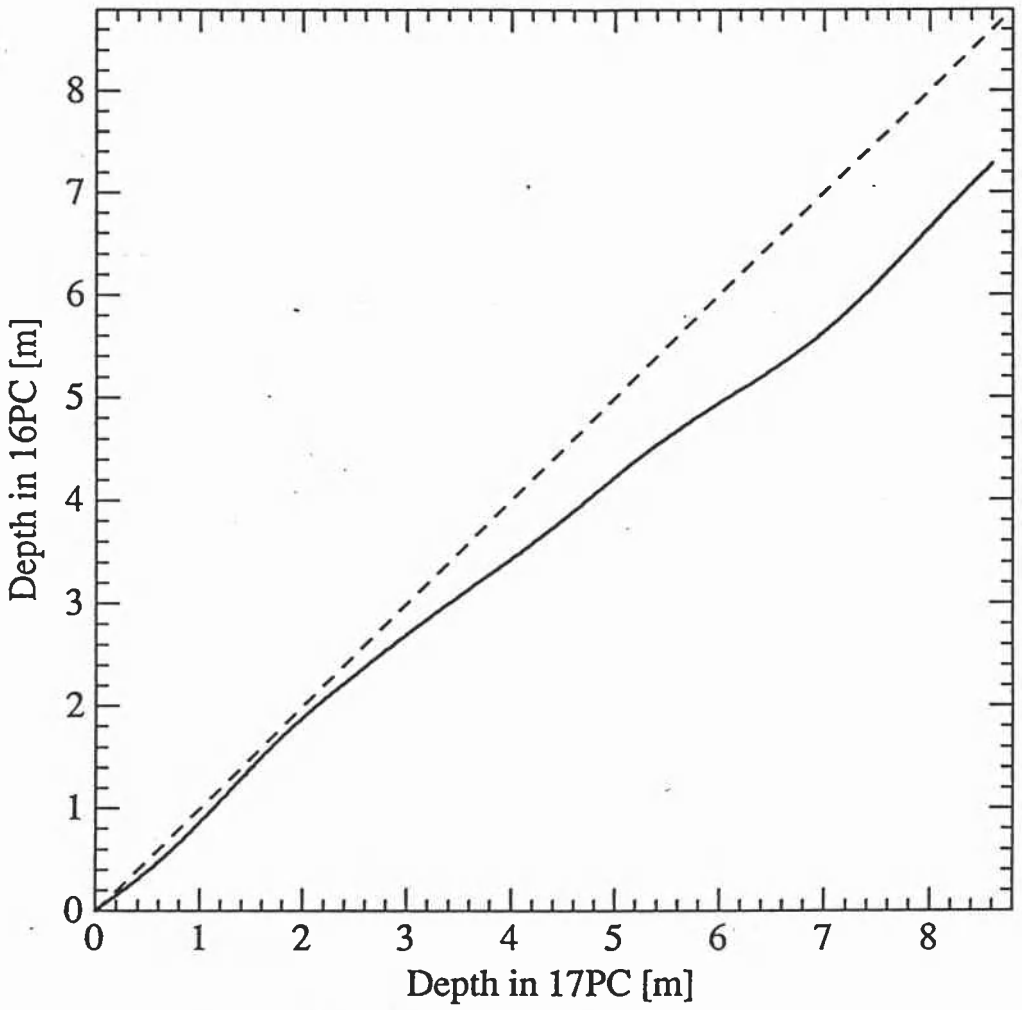

Figure 46. The mapping function that transfers depths in 16PC to depths in 17PC (see also Table 24). The mapping function was obtained by maximizing the correlation between the susceptibilities by the method of *Martinson et al.* [1982] using degree N=10. This mapping function results in a correlation of r = 0.86 between the signals in Figure 45.

VNTR01-19PC

Piston core 19 was taken on 25-Sep-1989 (7.918°N, 90.442°W, 3448 m water depth). The core is 10.89 m long, consisting of foram bearing siliceous clay. After the data selection we use 537 susceptibility determinations (range: 113.3 to 606.7, arithmetic mean: 234.9 (all 10^{-6} unitless SI)). The downcore susceptibility is shown in Figure 47, and Figure 48 shows details of individual measurements by sections.

Data selection. The measurements seem to be smooth across all the section boundaries and no data were deleted.

Chronology. Table 25 shows age-depth correlations, and the sedimentation rate is estimated to be about 5.3 cm/ky.

TABLE 25. Age-depth estimates from susceptibility correlations of 19PC

Piston Core	Event Name	Event Age (ka)	Position of Event Section (S-cm)	Position of Event Depth (m)	Sedimentation Rate (from top) (cm/ky)	Core Length (m)	Bottom Age (ka)
			Estimates Made During the Cruise:				
19	5.0	71		4.16	5.9		
19	6.0	128		6.37	5.0		180–220
			Estimates of this Report:				
19	5.0	74	5-86	4.16	5.62		
19	5.1	79	5-109	4.39	5.56		
19	5.2	91	4-3	4.84	5.32		
19	5.3	99	4-54	5.35	5.40		
19	5.4	111	4-94	5.75	5.18		
19	5.5	124	4-136	6.17	4.98		
19	6.0	130	3-4	6.37	4.90	10.89	180–220

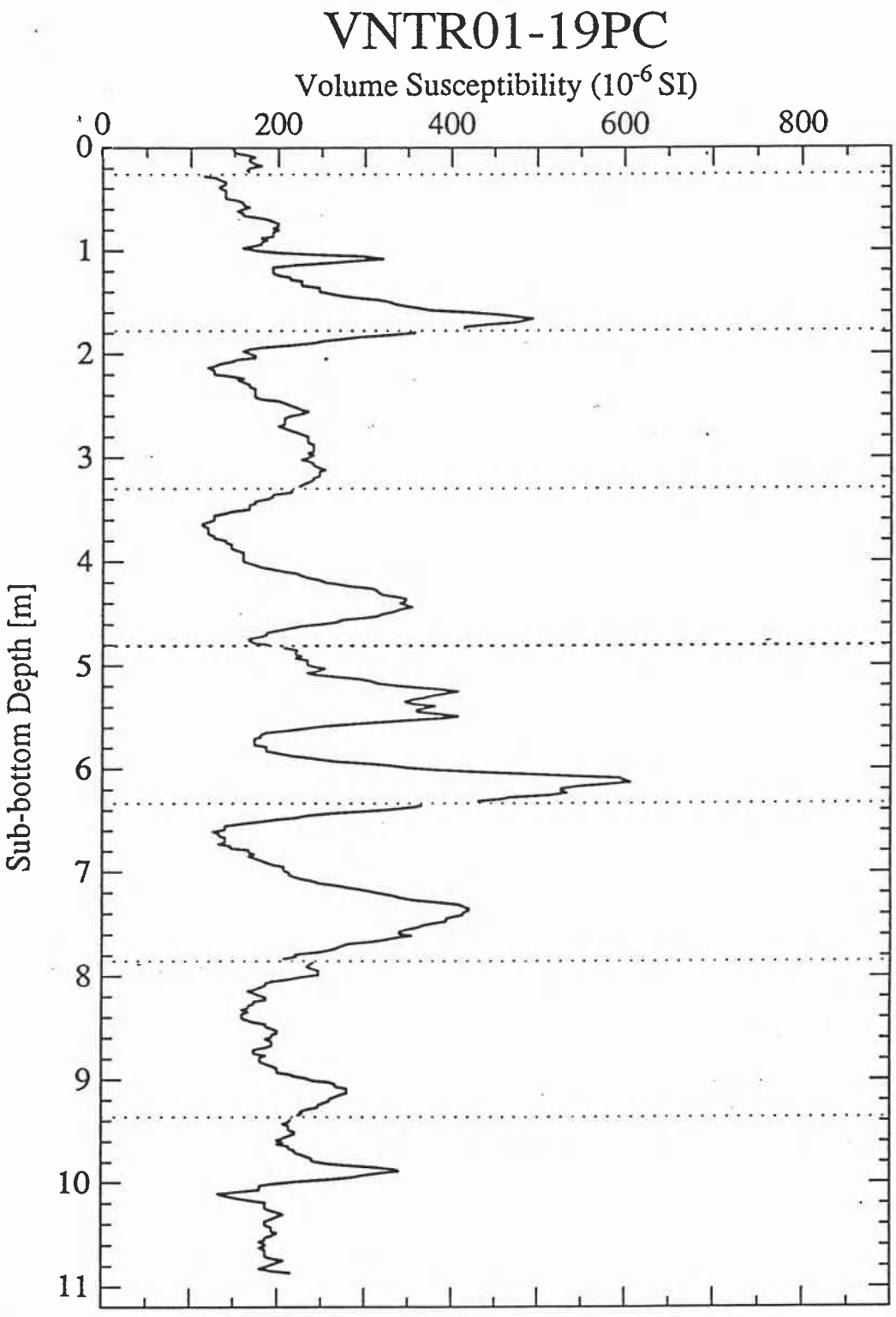

Figure 47. The downhole susceptibility in core VNTR01-19PC (8°N, 90°W). Section boundaries are shown by dotted lines.

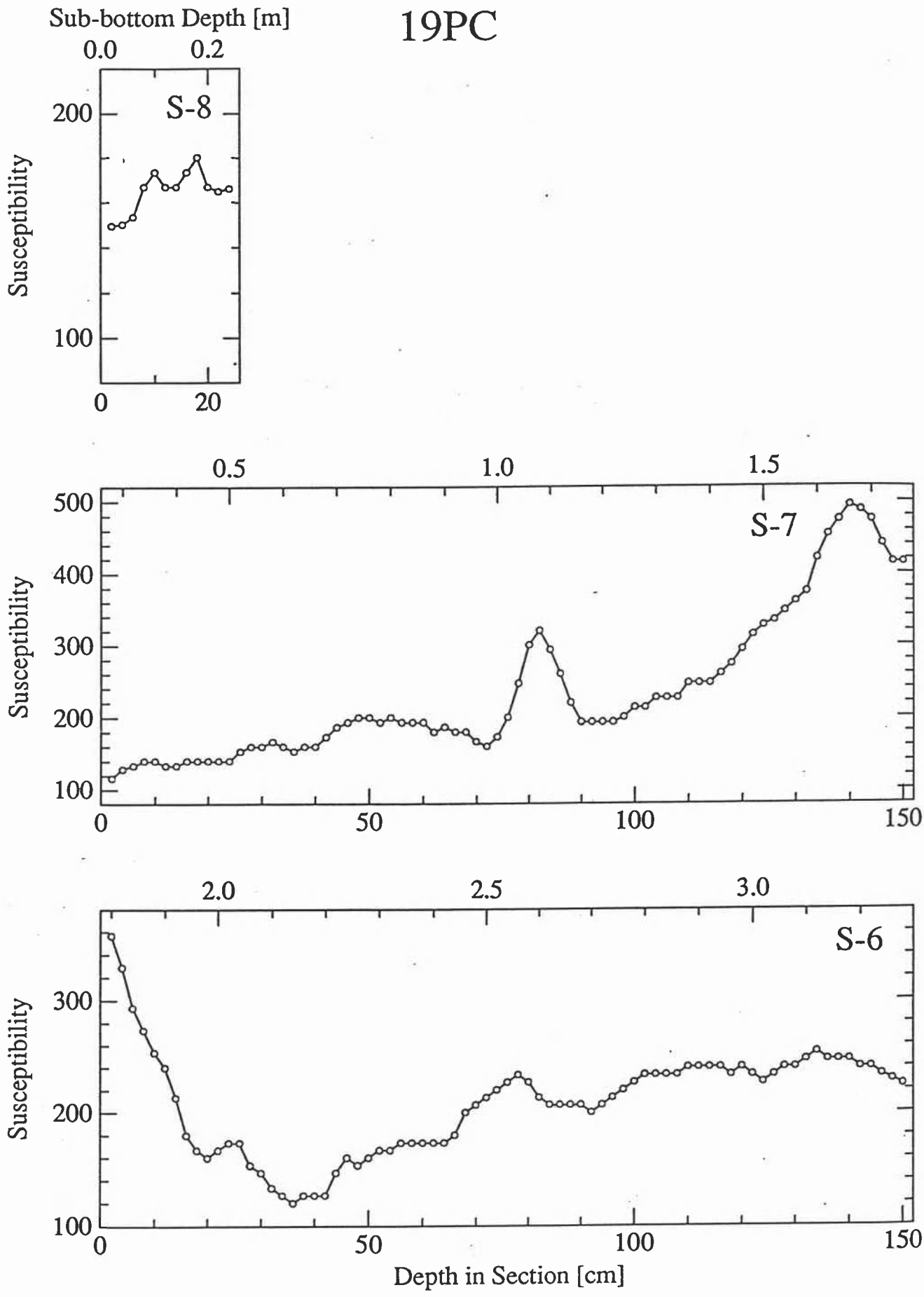

Figure 48. Details of the susceptibility data in core VNTR01-19PC by sections.

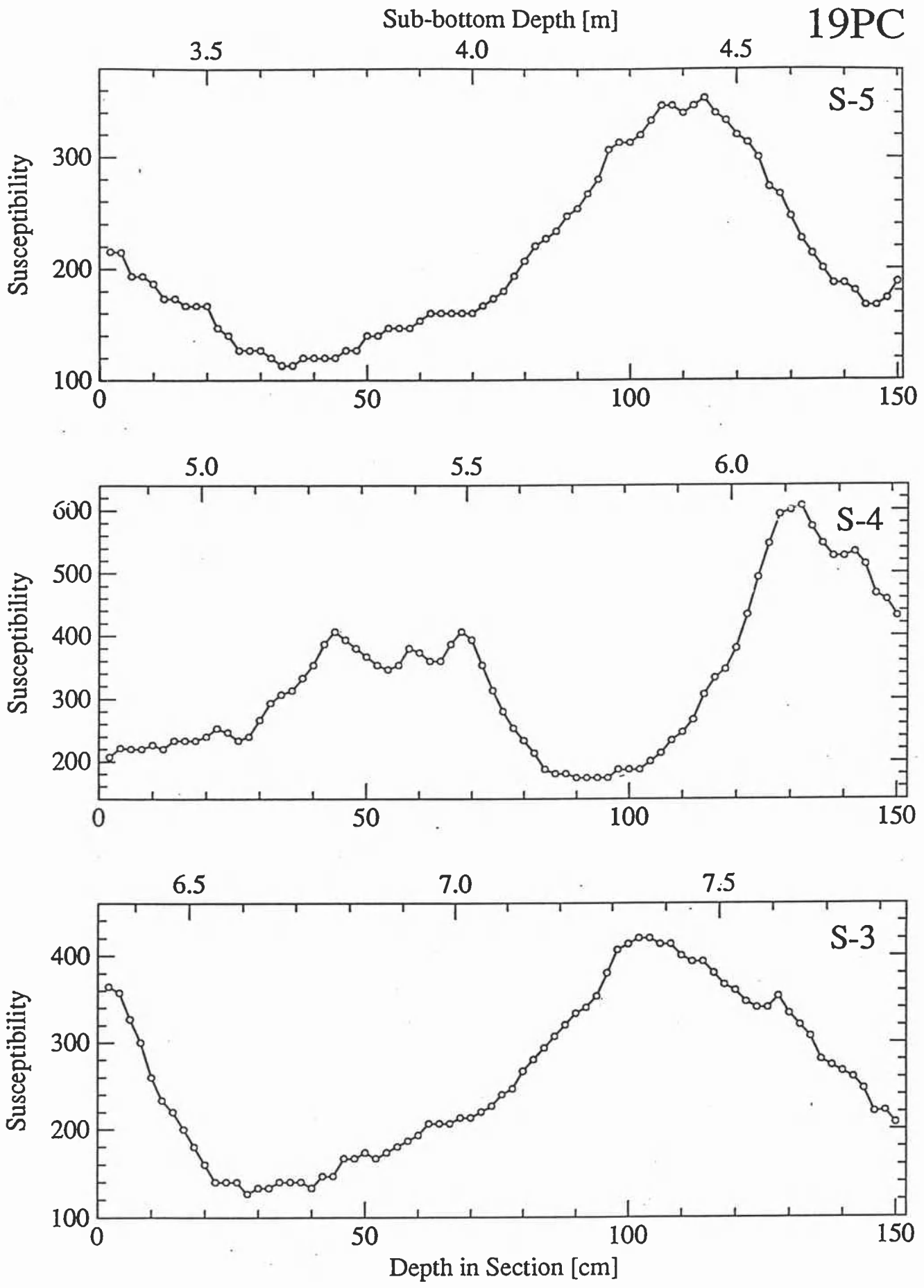
19PC
Sub-bottom Depth [m]
3.5
4.0
4.5
S-5
Susceptibility
300
200
100
0
50
100
150
5.0
5.5
6.0
S-4
600
500
400
300
200
6.5
7.0
7.5
S-3
400
300
200
100
Depth in Section [cm]

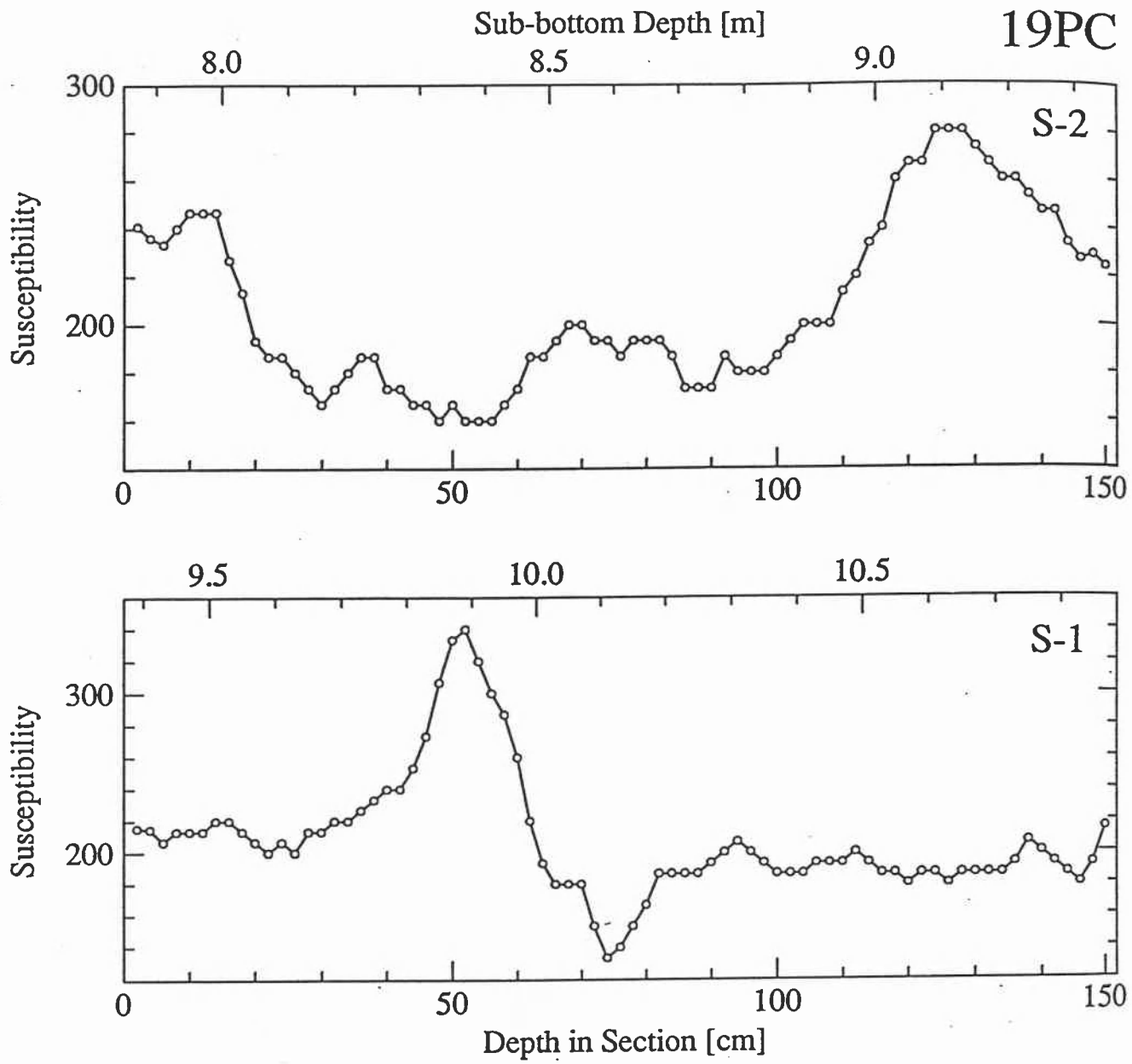
19PC
Sub-bottom Depth [m]
8.0
8.5
9.0
300
200
Susceptibility
S-2
0
50
100
150
9.5
10.0
10.5
S-1
300
200
Susceptibility
0
50
100
150
Depth in Section [cm]

VNTR01-20PC

Piston core 20 was taken on 27-Sep-1989 (5.632°N, 94.198°W, 3563 m water depth). The core is 12.62 m long, consisting of fossiliferous clay. After the data selection we use 619 susceptibility determinations (range: 108.0 to 253.3, arithmetic mean: 163.3 (all 10^{-6} unitless SI)). The downcore susceptibility is shown in Figure 49, and Figure 50 shows details of individual measurements by sections.

Data selection. Spikes at section boundaries S-9/S-8 and S-4/S-3 were fixed by deleting five data points (S-8: 4 cm and 6 cm, S-4: 100 cm and 102 cm, S-3: 2 cm).

Chronology. Table 26 shows age-depth correlations, and the sedimentation rate is estimated to be about 0.9 cm/ky. If these correlations are right this core should penetrate the Jaramillo subchron of the Matuyama.

TABLE 26. Age-depth estimates from susceptibility correlations of 20PC

Piston Core	Event Name	Event Age (ka)	Position of Event Section (S-cm)	Position of Event Depth (m)	Sedimentation Rate (from top) (cm/ky)	Core Length (m)	Bottom Age (ka)
			Estimates Made During the Cruise:				
20	6.0	128		1.21	0.9		1300 ?
			Estimates of this Report:				
20	5.0	74	9-53	0.53	0.72		
20	6.0	130	8-23	1.21	0.93	12.62	1100–1400

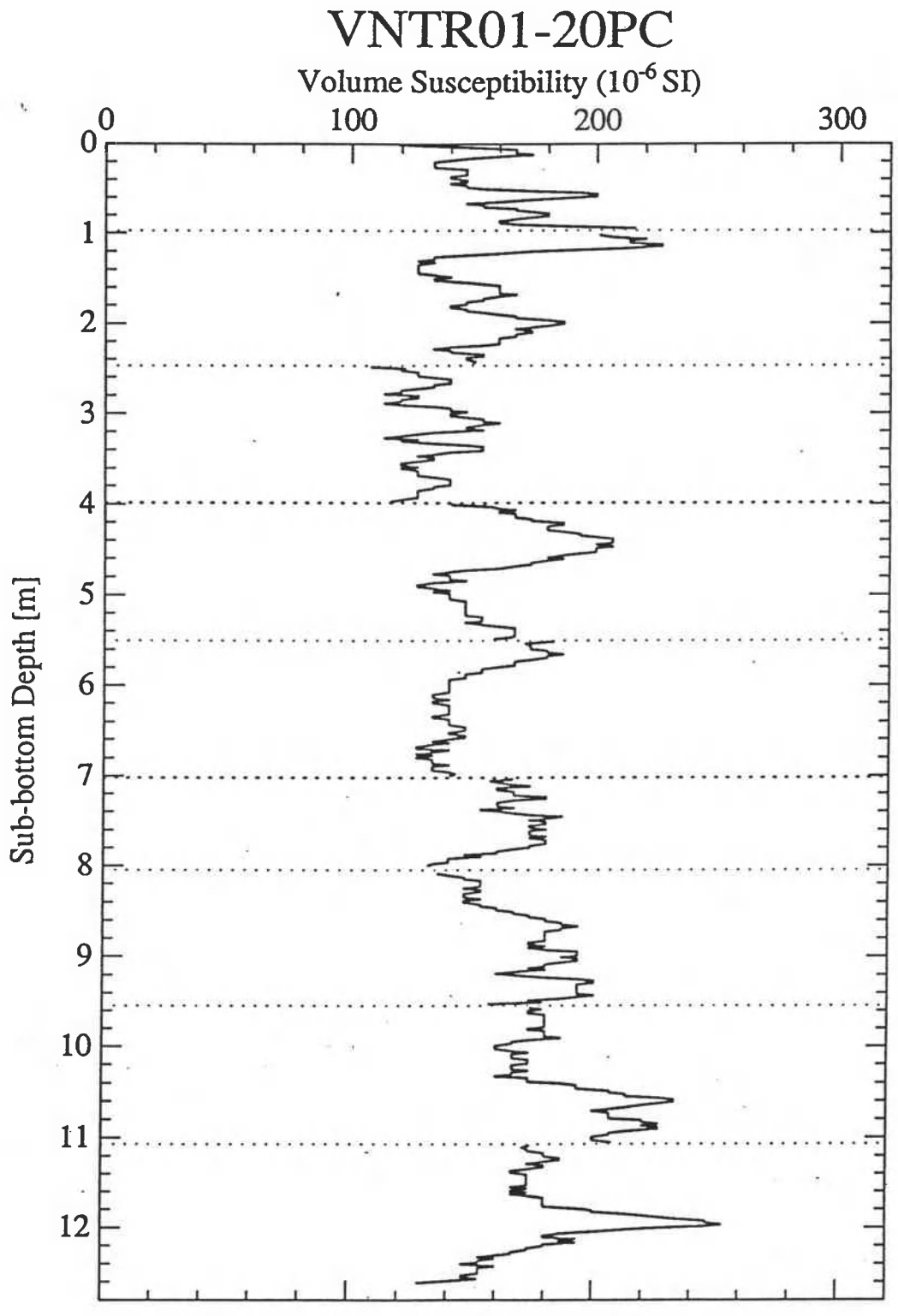

Figure 49. The downhole susceptibility in core VNTR01-20PC (6°N, 94°W). Section boundaries are shown by dotted lines.

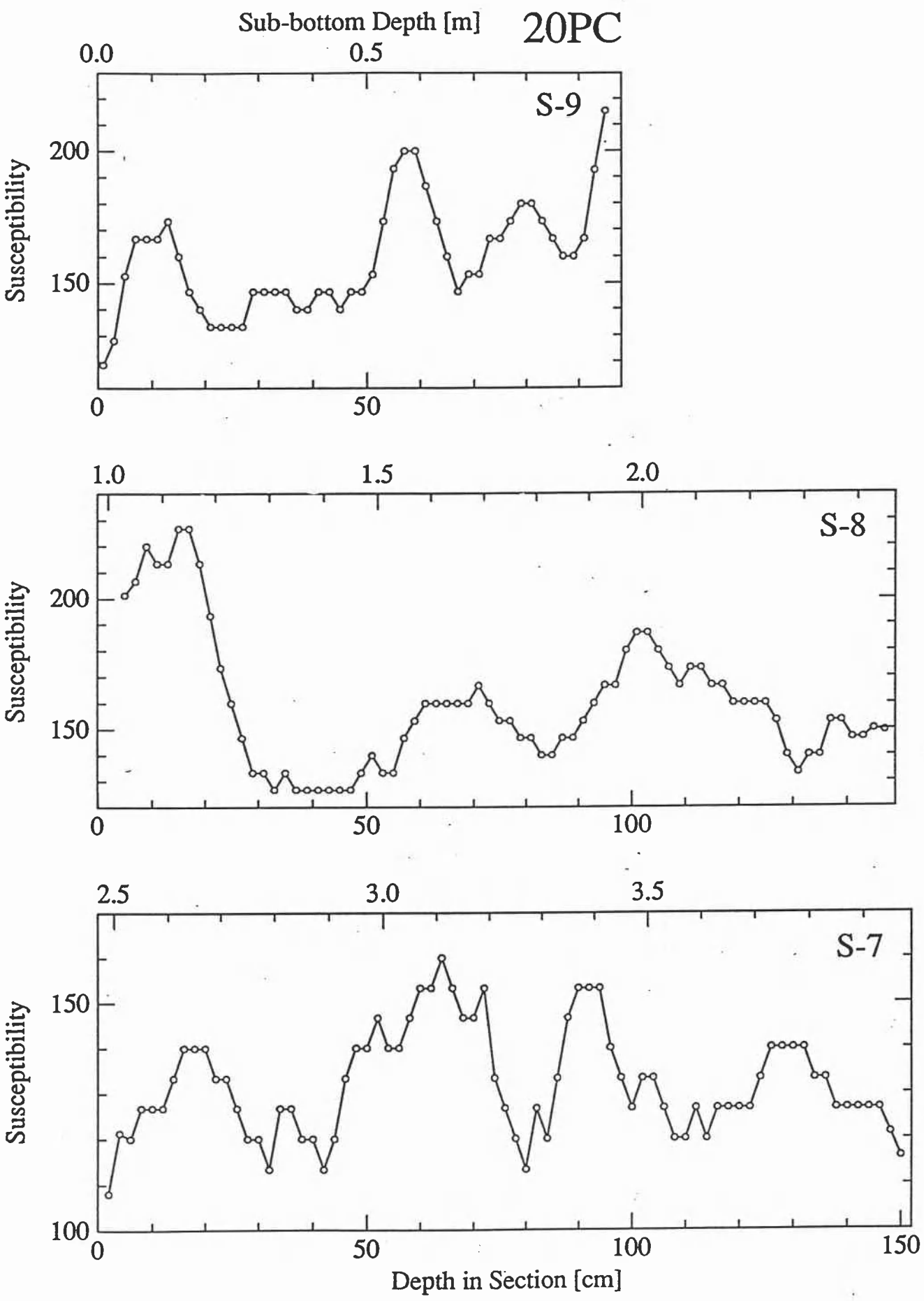

Figure 50. Details of the susceptibility data in core VNTR01-20PC by sections.

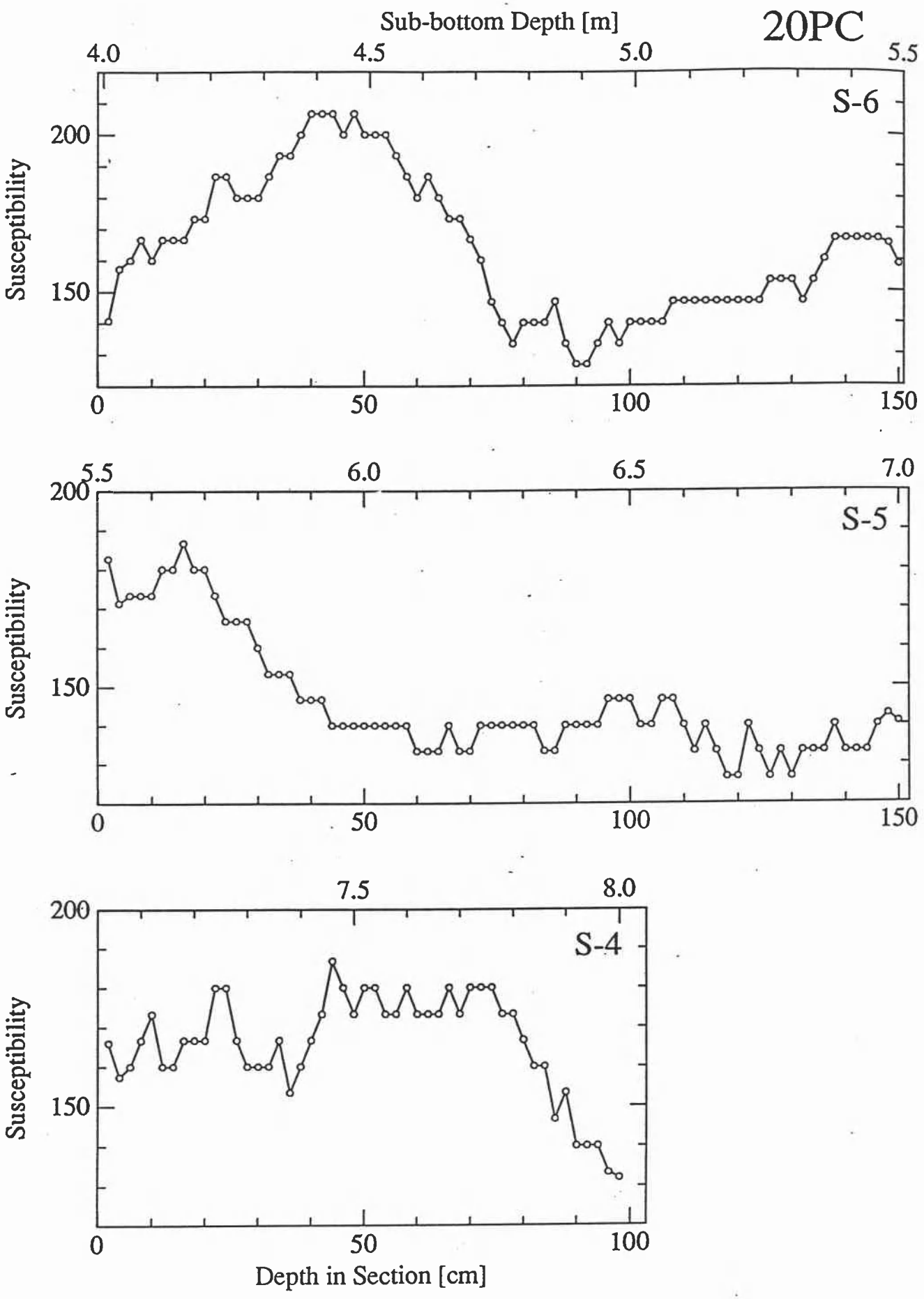
20PC
Sub-bottom Depth [m]
4.0
4.5
5.0
5.5
S-6
Susceptibility
200
150
0
50
100
150
5.5
6.0
6.5
7.0
S-5
7.5
8.0
S-4
Depth in Section [cm]

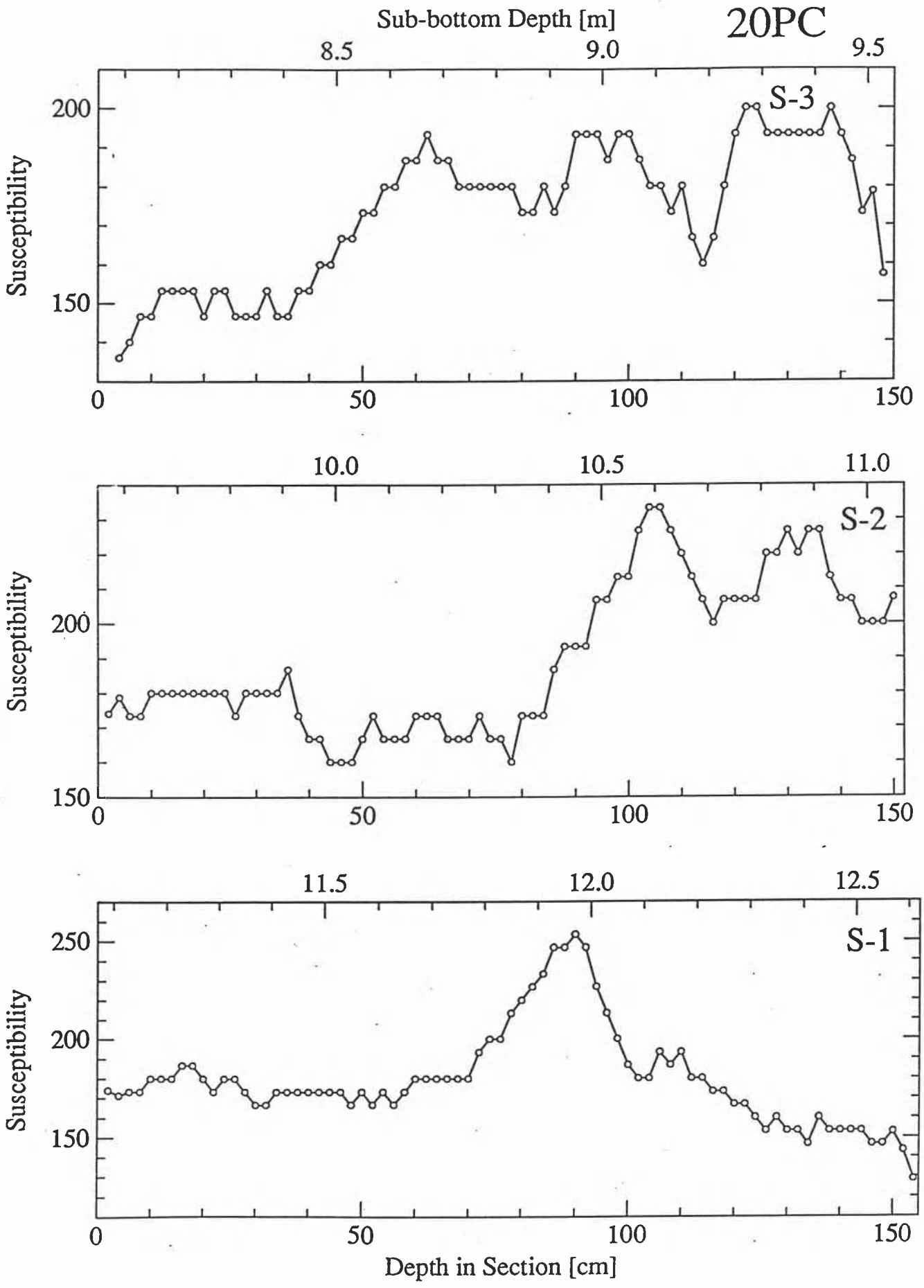
20PC
Sub-bottom Depth [m]
8.5
9.0
9.5
S-3
Susceptibility
200
150
0
50
100
150
10.0
10.5
11.0
S-2
Susceptibility
200
150
0
50
100
150
11.5
12.0
12.5
S-1
Susceptibility
250
200
150
0
50
100
150
Depth in Section [cm]

VNTR01-21PC

Piston core 21 was taken on 29-Sep-1989 (9.586°N, 94.603°W, 3710 m water depth). The core is 14.33 m long, consisting of foram bearing siliceous clay. After the data selection we use 699 susceptibility determinations (range: 16.7 to 253.3, arithmetic mean: 86.6 (all 10^{-6} unitless SI)). The downcore susceptibility is shown in Figure 51, and Figure 52 shows details of individual measurements by sections.

Data selection. Six data points at section boundaries were deleted (S-11: 12 cm, S-10:34 cm, S-9: 2 cm, S-7: 2 cm and 4 cm, S-4: 154 cm).

Chronology. Table 27 shows age-depth correlations, and the sedimentation rate is estimated to be about 2.2 to 2.5 cm/ky. There is a consistent sedimentation rate by correlating a major spike in the susceptibility to ash layer "K".

TABLE 27. Age-depth estimates from susceptibility correlations of 21PC

Piston Core	Event Name	Event Age (ka)	Position of Event Section (S-cm)	Depth (m)	Sedimentation Rate (from top) (cm/ky)	Core Length (m)	Bottom Age (ka)
			Estimates Made During the Cruise:				
21	6.0	128		2.79	2.2		
21	Ash L ?	256		8.28	3.2		400–700 ?
			Estimates of this Report:				
21	6.0	130	8-80	2.79	2.15		
21	Ash K	330	4-22	8.27	2.51	14.33	550–650

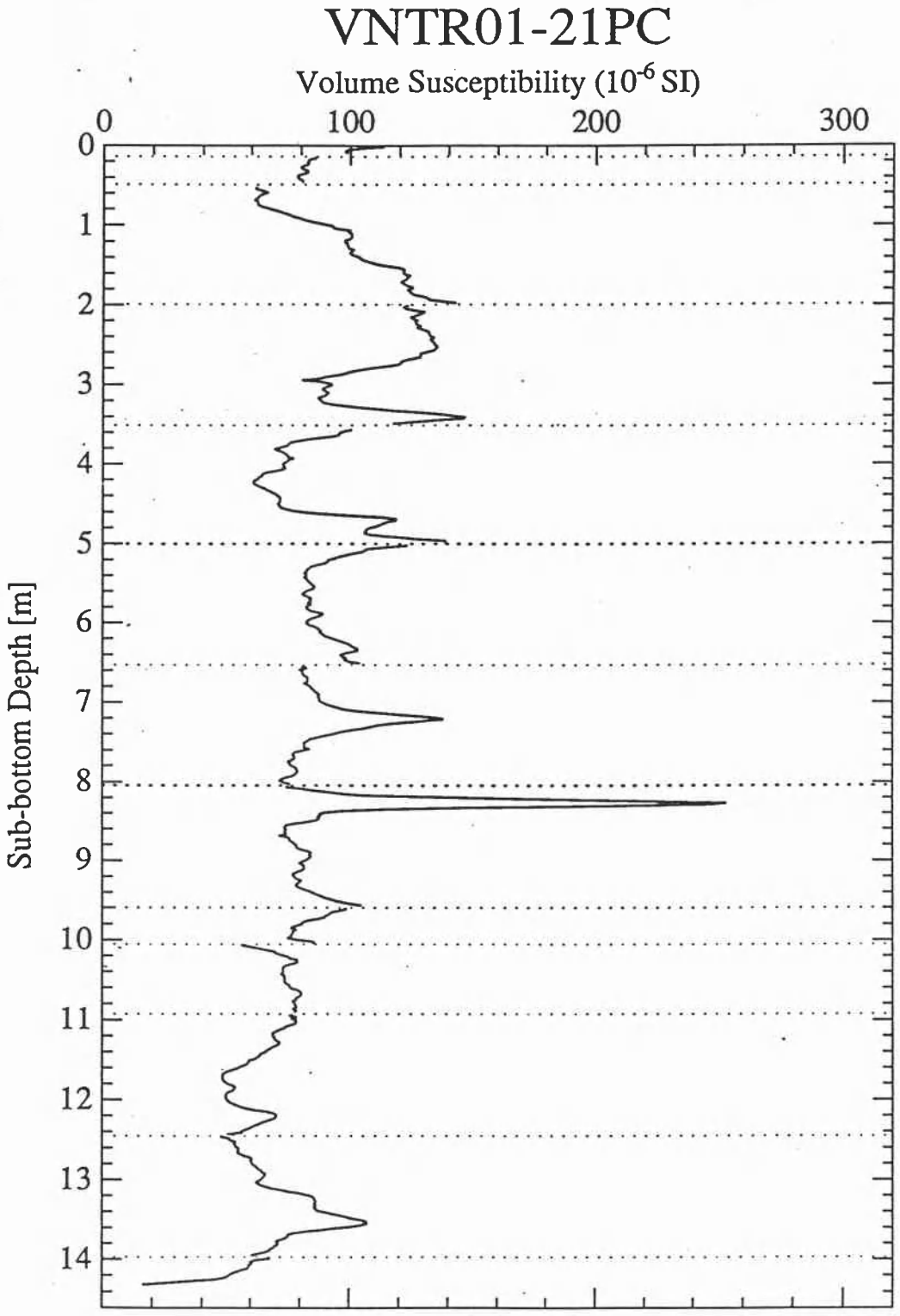

Figure 51. The downhole susceptibility in core VNTR01-21PC (10°N, 95°W). Section boundaries are shown by dotted lines.

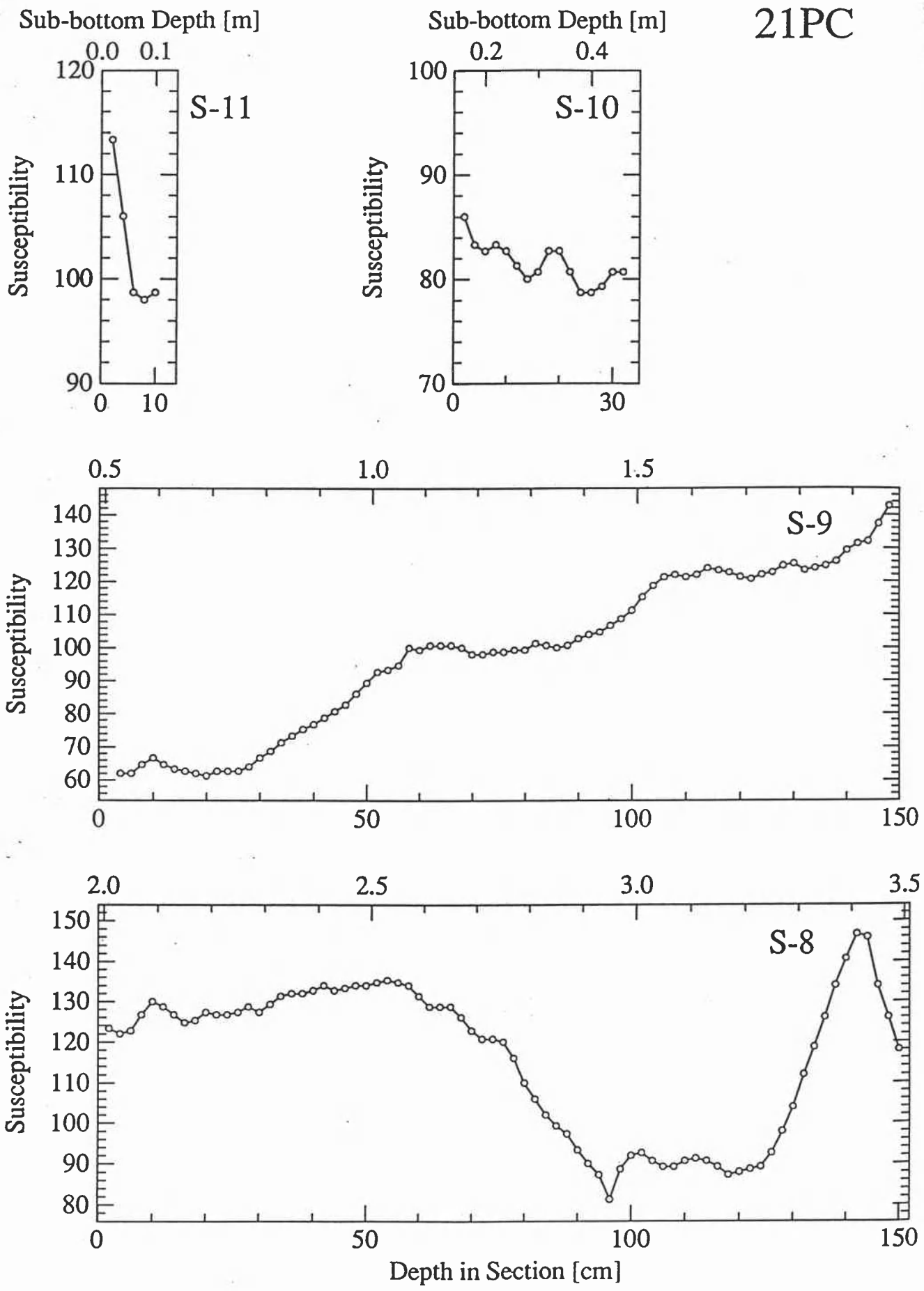

Figure 52. Details of the susceptibility data in core VNTR01-21PC by sections.

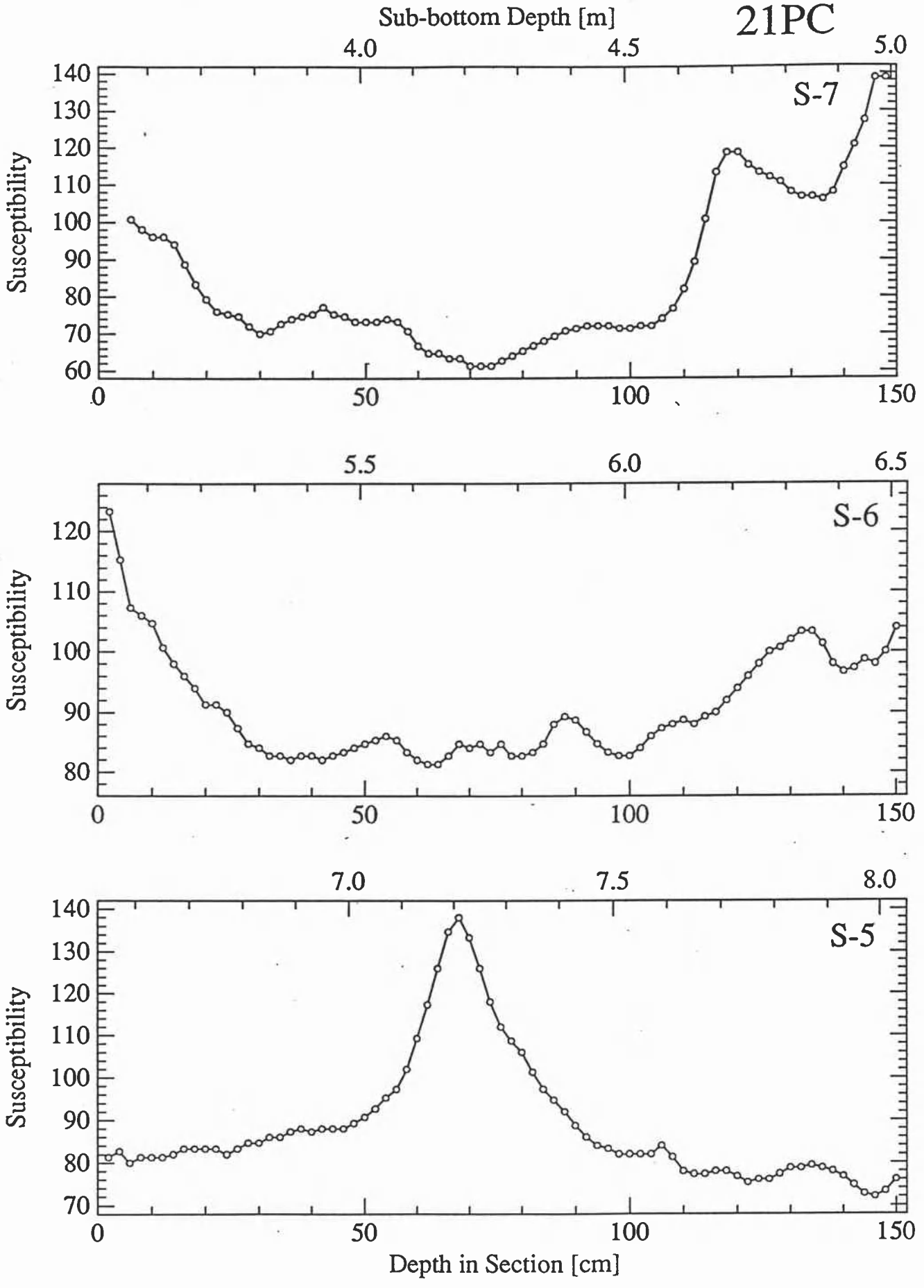
21PC
Sub-bottom Depth [m]
4.0
4.5
5.0
S-7
Susceptibility
140
130
120
110
100
90
80
70
60
0
50
100
150
5.5
6.0
6.5
S-6
Susceptibility
120
110
100
90
80
0
50
100
150
7.0
7.5
8.0
S-5
Susceptibility
140
130
120
110
100
90
80
70
0
50
100
150
Depth in Section [cm]

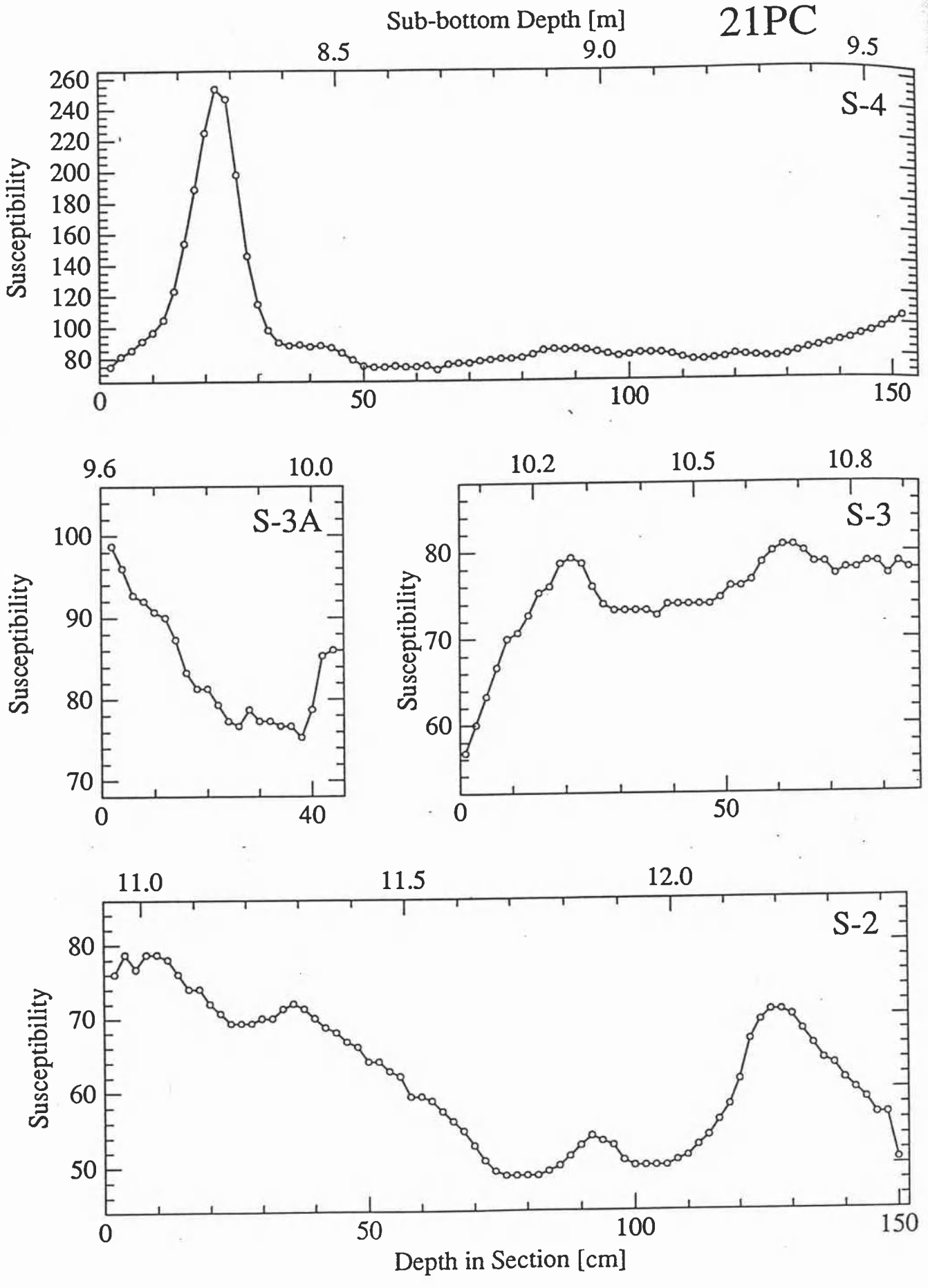
21PC
Sub-bottom Depth [m]
8.5
9.0
9.5
S-4
Susceptibility
260
240
220
200
180
160
140
120
100
80
0
50
100
150
9.6
10.0
S-3A
Susceptibility
100
90
80
70
0
40
10.2
10.5
10.8
S-3
Susceptibility
80
70
60
0
50
11.0
11.5
12.0
S-2
Susceptibility
80
70
60
50
0
50
100
150
Depth in Section [cm]

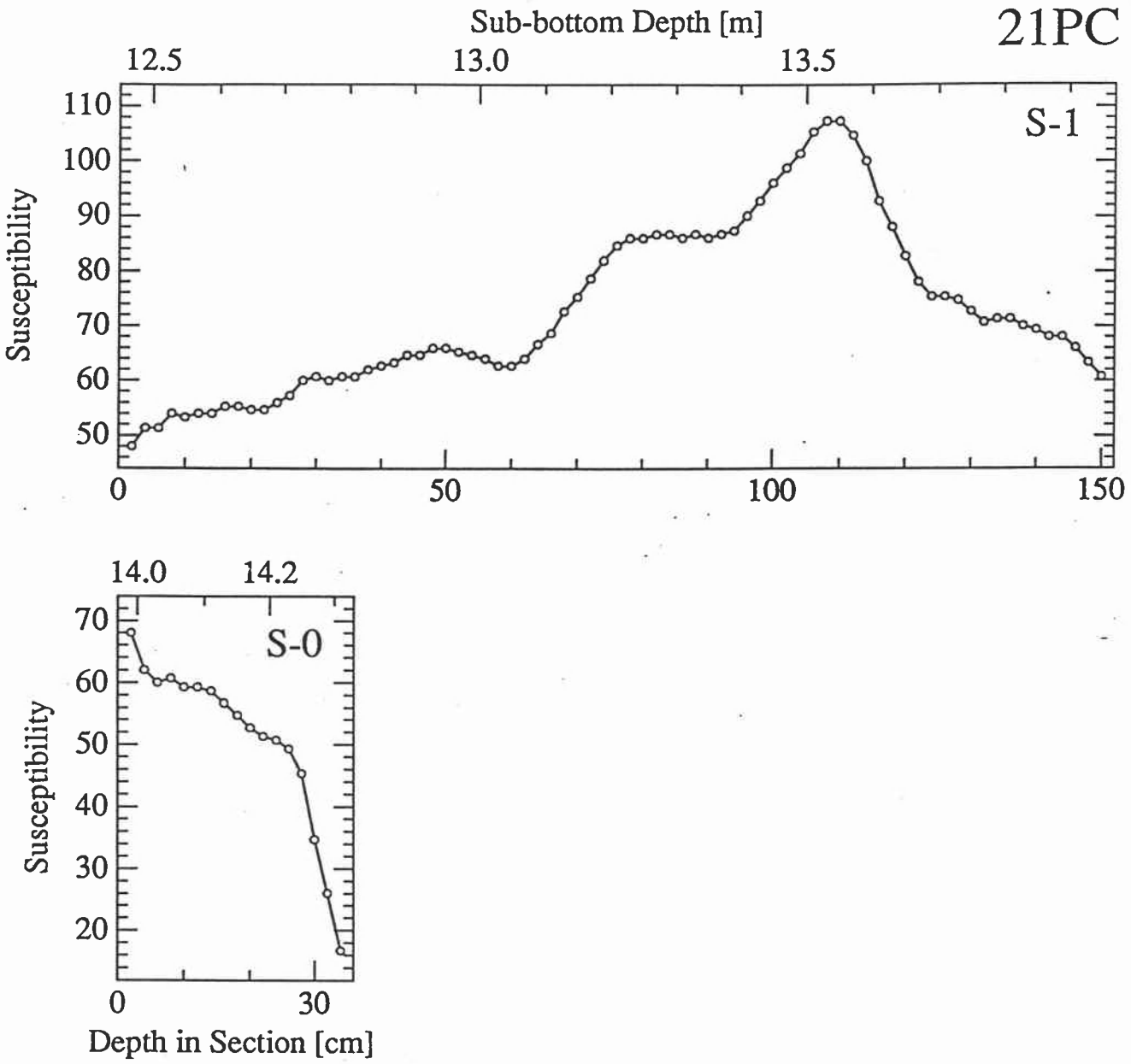
21PC
Sub-bottom Depth [m]
12.5
13.0
13.5
S-1
Susceptibility
110
100
90
80
70
60
50
0
50
100
150
14.0
14.2
S-0
Susceptibility
70
60
50
40
30
20
0
30
Depth in Section [cm]

VNTR01-22PC

Piston core 22 was taken on 30-Sep-1989 (13.001°N, 99.367°W, 3500 m water depth). The core is 10.97 m long, consisting of hemipelagic clay. After the data selection we use 539 susceptibility determinations (range: 107.3 to 502.0, arithmetic mean: 175.2 (all 10^{-6} unitless SI)). The downcore susceptibility is shown in Figure 53, and Figure 54 shows details of individual measurements by sections.

Data selection. Spikes at section boundaries were fixed by deleting three data points (S-5: 150 cm, S-4: 148 cm and 150 cm).

Chronology. The variation in susceptibility is not easily correlated to climatic timescales. There appears to be an ash layer at 3.98 m depth S-5: 60 cm. If this is ash layer "D" then the sedimentation rate is about 4.7 cm/ky. On the other hand it could represent ash layer "K" leading to a sedimentation rate of 1.2 cm/ky.

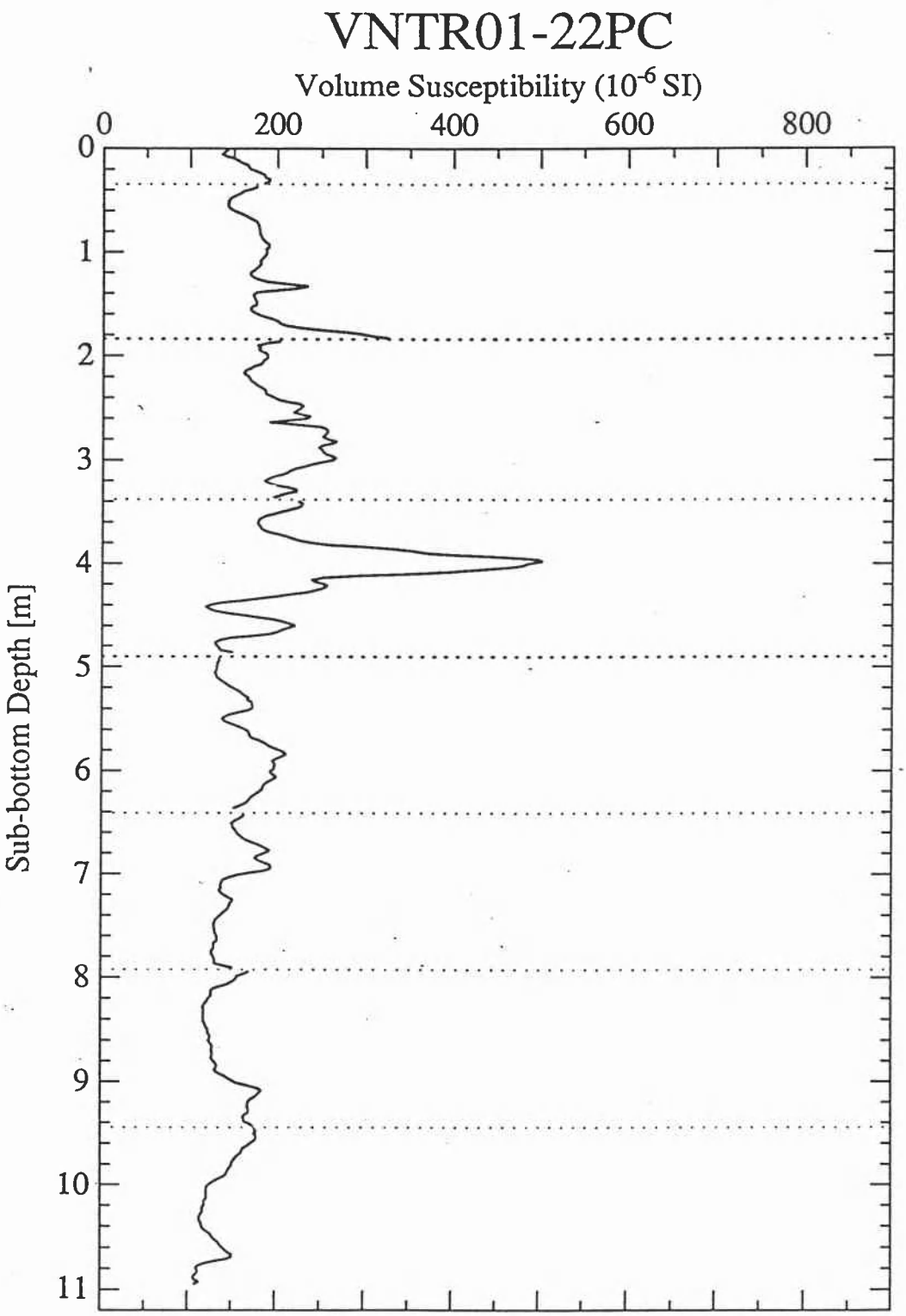

Figure 53. The downhole susceptibility in core VNTR01-22PC (13°N, 99°W). Section boundaries are shown by dotted lines.

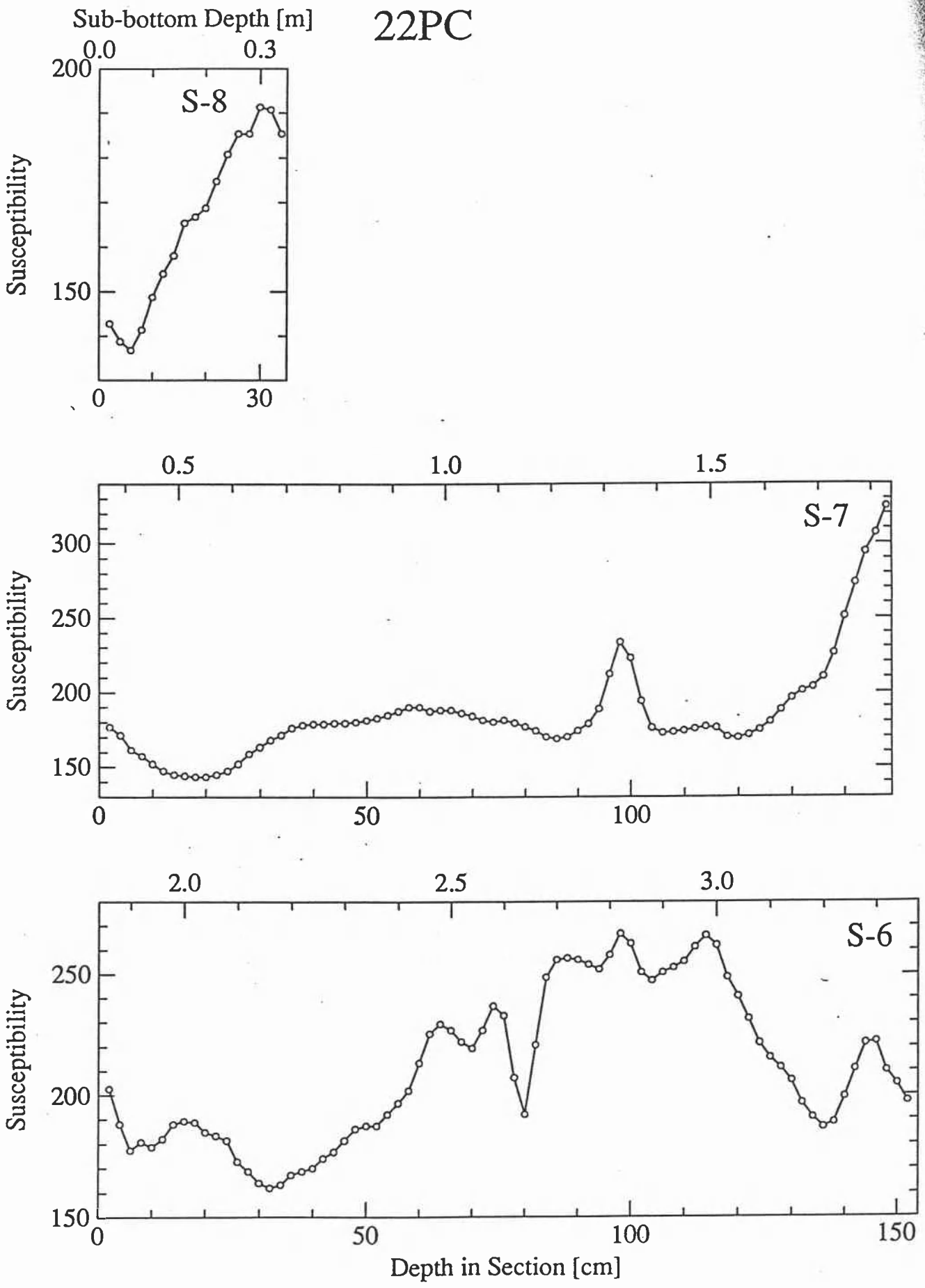

Figure 54. Details of the susceptibility data in core VNTR01-22PC by sections.

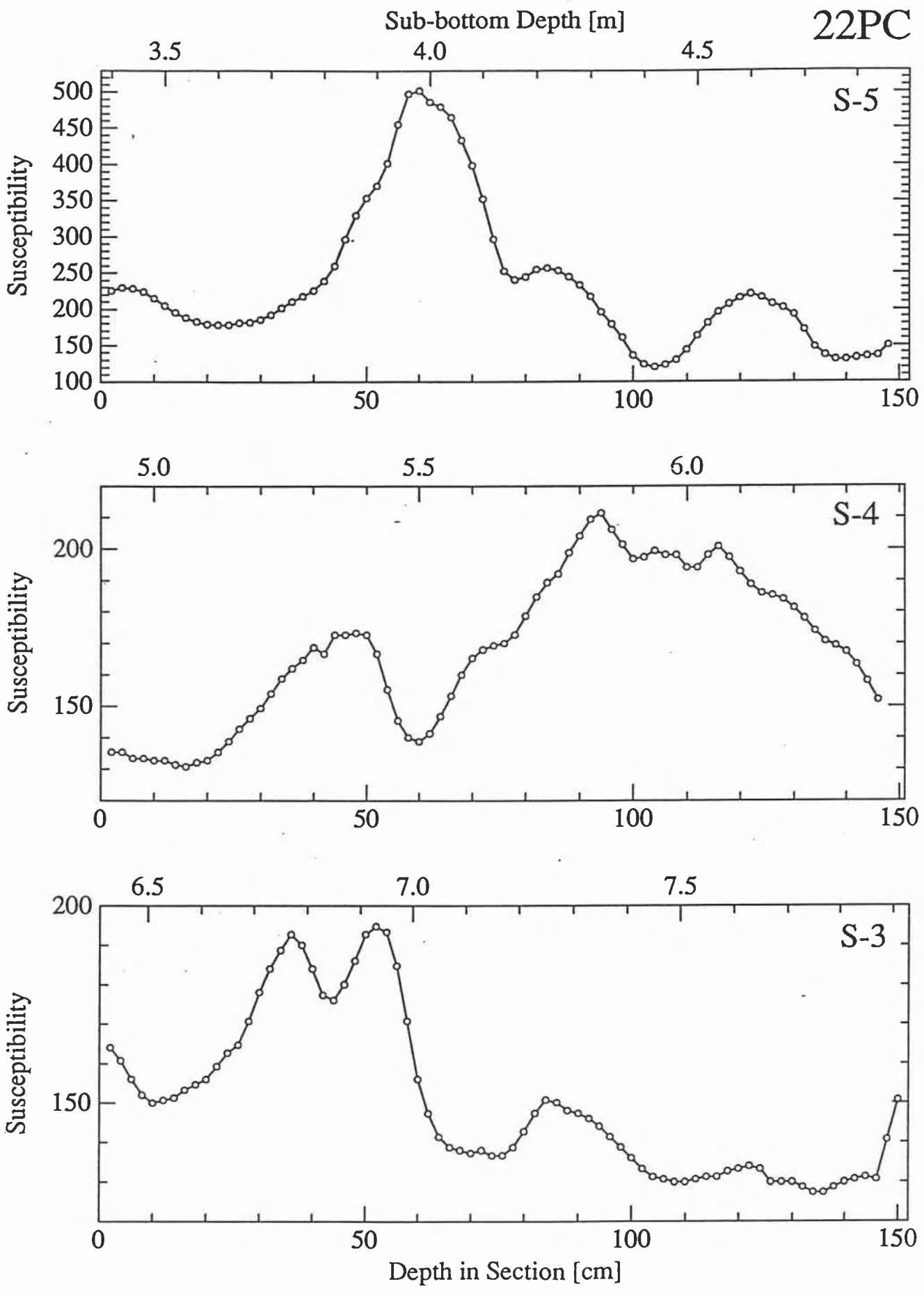
22PC
Sub-bottom Depth [m]
3.5
4.0
4.5
S-5
Susceptibility
500
450
400
350
300
250
200
150
100
0
50
100
150
5.0
5.5
6.0
S-4
Susceptibility
200
150
0
50
100
150
6.5
7.0
7.5
S-3
Susceptibility
200
150
0
50
100
150
Depth in Section [cm]

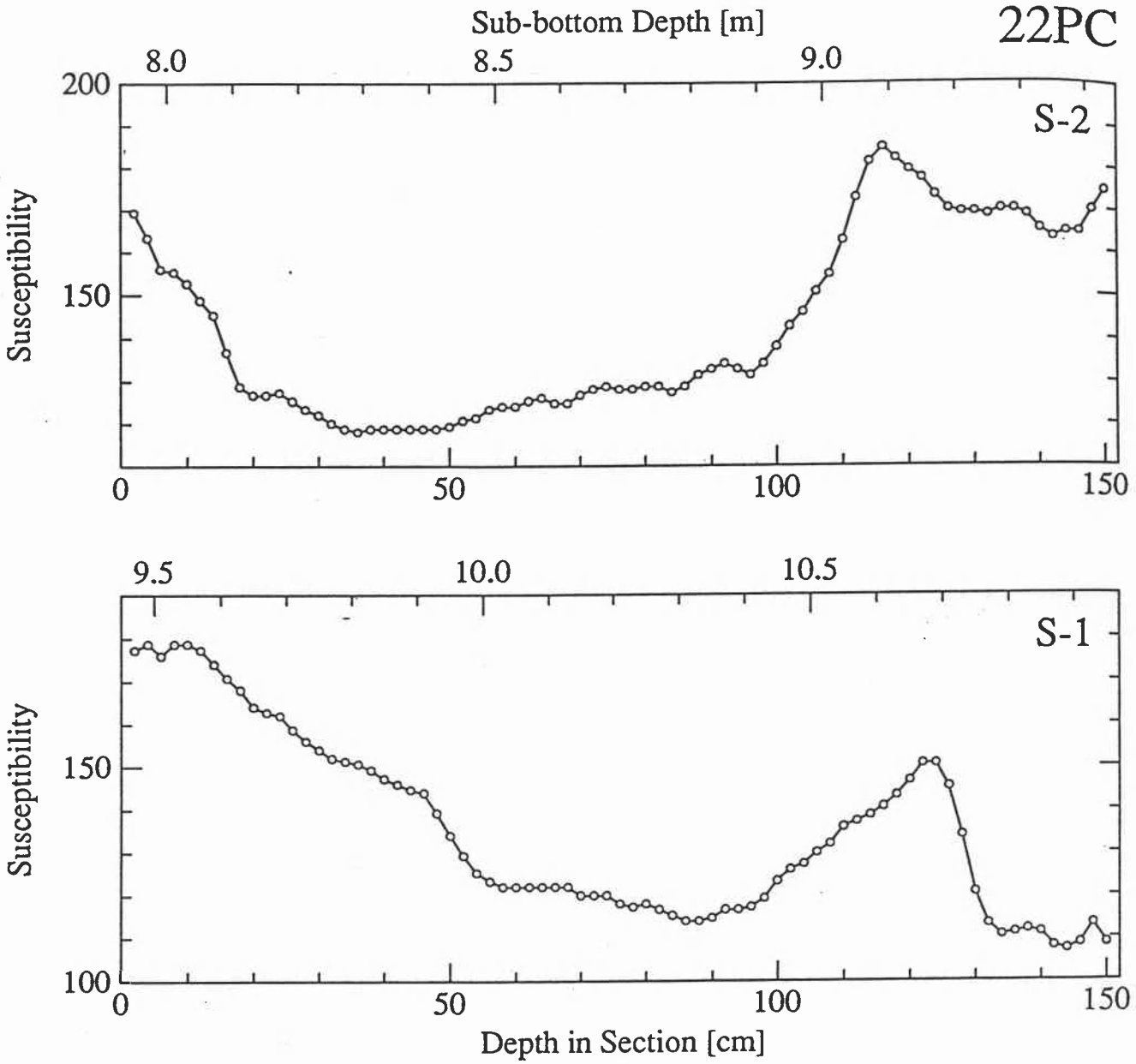
22PC
Sub-bottom Depth [m]
8.0
8.5
9.0
200
150
Susceptibility
S-2
0
50
100
150
9.5
10.0
10.5
S-1
150
100
Susceptibility
0
50
100
150
Depth in Section [cm]

Tephrochronology

The study area is relatively close to the volcanoes of Central and South America and previous studies show that several cores, especially close to land, contain ash layers. Since volcanic ashes have usually high susceptibilities, ash layers in the cores may show up as significant spikes in the downhole susceptibility signal. Distribution of prominent dated ash layers of this area have been studied in some detail [e.g., *Ninkovich and Shackleton*, 1975; *Drexler et al.*, 1980; *Ledbetter*, 1985].

The susceptibility signals in some of the cores show very distinct spikes that are correlated in this study to some of the known ash layers of the area. A spike in the downhole susceptibility signal may be related to other features than ash layers, for instance metallic contaminants during coring. Even by assuming that the spikes are volcanic ash layers, it is difficult to choose the right ash layer as the source of a given spike. Since there is only one major spike in a core the areal distribution of the most prominent ash layers is used as well as the approximate sedimentation rate, deduced from position of oxygen isotope stage five and correlation to surrounding cores, to correlate a given susceptibility spike to a dated ash layer.

Ash "K" at 330 ka. Figure 55 shows the distribution of ash layer "K" in the northern part of the study area [*Ledbetter*, 1985]. Ash "K" has now a revised date at about 330 ka [*Finney*, 1986; *Lyle et al.*, 1988]. Spikes in cores 01PC at 4.20 m (top of the spike) (half-heights at 4.08–4.28 m) and 21PC at 8.27 m (8.22–8.32 m) are both correlated in this study to ash "K".

Ash "D" at 84 ka. Also in the northern area, ash layer "D", has been correlated to the Los Chocoyos ash, originating in an eruption dated at 84 ka from the Lake Atitlan caldera, Guatemala, (Figure 56) [*Drexler et al.*, 1980; *Ledbetter*, 1985]. A spike in core 22PC at 3.98 m (3.90–4.10 m) is possibly due to ash "D". In core 22PC there are no other features that can support this particular pick, and although this correlation is favored this spike might represent ash "K".

Ash "L" at 230 ka. In the south-eastern part of the study area is ash layer "L", dated at 230 ka (Figure 57) [*Ninkovich and Shackleton*, 1975; *Ledbetter*, 1985]. Spikes in cores 14PC at 4.62 m (4.55–4.68 m) (Figure 58), 16PC at 3.75 m (3.70–3.79 m) (Figure 59), and 17PC at 4.42 m (4.37–4.46 m) (Figure 60) are all correlated in this study to ash "L".

Fingerprints of bioturbation. The thickness of most of the proposed ash layers is somewhat troublesome. For instance, cores 14PC, 16PC, and 17PC are all outside the currently recognized "extent" of ash layer "L". Still the susceptibility measurements indicate that the layers are 9 to 13 cm thick. The thickness of ash "L" in known cores indicates that the

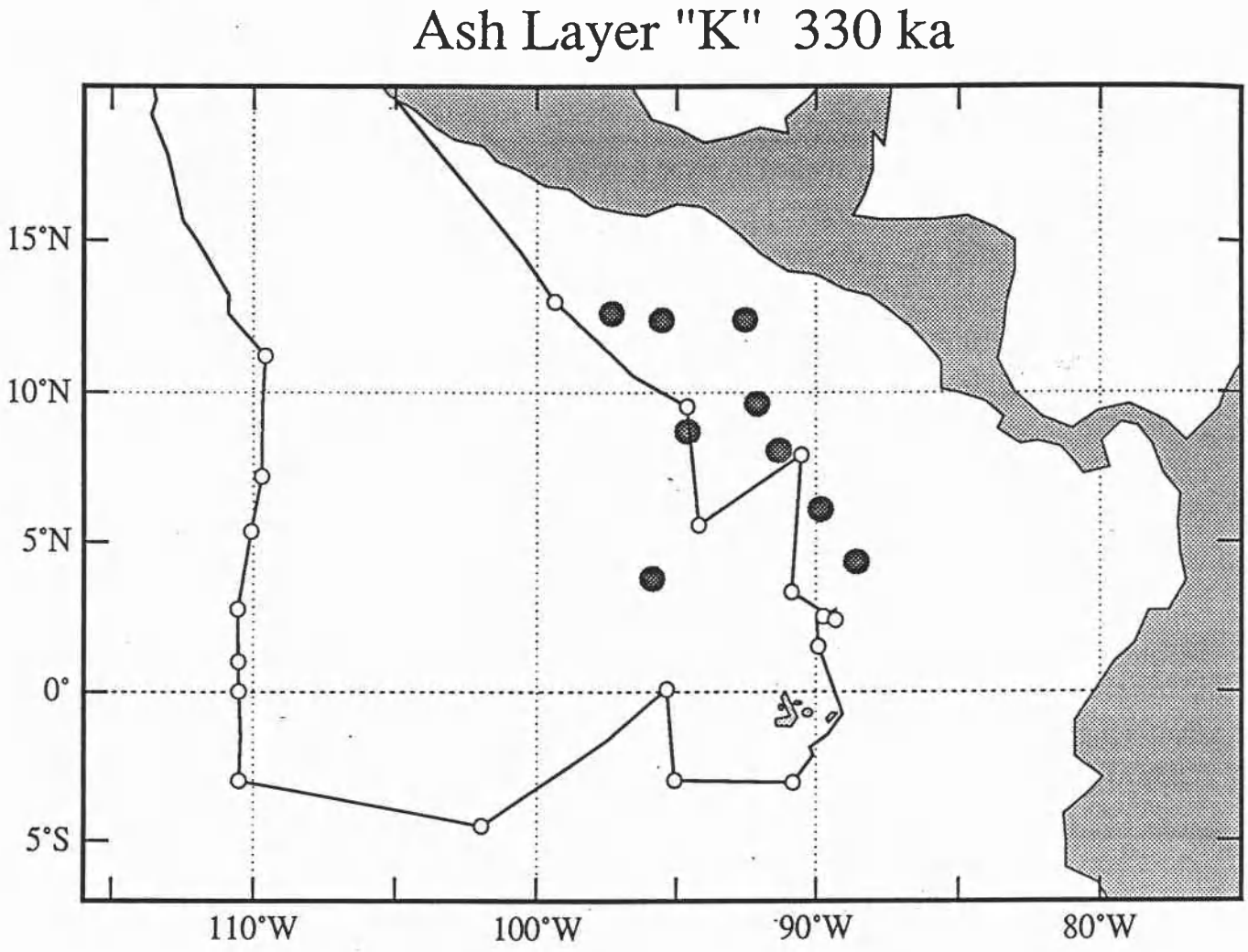

Figure 55. Distribution of ash layer "K" dated at 330 ka. Dots show cores where ash "K" has been found [*Ledbetter*, 1985].

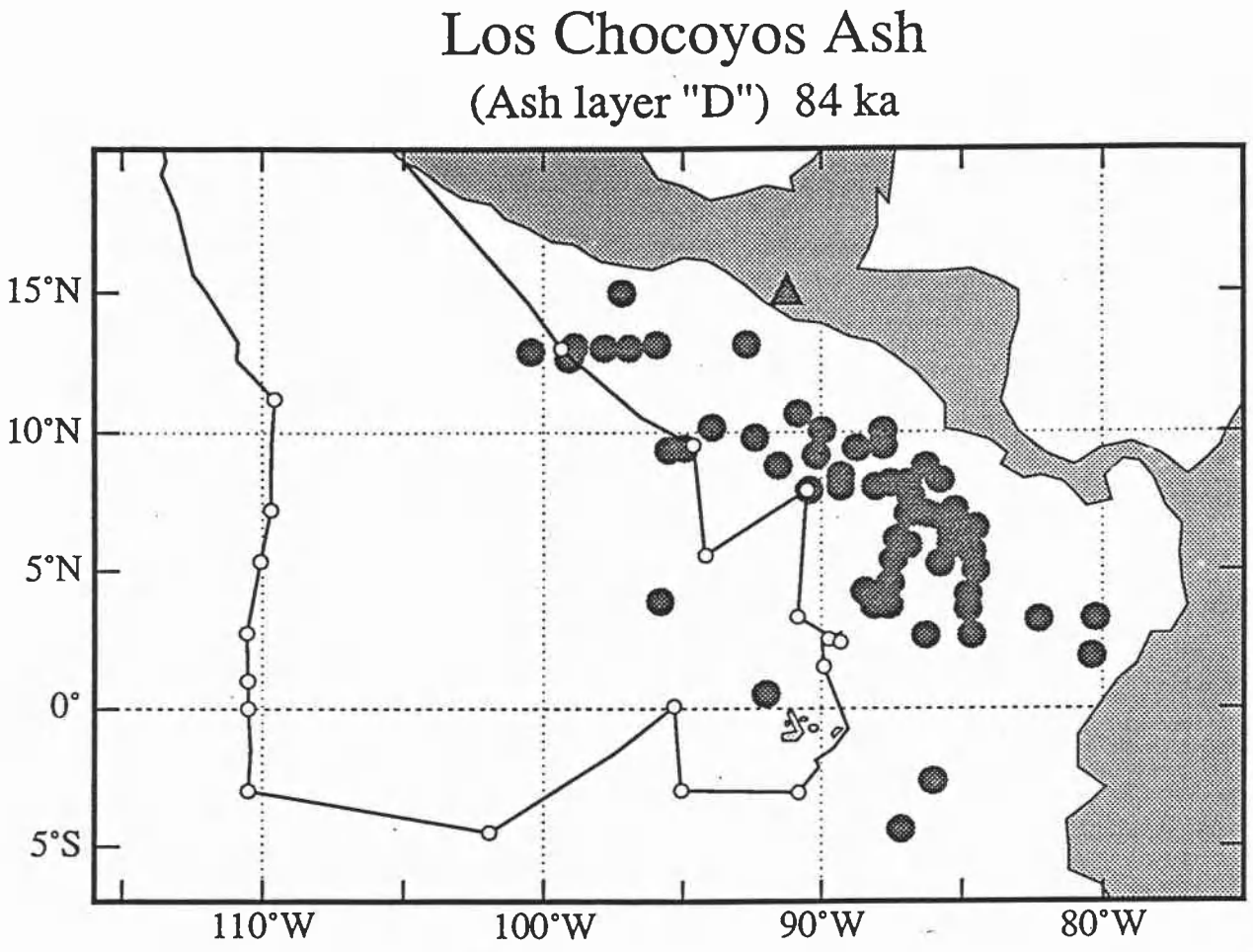

Figure 56. Distribution of ash layer "D" dated at 84 ka. Dots show cores where ash "D" has been found [*Drexler et al.*, 1980; *Ledbetter*, 1985]. Triangle shows the source of ash "D" in Guatemala.

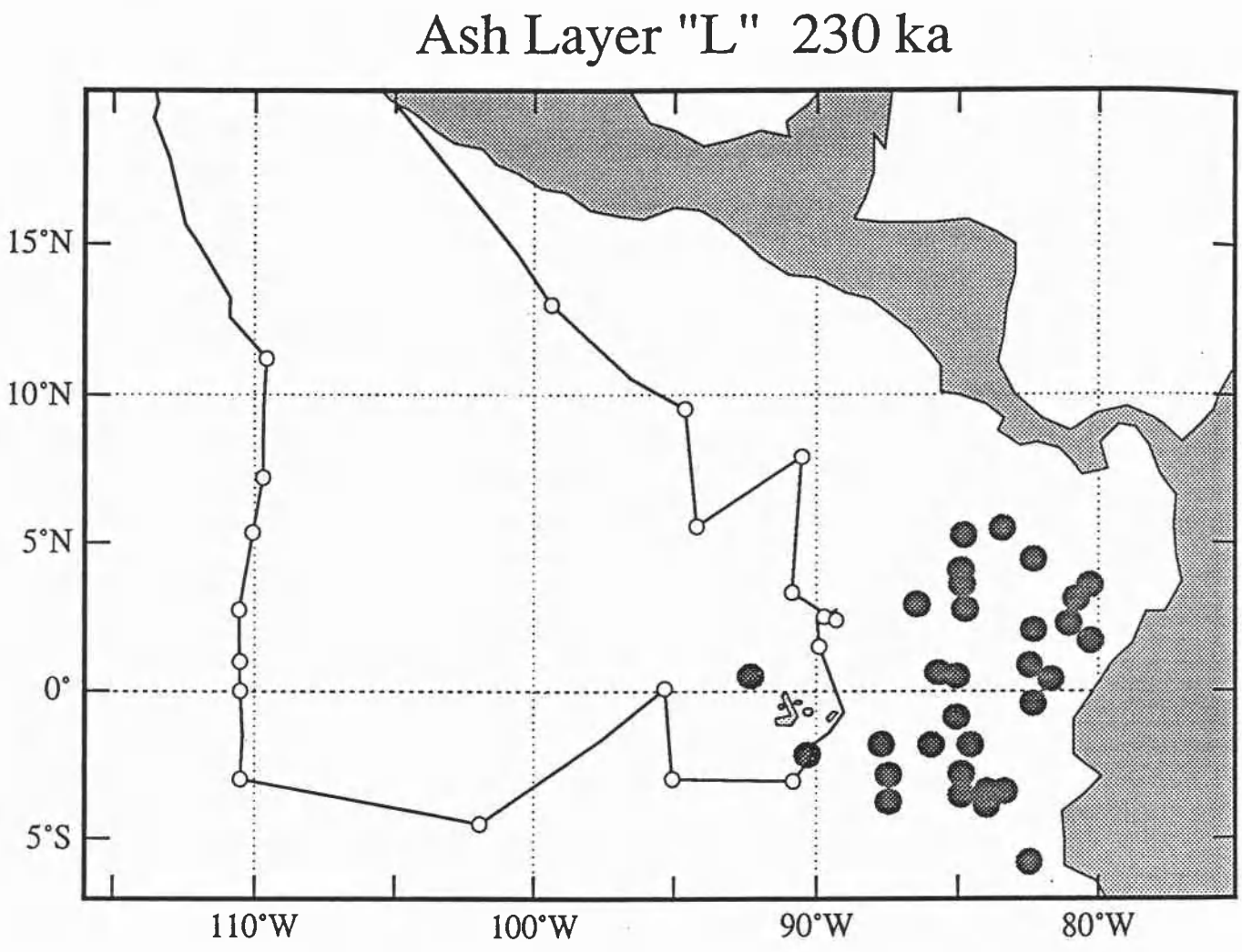

Figure 57. Distribution of ash layer "L" dated at 230 ka. Dots show cores where ash "L" has been found [*Ninkovich and Shackleton*, 1975; *Ledbetter*, 1985].

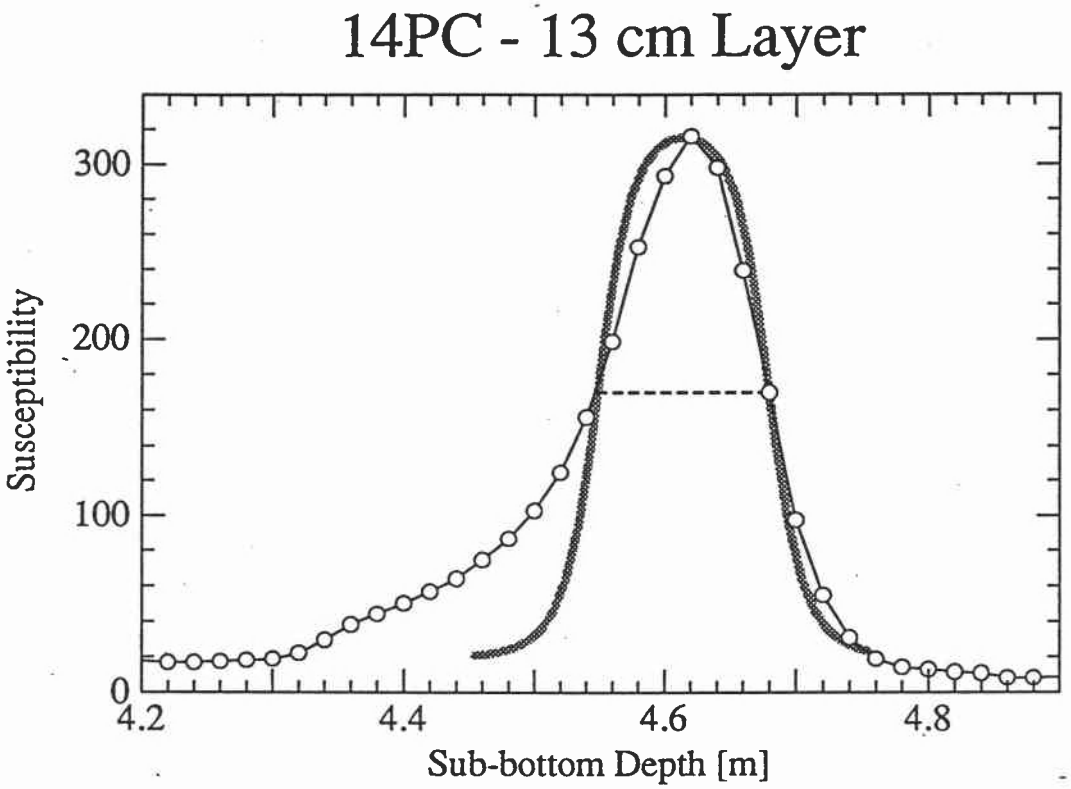

Figure 58. Details of the proposed ash layer "L" in VNTR01-14PC. The circles represent susceptibility measurements and the shaded curve is a calculated response of a 13 cm thick sharp layer. Note that the bottom of the "ash" layer is nearly a sharp boundary, but the top is a gradual boundary. The shape is interpreted as the fingerprints of bioturbation of an initially very thin layer.

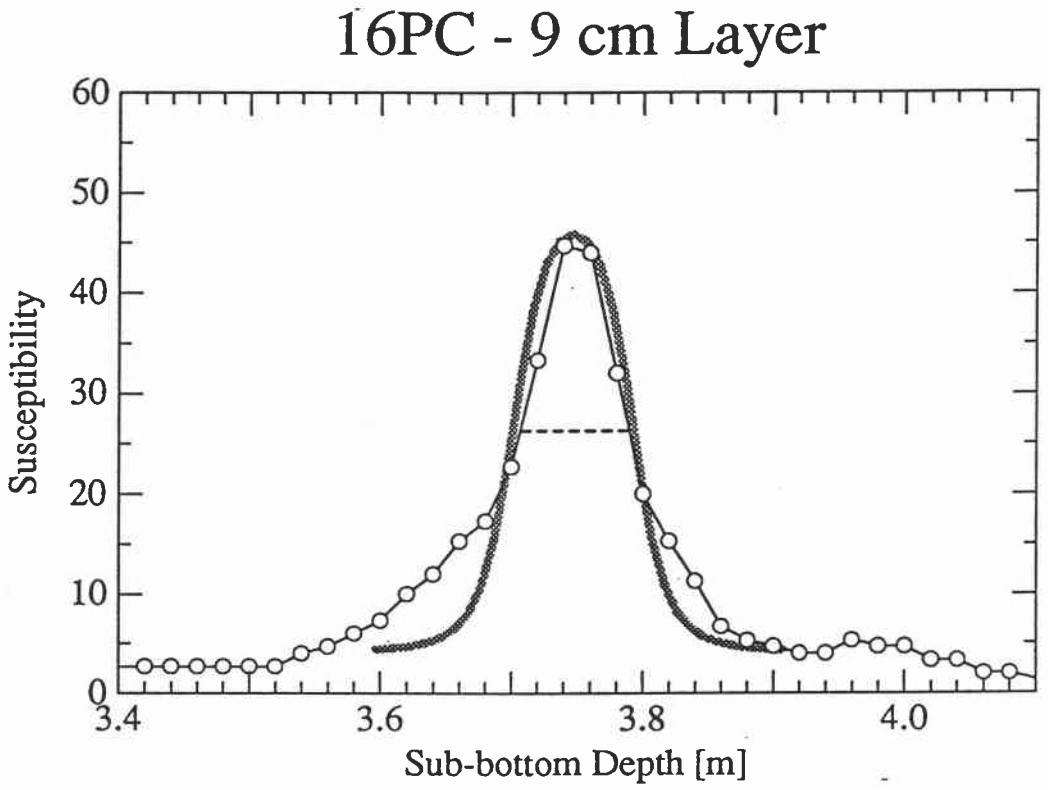

Figure 59. Details of the proposed ash layer "L" in VNTR01-16PC. The circles represent susceptibility measurements and the shaded curve is a calculated response of a 9 cm thick sharp layer.

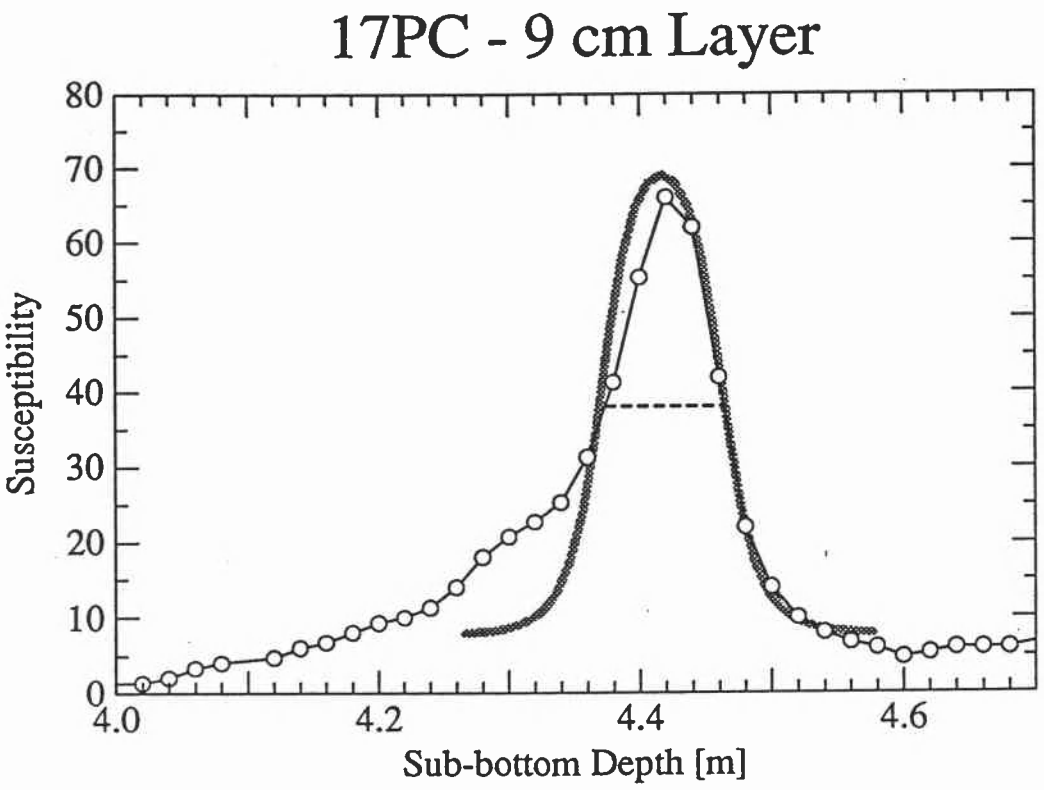

Figure 60. Details of the proposed ash layer "L" in VNTR01-17PC. The circles represent susceptibility measurements and the shaded curve is a calculated response of a 9 cm thick sharp layer.

thickness should be much thinner and possibly less than 1 cm in our cores. Here, it is worthwhile to note that the susceptibility reaches 316×10^{-6} in 14PC but only 45×10^{-6} in 16PC and 66×10^{-6} in 17PC, so the ash is diluted by a factor of 5–7 in cores 16PC and 17PC compared to core 14PC. Furthermore, a susceptibility of 316×10^{-6} might even be considered low for a 100% ash. It is therefore likely that the ash layers were initially very thin, but bioturbation mixed the ash downward into a certain zone, with relatively sharp bottom, but as more sediment is accumulated, the top of the ash gets mixed and diluted exponentially upward. The thickness of 9 to 13 cm is therefore indicative of the bioturbation process (see also *Glass* [1969]). This conclusion is probably also valid for all the ash layers of this study ranging in thickness of 9 to 20 cm. It is also interesting to note that the susceptibility spikes seem to be very sharp at the bottom and have gradual boundary at the top.

Latitudinal Variation in Susceptibility

A very strong latitudinal change in the average susceptibility was observed during the transect at 110°W as shown in Figure 61. The cores closer to land show similar change, but local effects become important for some. Increased biogenic sedimentation on the equator is thought to be partly responsible for the decrease in the susceptibility toward the equator (dilution effects). However, by estimating the accumulation rate of susceptible material there is still a factor of up to 10 in unexplained decrease toward the equator. Flux of eolian sediment is known to decrease rapidly toward the equator. Therefore the susceptible material is probably of terrigenous origin.

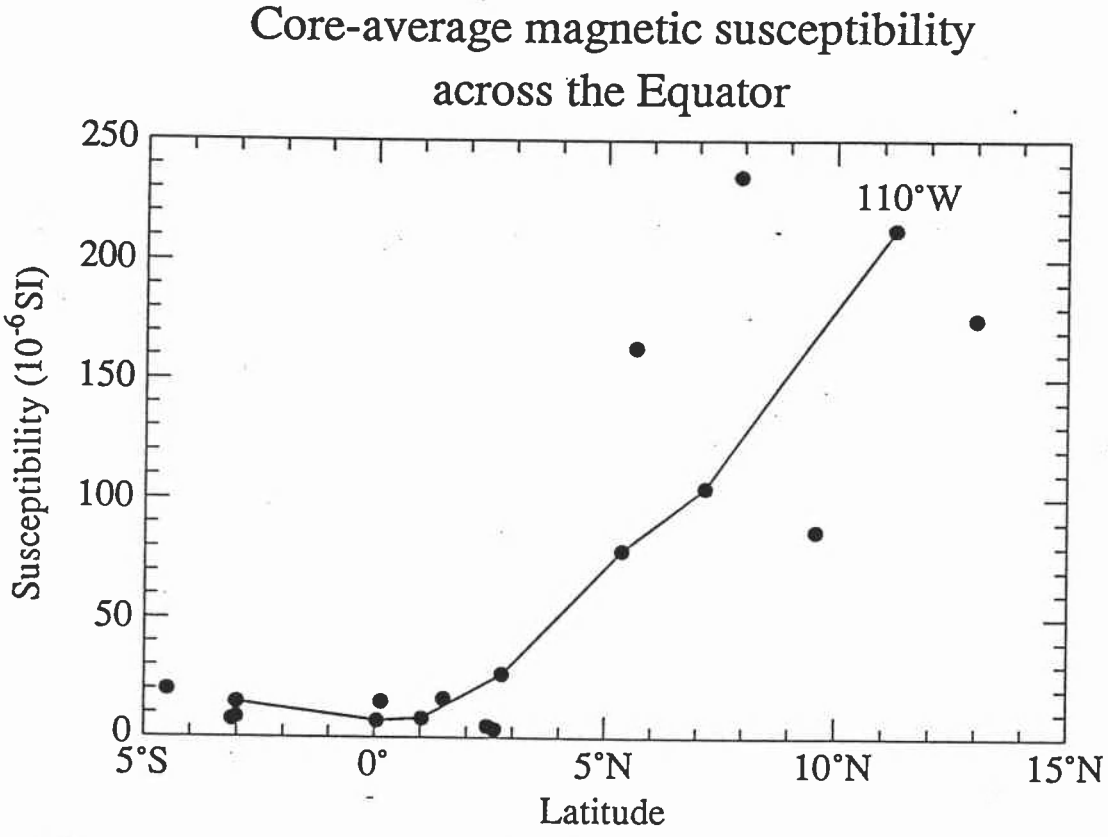

Figure 61. Core-average susceptibility across the equator. The cores on the transect at 110°W are connected by a line. The decrease towards the equator is probably due to increased biogenic sedimentation and decreased eolian input.

Conclusions

1) This report demonstrates that magnetic susceptibility can be measured rapidly on unopened cores during a coring cruise. The instruments needed are relatively cheap and the measurements do not affect the sediment. Before sampling the cores these measurements are a powerful reconnaissance tool.

2) The susceptibility is probably a good proxy parameter for calcium carbonate content of the sediment. Some of the downhole susceptibility features are seen over large distances and others are very localized. The characteristics of individual susceptibility logs are possibly related to paleoceanographic parameters.

3) The susceptibility is very powerful in correlating depth horizons between close cores. An example of this is seen in cores 16PC and 17PC that are 49 km apart. Although the susceptibilities are very low and close to the noise level they can easily be correlated (see Figures 45 and 46, and Table 24).

4) Rough estimates of chronology were made by correlating variations in the susceptibility to climatic oscillations. The age-depth correlations are summarized in Figure 62. Probably the best correlations come from core 06PC for which dating was possible down the entire core (see Figures 5 and 6, and Tables 12 and 13). It is not fully understood why such good correlations are possible.

5) Only after the sampling and dating the sediment by traditional methods will it be possible to determine the success of the age-depth correlations of this study.

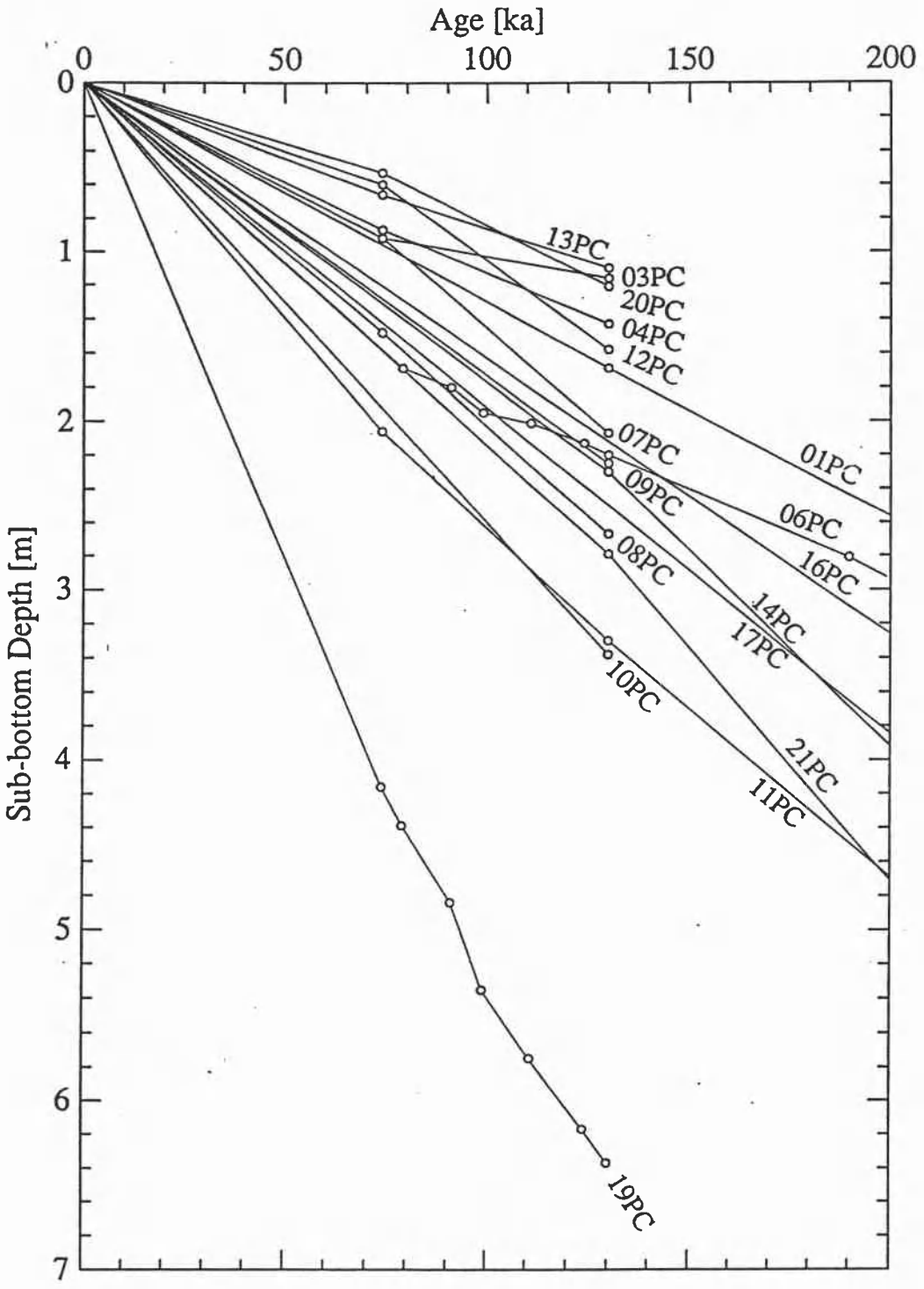

Figure 62. A summary of the age-depth picks of this study for the last 200 ky. Most of the cores have sedimentation rates between 0.8 and 2.5 cm/ky.

Bibliography

Amerigian, C., Sea-floor dynamic processes as the possible cause of correlations between paleoclimatic and paleomagnetic indices in deep-sea sedimentary cores, *Earth Planet. Sci. Lett.*, *21*, 321-326, 1974.

Arason, P., Automated magnetic susceptibility recording of borecores, Multicopied Report, 16 pp., Oregon State University, Corvallis, 1987.

Arason, P., A system for whole core magnetic susceptibility recording, Multicopied Report, 17 pp., Oregon State University, Corvallis, 1988.

Bartington Instruments, *Operation manual, Bartington model M.S.2., Magnetic susceptibility system*, Oxford, England, 38 pp., 1987.

Bloemendal, J., B. Lamb, and J. King, Paleoenvironmental implications of rock-magnetic properties of Late Quaternary sediment cores from the eastern equatorial Atlantic, *Paleoceanography*, *3*, 61-87, 1988.

Chikazumi, S., *Physics of Magnetism*, 554 pp., John Wiley, New York, 1964.

Collinson, D. W., *Methods in Rock Magnetism and Palaeomagnetism*, 503 pp., Chapman and Hall, London, 1983.

Dankers, P. H. M., Magnetic properties of dispersed natural iron-oxides of known grain-size, Ph.D. thesis, 143 pp., Utrecht University, Netherlands, 1978.

Drexler, J. W., W. I. Rose Jr., R. S. J. Sparks, and M. T. Ledbetter, The Los Chocoyos ash, Guatemala: A major stratigraphic marker in Middle America and in three ocean basins, *Quat. Res.*, *13*, 327-345, 1980.

Finney, B. P., Paleoclimatic influence on sedimentation and manganese nodule growth during the past 400,000 years at MANOP site H (eastern equatorial Pacific), Ph.D. thesis, 195 pp., Oregon State University, Corvallis, 1986.

Glass, B. P., Reworking of deep-sea sediments as indicated by the vertical dispersion of the Australasian and Ivory Coast microtectite horizons, *Earth Planet. Sci. Lett.*, 6, 409-415, 1969.

Imbrie, J., J. D. Hays, D. G. Martinson, A. McIntyre, A. C. Mix, J. J. Morley, N. G. Pisias, W. L. Prell, and N. J. Shackleton, The orbital theory of Pleistocene climate: Support from a revised chronology of the marine $\delta^{18}O$ record, in Berger, A., J. Imbrie, J. Hays, G. Kukla, and B. Saltzman (Eds.), *Milankovitch and Climate*, part 1, 269-305, Reidel Publ., Netherlands, 1984.

Kent, D. V., Apparent correlation of palaeomagnetic intensity and climatic records in deep-sea

sediments, *Nature*, *299*, 538-539, 1982.

King, J. W., Paleomagnetic and rock-magnetic stratigraphy of Pigmy basin, deep sea drilling project site 619, leg 96, in Bouma, A. H., J. M. Coleman, A. W. Meyer, et al., *Init. Repts. DSDP*, *96*, Washington (U.S. Govt. Printing Office), 677-684, 1986.

Ledbetter, M. T., Tephrochronology of marine tephra adjacent to Central America, *Geol. Soc. Am. Bull.*, *96*, 77-82, 1985.

Lyle, M., D. W. Murray, B. P. Finney, J. Dymond, J. M. Robbins, and K. Brooksforce, The record of late Pleistocene biogenic sedimentation in the eastern tropical Pacific Ocean, *Paleoceanography*, *3*, 39-59, 1988.

Martinson, D. G., W. Menke, and P. Stoffa, An inverse approach to signal correlation, *J. Geophys. Res.*, *87*, 4807-4818, 1982.

Martinson, D. G., N. G. Pisias, J. D. Hays, J. Imbrie, T. C. Moore Jr., and N. J. Shackleton, Age dating and the orbital theory of ice ages: Development of a high-resolution 0 to 300,000-year chronostratigraphy, *Quat. Res.*, *27*, 1-29, 1987.

Molyneux, L., and R. Thompson, Rapid measurement of the magnetic susceptibility of long cores of sediment, *Geophys. J. Roy. Astron. Soc.*, *32*, 479-481, 1973.

Ninkovich, D., and N. J. Shackleton, Distribution, stratigraphic position and age of ash layer "L", in the Panama basin region, *Earth Planet. Sci. Lett.*, *27*, 20-34, 1975.

Radhakrishnamurty, C., S. D. Likhite, B. S. Amin, and B. L. K. Somayajulu, Magnetic susceptibility stratigraphy in ocean sediment cores, *Earth Planet. Sci. Lett.*, *4*, 464-468, 1968.

Robinson, S. G., The late Pleistocene paleoclimatic record of North Atlantic deep-sea sediments revealed by mineral-magnetic measurements, *Phys. Earth Planet. Inter.*, *42*, 22-47, 1986.

Sager, W. W., Magnetic-susceptibility measurements of metal contaminants in ODP leg 101 cores, in Austin, J. A., Jr., W. Schlager, A. A. Palmer, et al., *Proc. Init. Repts. ODP*, *101*, Washington (U.S. Govt. Printing Office), 39-45, 1986.

Somayajulu, B. L. K., T. J. Walsh, and C. Radhakrishnamurty, Magnetic susceptibility stratigraphy of Pacific Pleistocene sediments, *Nature*, *253*, 616-617, 1975.

Thompson, R., and F. Oldfield, *Environmental Magnetism*, 227 pp., Allen and Unwin, London, 1986.

Wollin, G., D. B. Ericson, W. B. F. Ryan, and J. H. Foster, Magnetism of the earth and climatic changes, *Earth Planet. Sci. Lett.*, *12*, 175-183, 1971.